The novel application of high resolution peripheral quantitative ct imaging in distal radius and scaphoid fractures

The novel application of High Resolution peripheral Quantitative CT imaging in distal radius and scaphoid fractures

Anne Daniels

The novel application of
High Resolution peripheral Quantitative CT imaging
in distal radius and scaphoid fractures

Proefschrift

ter verkrijging van de graad van doctor aan de Universiteit Maastricht,
op gezag van de Rector Magnificus, Prof. dr. Pamela Habibović
volgens het besluit van het College van Decanen,
in het openbaar te verdedigen
op vrijdag 30 juni 2023 om 13.00 uur

door

Anne Marjan Daniels
geboren op 11 november 1991
te Sittard

ISBN: 978-94-93315-80-8

Layout and printing: proefschrift-aio.nl

Publication of this thesis was financially supported by Maastricht University, maatschap chirurgie VieCuri MC Venlo, Maastricht UMC+, VieCuri MC Venlo, SCANCO medical AG, SWOAHS, Nederlandse Vereniging voor Traumachirurgie, ABN AMRO bank and Chipsoft.

Promotoren

Prof. dr. J.P. van den Bergh
Prof. dr. M. Poeze

Copromotoren
Dr. H.M.J. Janzing - *VieCuri MC Venlo*
Dr. C.E. Wyers - *VieCuri MC Venlo*

Beooordelings commissie
Prof. dr. P. Willems - *voorzitter*
Prof. dr. A.E. Boonen
Dr. A.J.M. Janus - *Isala Zwolle*
Dr. ir. J.J.A. de Jong
Prof. dr. M.H.J. Verhofstad - *Erasmus MC Rotterdam*

Het Fonds Wetenschap en Innovatie van het VieCuri MC Venlo heeft financieel bijgedragen aan de totstandkoming van dit proefschrift.

Table of contents

Chapter 1

Introduction and outline

Introduction

The evolution of an elevated posture of the human body leads to different risks, for example fall from a standing height. This resulted in an increase in the occurrence of hand and wrist injuries [1]. At the end of the 18th century, Petit and Pouteau [2] suggested that the injury resulting from a fall on outstretched hand, up till then referred to as dislocation as stated by Hippocrates, was a fracture. This hypothesis was supported for distal radius fractures (DRFs) by Colles (1814), Barton (1838), Dupuytren (1841) and Smith (1847) in the subsequent years. Followed by Destot, who was the first to describe a scaphoid fracture in 1905 [3].

Nowadays, DRFs are among the most common fractures in adults and scaphoid fractures the most common carpal fractures. In 2015, 99.000 patients were diagnosed with hand and wrist injuries in the Dutch hospitals. There is a bimodal distribution of distal radius and scaphoid fractures with an incidence peak around the age of 15-20 years and 45-65 years, both equating 30.000 injuries and thereby representing more than half of all hand/wrist injuries per year in the Netherlands [4]. Men account for approximately 75 percent to the peak incidence at young age, presumably as result of sports- and/or high-energy trauma. The peak incidence later in life mainly reflects a high incidence in women, since 70 percent of all fractures at this age occur in women mostly as a result of low-energy injuries [5-7].

Hand and wrist anatomy

The distal articular surface of the radius forms the anatomic foundation of the wrist joint and is divided into two articular facets – the scaphoid and lunate fossa – by a longitudinal sagittal ridge. At the ulnar side of the distal radius, the concave sigmoid notch facilitates the articulation with the ulna. The triangular fibrocartilage complex (TFCC) stabilizes the distal radioulnar joint [8]. The scaphoid bone is a boat-shaped ('skaphos' in Greek) bone positioned in the first carpal row. To a large extent, the scaphoid is covered with cartilage. As it is the only carpal bone bridging the proximal and distal carpal row and thereby articulating with five surroundingbones – trapezium, trapezoid, capitate, lunate and distal radius [Figure 1] –, it serves a key role in the function of the wrist [9].

Figure 1. Anatomy of the wrist and hand

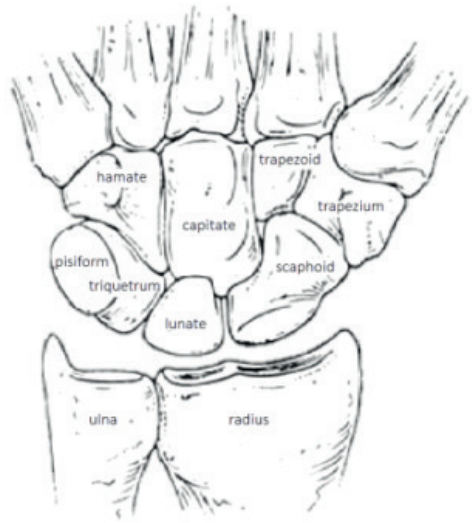

Osteoporosis

The most common method to evaluate bone mineral density (BMD) in daily practice is by using dual-energy X-ray absorptiometry (DXA) measurement in the spine and hip. DXA was first approved for the measurement of BMD in clinical practice by the United States Food and Drug Administration (FDA) in 1988. Six years later, in 1994, the WHO released criteria for diagnosing osteoporosis according to variation of a patient's BMD from the mean BMD of a young-adult reference population expressed as a T-score. BMD measurements are classified according to the lowest T-score in the total hip/femoral neck or lumbar spine: osteoporosis as T-score ≤–2.5, osteopenia as T-score between –2.5 and –1.0 and normal BMD as T-score ≥–1.0 [10,11].

Distal radius fractures

Epidemiology

Low-energy trauma such as a fall from standing height is the most reported cause of DRFs [5-7]. In 2017, women were diagnosed with osteoporosis 3.5 times more often than men [12]. It is well known that osteoporosis is related to fracture risk and thereby contributes to the occurrence of DRFs [6,11,13-18]. In addition, of all distal forearm fractures in 2010 in the Netherlands, 32% could be attributed to osteoporosis (35% for women vs 16% for men) [18].

Classification

From 1814 on, more than twenty classification systems for DRFs were developed. Despite general conformity regarding the classification systems, there is a large variation regarding details such as ulnar styloid involvement. The most commonly used classification systems are the Arbeitsgemeinschaft für Osteosynthesefragen/Orthopaedic Trauma Association (AO/OTA), Fernandez, Melone, Frykman and Universal (Cooney) classification [19-22]. In the AO/OTA classification [Figure 2] three main types being extra-articular (type A), partly articular (type B) and complete articular (type C) fractures are enclosed. Classifying fractures into one of the AO/OTA main types is the most reliable way to classify a DRF according to existing literature [23]. Each main type is divided into three subgroups addressing the comminution and dislocation of the fracture (A1-3, B1-3, C1-3) and is then again subdivided into three groups. However, inter- and intra- observer agreement of subgroup assessment is poor and therefore classification of DRFs into subgroups is not recommended [24].

Figure 2. AO/OTA classification: three main types (A/B/C) with subgroups (1-3)

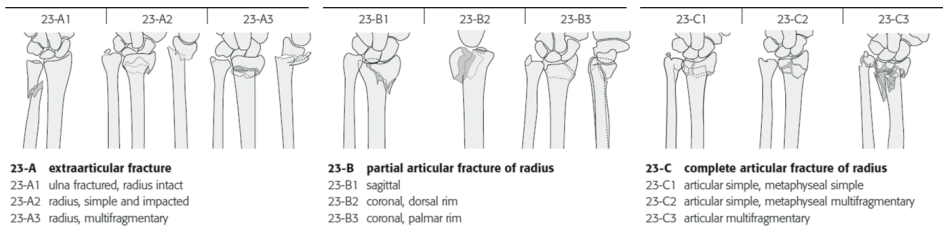

Figure 3. Radiographic alignment parameters (RI/UV/DA/VA) to assess the distal radius

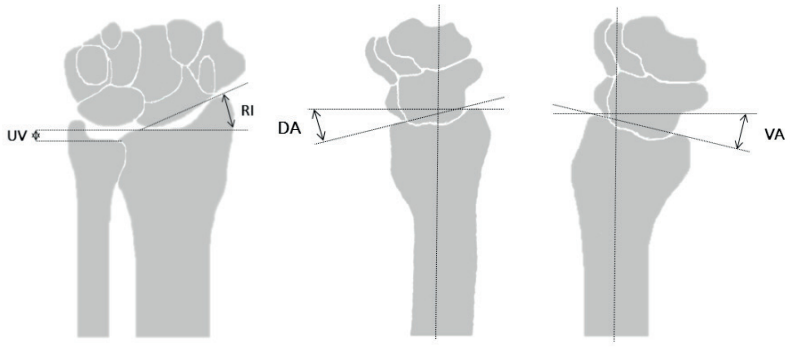

Treatment

Standard initial management at the emergency department (ED) is closed reduction followed by cast immobilization. In case of a clear indication for surgical repair, not reducing the fracture at first presentation should be considered. With maximizing functional outcome at long term as primary treatment focus, the importance of radiographic alignment was frequently studied. Papers report that large deviation from radiographic alignment to the anatomic position is related to worse functional results (range of movement, grip strength, pain), especially in younger people. Small deviations from radiographic alignment appear to be less important to the patient's functional outcome on both short and long term [25-31]. In order to select fractures with an acceptable position, the following range of radiographic alignment [Figure 3] are generally defined: dorsal angulation (DA) ≤15°, volar angulation (VA) <20°, radial inclination (RI) ≥15° and ulnar variance (UV) < 5mm [24,30,32].

Surgical treatment is considered for fractures with an unacceptable position (despite reduction). Patient characteristics such as age, physical demand and comorbidities should be taken into account when making this decision. Surgical treatment for DRFs includes internal fixation with volar and/or dorsal locking plates, percutaneous Kirschner wire fixation and an external fixation.

Fractures with an acceptable position can be treated conservatively. Despite the widespread acceptance of immobilization as conservative treatment for DRFs, the duration and kind of immobilization is still debated. Generally, minimally or non-displaced fractures at time of presentation are treated with cast immobilization for three (up to five) weeks [24]. Alternative immobilization encompasses functional treatment with a brace for stable fractures. Fractures that require reduction at first presentation should be considered potentially unstable and therefore always require cast immobilization with follow-up radiographs [24]. Research has been conducted on the identification of factors associated with secondary displacement of a DRF. For example DA >20°, dorsal comminution, radial shortening before reduction and age >60 years were identified and some of them again invalidated by other studies [33-40].

Scaphoid fractures

Epidemiology

Scaphoid fractures represent 2-6% of all fractures and account for almost 90% of all carpal fractures in the Netherlands [41-43]. There is male predominance with a peak incidence at young age (15-25 years). This is most likely explained by the participation in high-risk contact sports, one of the risk factors for scaphoid

fractures. Possible other risk factors include reduced BMD and smoking. Although the mechanism of impact might vary, the most common cause of a scaphoid fracture is a fall on outstretched hand.

Classification

The scaphoid has a natural tendency to flex in the palmar direction with longitudinal load [44] and is therefore easily mechanically predisposed to fracture. If the impact to the palm occurs with the wrist in extension and radial deviation, the proximal two-third of the scaphoid and distal radius meet and the waist of the scaphoid is at risk. An impact with the wrist in extension and neutral (anatomic) position may lead to a fracture in the proximal pole of the scaphoid. Besides classifying scaphoid fractures based on location (proximal, waist, distal) as described by Bohler, Cooney (Mayo), Schernberg and the AO/OTA [45-48], classification based on fracture plane orientation (horizontal oblique, transvers, vertical oblique) as described by Bohler and Russe [48,49] and based on displacement and/or instability as described first by McLauglin and Parkes and later on by Cooney (Mayo), Weber and Herbert and Fisher [46,50-52] is possible. This last classification system was designed in relation to the introduction of a new bone screw, as this technique was designated for the displaced and/or unstable fractures. The (modified) Herbert classification system encompasses type A and B fractures, being stable respectively unstable fractures with subtypes addressing the location and displacement/comminution [Figure 4].

Figure 4. Herbert classification system; two main types (A/B) with subgroups (1-2,1-5)

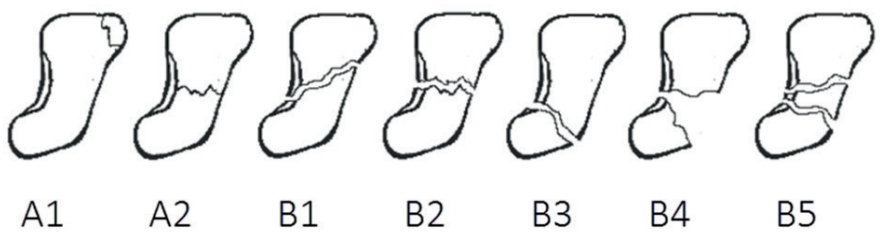

Although inter- and intra- observer reliability outcomes of all mentioned systems vary with mostly fair rates [53,54], the Herbert classification system is currently the most frequently used system. Assessment of displacement of scaphoid fractures is best done on computed tomography (CT) or radiographs combined with CT instead of radiographs alone [55-57].

Treatment

Early and accurate diagnosis is of great importance as the complications such as malunion, nonunion and early osteoarthritis of the radiocarpal joint [58-61] are associated with serious pain and impairment of hand and wrist function. Adequate treatment of a scaphoid fracture can reduce these complications. Since up to 25% of scaphoid fractures remain radiographically occult with conventional imaging [53,58,62,63], patients with a suspected scaphoid fracture (tenderness at the anatomic snuffbox and/or pain on axial compression of the thumb) are usually treated with cast immobilization and reassessment takes place after 7-10 days. If a suspicion of a scaphoid fracture remains after reassessment, additional imaging such as CT, magnetic resonance imaging (MRI) or bone scintigraphy (BS) is suggested in current local protocols.

If diagnosis is obtained, scaphoid fractures can be treated either conservative or operatively with screw or plate fixation. A fracture of the proximal pole or a fracture with comminution is susceptible to displacement due to the opposing forces and ligament distribution [64] and therefore surgical intervention is suggested. Conservative treatment consists of six (for distal scaphoid fractures) up to twelve weeks (for mid/distal scaphoid fractures) cast immobilization.

Current bone imaging techniques for diagnosis of distal radius and scaphoid fractures

Conventional radiographs

In 1895, the 'roentgenography' was discovered and resulted in rapid involvement of fracture understanding. The technique relies upon the absorption of ionizing radiation differing for each type of tissue in the body resulting in contrast differences between fat and bone [65]. Thereby, fractures can be diagnosed. Conventional views of the distal radius obtained in daily practice are the antero-posterior and lateral view. Although management of DRFs remained predominantly conservative, the introduction of this imaging technique made assessment of reduction and follow-up of fracture healing possible.

For scaphoid fracture detection, usually two additional views are obtained being a semi-pronated oblique and antero-posterior view with the wrist in ulnar deviation. Although radiographs are readily available in every hospital and can provide a rapid first impression of the diagnosis, it lacks the possibility to demonstrate bone loss and soft-tissue evaluation. Moreover, up to 25% of all scaphoid fractures remain occult on conventional radiographs [62,66,67] and preoperative evaluation of complex fractures with conventional radiographs is inferior to CT [68,69].

Computed tomography (CT)

In 1957, a method for calculating radiation absorption distributions in the human body was developed, but not put into practice with success until the first CT in 1972 [70,71]. Following generations of CT scanners were characterized by an increased number of detectors and expanded movement of detectors.

Images are acquired in the axial plane and can be reconstructed into any other anatomical plane. CT is readily available in most hospitals and perfectly suited for the detailed three-dimensional evaluation of bony structures and soft-tissue calcification. However, the shortcoming of conventional radiographs, i.e. soft-tissue evaluation, cannot be fully mastered with CT. Moreover, relatively high dose ionizing radiation is necessary even for imaging of the extremities (46 µSv for a hand/wrist CT). This technique is frequently used as preoperative imaging for more detailed information on DRFs and as diagnostic tool for clinically suspected scaphoid fractures. A limitation of CT in diagnosing scaphoid fractures is the relatively low sensitivity compared to MRI [72-75].

Magnetic Resonance Imaging (MRI)

After multiple large discoveries, starting with the resonance phenomenon in 1946, MRI was developed and implemented in clinical practice at the beginning of the 1980s. he MRI signal is derived from the hydrogen protons as they move back into alignment with the magnetic field and fall out of "phase" with each other. MR images are generated by the alignment of the hydrogen nuclei with the magnetic field. The potential risks of ionizing radiation are not applicable to this technique. Similar to CT, metallic devices result in problematic artefacts making evaluation difficult [76].

High signals in bone marrow on MRI might be an indication for trauma. This finding has to be judged in light of clinical or other imaging findings. MRI is rarely used in DRF diagnostics but is appropriate to exclude a scaphoid fracture (specificity 94-100%) [77-81]. However, MRI is expensive, has limited availability in hospitals and is time consuming.

Bone Scintigraphy (BS)

The first to investigate the skeletal metabolism were Hevesy (1930) and Pecher (1940). This nuclear medicine scintigraphy procedure requires the infusion of radiopharmaceutical agents. Different radiopharmaceutical agents were tested which lead in 1971 to the discovery of the currently used agent; technetium-labeled methylene diphosphonate in [82]. After administration of this agent to the patients, radiation is detected by a camera and displayed in a comparable way as

in conventional radiographs. With this technique, changes in bone metabolism can be identified. Although its sensitivity for diagnosing scaphoid fractures is high (95-100%), specificity rates vary from 50-90% as bone turnover can, similar to MRI findings, indicate as well trauma, trabecular vs cortical injury, as degeneration, infection and malignancy [74,83,84]. Due to these specificity rates, the applicability of bone scintigraphy in scaphoid fracture detection is limited [75,77-79,81]. Moreover, accurate localization can be difficult, radiation dose is high, spatial resolutions are low and it is invasive and time consuming.

High Resolution peripheral Quantitative CT

Technique

The advancement of CT imaging techniques lies in retaining quality and reducing radiation dose at the same time [85]. Recently, High Resolution peripheral Quantitative CT (HR-pQCT), a three-dimensional quantitative imaging technique, of the distal radius and distal tibia has been developed. In addition to the BMD measured by DXA, this low radiation technique allows in vivo measurement of bone microarchitecture at the extremities by performing a 'virtual bone biopsy' [86-91]. Thereby, bone microstructure can be assessed in greater detail in a clinical setting to acquire the information that could, up till the introduction of HR-pQCT, only be obtained by taking a bone biopsy. A standard protocol is available for image acquisition and reconstruction. The cortical and trabecular bone at the distal radius and tibia can be assessed with an isotropic voxel size of 82 µm [87]. Moreover, three-dimensional evaluation of HR-pQCT makes micro finite element analysis (µFEA) possible [92-94]. Using µFEA, bone stiffness (resistance) and strength (breaking capacity) can be calculated.

Current applications

Validation and reproducibility studies of HR-pQCT have been performed extensively [88,94-99] and in the last decade widespread experience has been gathered concerning the use of this technique in clinical research. Recently it has been reported that assessment of cortical and trabecular bone microarchitecture by HR-pQCT improves overall fracture prediction in mostly normal or osteopenic elderly subjects beyond BMD [100]. In addition, HR-pQCT is proven to be feasible in assessment of changes in bone density, microarchitecture and bone stiffness during anti-osteoporosis treatment [101,102]. More recently HR-pQCT was used to study the facture healing process of stable distal radius fractures [103-105]. Its application in patients with rheumatoid arthritis (RA) was investigated as well [106-108]. Studies reported cortical erosions in finger joints of patients with RA detected with HR-pQCT while no erosions were visible on conventional radiographs and MRI [107,109-112]. This suggests that HR-pQCT is more sensitive in the

detection of bone damage on structural level and that HR-pQCT is able and highly sensitive to detect small cortical interruptions in comparison to the gold standard micro CT (μCT) [109,113,114]. A disadvantage of HR-pQCT in current practice is the limited availability in a clinical setting and the relatively small scanned region compared to CT.

Focus of this thesis

Distal radius fractures

Although BMD is proven to be an important component of fracture risk, the contribution of decreased BMD (measured by DXA) to DRF pattern complexity [16,115-118] and secondary displacement of a DRF [115,119] is reported with controversial results. Moreover, the association of other characteristics, such as prevalent vertebral fractures, vitamin D levels and bone microarchitecture and strength with DRF complexity has not been studied.

By being able to anticipate early stage instability, unnecessary manipulation at first presentation may be prevented, timely surgical treatment achieved, soft tissue swelling may be reduced and a reduction in complications such as malunion might be accomplished. We hypothesized that the standard assessment of bone quality and bone strength at the distal radius and tibia could attribute to the understanding DRF complexity and secondary displacement beyond the current clinical and bone density characteristics of patients.

Therefore, in this thesis the association of patient characteristics, BMD, bone microarchitecture and bone strength assessed with HR-pQCT with the pattern complexity and secondary displacement of a DRF will be addressed.

Scaphoid fractures

According to existing literature, only 10-20% of the clinically suspected scaphoid fractures are true fractures [42,62,74,120-122]. This implies most patients are over-diagnosed and -treated with unnecessary socio-economic effects as result of cast immobilization [43]. In addition, clinical reassessment is, despite widely varying diagnostic performance characteristics [123,124], guiding in decision-making for additional imaging in current practice.

Although conventional radiographs, CT, MRI and BS are frequently used nowadays, there is no consensus regarding the best modality for detecting scaphoid fractures [73-75,79-81,120,121,123,125-128] resulting in inconsistency in the imaging of acute scaphoid injury [129].

Altogether, there is a clear need for more data on diagnostic methods to ensure adequate diagnosis of scaphoid fractures in order to achieve fracture consolidation, function recovery and to prevent complications. We hypothesized that the application of HR-pQCT could be of additional value for the diagnosis of scaphoid fractures given its high resolution. Therefore, in this thesis, the application of HR-pQCT for detection of scaphoid fractures will be studied.

Outline of this thesis

We aimed to study the association of patient characteristics, BMD (measured by DXA and HR-pQCT), bone microarchitecture and calculated bone strength (by HR-pQCT) with the pattern complexity and secondary displacement of distal radius fractures. In ***chapter 2***, we focused on patient- and bone/fracture related factors associated with fracture pattern complexity and in ***chapter 3***, we focused on patient- and bone/fracture related factors associated with secondary distal radius fracture displacement.

In ***chapter 4 to 7***, we aimed to develop a novel application of HR-pQCT for detection of scaphoid fractures. Since HR-pQCT imaging of the scaphoid bone was never described in literature before, we first intended to study the feasibility of in vivo scanning of the scaphoid bone in ***chapter 4.*** In this study,we aimed to compare a fully automated and a semi-automated contouring procedure of the scaphoid bone and to compare the micro architectural indices in good- and poor- quality scans. In ***chapter 5*** we focused on the interobserver variability of scaphoid fracture classification, based on HR-pQCT images. Subsequently, we compared the detection of scaphoid fractures with HR-pQCT and conventional CT in ***chapter 6***. Finally, we evaluated the diagnostic performance of initial radiographs and the clinical reassessment at 7-14 days in relation to CT and HR-pQCT diagnosed scaphoid fractures in ***chapter 7.***

Chapter 8 will comprise a discussion of our main findings and provides final conclusions and recommendations and in ***chapter 9*** the findings of this thesis are summarized**.**

References

1. Kivell, T.L., et al., *Australopithecus sediba hand demonstrates mosaic evolution of locomotor and manipulative abilities.* Science, 2011. 333(6048): p. 1411-7.
2. Pouteau, C., *Memoire, contenant quelques reflexions sur quelques fractures de l'avant-bras sur les luxations incomplette du poignet sur les diastasis.* Oeuvres Posthumes de M Pouteau, Paris, 1783: p. 1783;2:251-266
3. Destrot, E., *La poignet et les accidents du travail: étude radiographique et clinique*. Paris, Vitot Freres, 1905.
4. Centraal Bureau voor de Statistiek, *Medisch Specialistische Zorg.* 2018; Available at: https://opendata.cbs.nl/statline.
5. Beerekamp, M.S.H., et al., *Epidemiology of extremity fractures in the Netherlands.* Injury, 2017. 48(7): p. 1355-1362.
6. Koo, O.T., et al., *Distal radius fractures: an epidemiological review.* Orthop Surg, 2013. 5(3): p. 209-13.
7. Riggs, B.L., et al., *Population-based study of age and sex differences in bone volumetric density, size, geometry and structure at different skeletal sites.* J Bone Miner Res, 2004. 19(12): p. 1945-1954.
8. Cohen, M. and R. Wysocki, F*ractures of the Distal Radius, in Skeletal Trauma: Basic Science, Management and Reconstruction*. 2015. Edition 5.
9. Taljanovic, M.S., et al., *Imaging and treatment of scaphoid fractures and their complications.* Semin Musculoskelet Radiol, 2012. 16(2): p. 159-73.
10. Dutch Institute for Healthcare Improvement CBO. *Richtlijn Osteoporose en Fractuurpreventie*, 2011.
11. Kanis, J.A.*, Diagnosis of osteoporosis and assessment of fracture risk.* Lancet, 2002. 359(9321): p. 1929-36.
12. Ministerie van Volksgezondheid, Welzijn en Sport, *Zorgregistraties eerste lijn*. 2018. Available at: https://nivel.nl/zorgregistraties.
13. Oyen, J., et al., *Osteoporosis as a risk factor for distal radial fractures: a case-control study*. J Bone Joint Surg Am, 2011. 93(4): p. 348-56.
14. Oyen, J., et al., *Low bone mineral density is a significant risk factor for low-energy distal radius fractures in middle-aged and elderly men: a case-control study.* BMC Musculoskelet Disord, 2011. 12: p. 67.
15. Dias, J.J., et al., *Osteoporosis and Colles' fractures in the elderly.* J Hand Surg Br, 1987. 12(1): p. 57-9.
16. Itoh, S., et al., *Relationship between bone mineral density of the distal radius and ulna and fracture characteristics.* J Hand Surg Am, 2004. 29(1): p. 123-30.
17. Porrino, J.A., et al., *Fracture of the distal radius: epidemiology and premanagement radiographic characterization.* AJR Am J Roentgenol, 2014. 203(3): p. 551-9.
18. Lotters, F.J., et al., *Current and Future Incidence and Costs of Osteoporosis-Related Fractures in The Netherlands: Combining Claims Data with BMD Measurements.* Calcif Tissue Int, 2016. 98(3): p. 235-43.
19. Lill, C.A., et al., *Impact of bone density on distal radius fracture patterns and comparison between five different fracture classifications.* J Orthop Trauma, 2003. 17(4): p. 271-8.
20. Plant, C.E., et al., *Is it time to revisit the AO classification of fractures of the distal radius? Inter- and intra-observer reliability of the AO classification.* Bone Joint J, 2015. 97-b(6): p. 818-23.
21. Arealis, G., et al., *Does the CT improve inter- and intra-observer agreement for the AO, Fernandez and Universal classification systems for distal radius fractures?* Injury, 2014. 45(10): p. 1579-84.
22. Ferrero, A., et al.*, Analysis of the inter- and intra-observer agreement in radiographic evaluation of wrist fractures using the multimedia messaging service.* Hand (N Y), 2011. 6(4): p. 384-9.
23. Muller, M.E., Nazarian, S., Koch, P. and Schatzker, J., *The comprehensive classification of fractures of long bone*. Springer-Verlag, London 1990. Current Orthopaedics, 1991.
24. Nederlandse Vereniging voor Heelkunde, *Richtlijn distale radius fracturen: diagnostiek en behandeling*. Richlijnendatabase, 2010.
25. Howard, P.W., et al., *External fixation or plaster for severely displaced comminuted Colles' fractures? A prospective study of anatomical and functional results.* J Bone Joint Surg Br, 1989. 71(1): p. 68-73.
26. Dario, P., et al., *Is it really necessary to restore radial anatomic parameters after distal radius fractures?* Injury, 2014. 45 Suppl 6: p. S21-6.
27. Kodama, N., et al., *Acceptable parameters for alignment of distal radius fracture with conservative treatment in elderly patients.* J Orthop Sci, 2014. 19(2): p. 292-297.
28. Gutierrez-Monclus, R., et al., *Correlation Between Radiological Parameters and Functional Outcomes in Patients Older Than 60 Years of Age With Distal Radius Fracture.* Hand (N Y), 2018: p. 1558944718770203.
29. McQueen, M.M., et al., *Redisplaced unstable fractures of the distal radius: a prospective randomised comparison of four methods of treatment.* J Bone Joint Surg Br, 1996. 78(3): p. 404-9.
30. McQueen, M. and Caspers, J.*, Colles fracture: does the anatomical result affect the final function?* J Bone Joint Surg Br, 1988. 70(4): p. 649-51.
31. Ng, C.Y. and McQueen, M.*, What are the radiological predictors of functional outcome following fractures of the distal radius?* J Bone Joint Surg Br, 2011. 93(2): p. 145-50.

32. Cooney, W.P., *Management of Colles' fractures.* J Hand Surg Br, 1989. 14(2): p. 137-9.
33. Abbaszadegan, H., et al., *Prediction of instability of Colles' fractures.* Acta Orthop Scand, 1989. 60(6): p. 646-50.
34. Adolphson, P., et al., *Computer-assisted prediction of the instability of Colles' fractures.* Int Orthop, 1993. 17(1): p. 13-5.
35. Hove, L.M., et al., *Prediction of secondary displacement in Colles' fracture*. J Hand Surg Br, 1994. 19(6): p. 731-6.
36. Lafontaine, M., et al., *Stability assessment of distal radius fractures.* Injury, 1989. 20(4): p. 208-10.
37. Mackenney, P.J., et al., *Prediction of instability in distal radial fractures.* J Bone Joint Surg Am, 2006. 88(9): p. 1944-51.
38. Nesbitt, K.S., et al., *Assessment of instability factors in adult distal radius fractures.* J Hand Surg Am, 2004. 29(6): p. 1128-38.
39. Walenkamp, M.M., et al., *Predictors of unstable distal radius fractures: a systematic review and meta-analysis.* J Hand Surg Eur Vol, 2016. 41(5): p. 501-15.
40. Walenkamp, M.M.J., et al., *Prediction of Distal Radius Fracture Redisplacement: A Validation Study.* J Orthop Trauma, 2018. 32(3): p. e92-e96.
41. Duckworth, A.D., et al., *Scaphoid fracture epidemiology.* J Trauma Acute Care Surg, 2012. 72(2): p. E41-5.
42. Kozin, S.H., *Incidence, mechanism and natural history of scaphoid fractures*. Hand Clin, 2001. 17(4): p. 515-24.
43. van der Molen, A.B., et al., *Time off work due to scaphoid fractures and other carpal injuries in The Netherlands in the period 1990 to 1993.* J Hand Surg Br, 1999. 24(2): p. 193-8.
44. Wolfe, S.W.M.D., et al., *Fractures of the Carpal Bones.* Green's Operative Hand Surgery, 2017.
45. Schernberg, F., et al., *Anatomo-radiological study of fractures of the carpal scaphoid bone. Problems of abnormal callus.* Rev Chir Orthop Reparatrice Appar Mot, 1984. 70 Suppl 2: p. 55-63.
46. Cooney, W.P., et al., *Fractures of the scaphoid: a rational approach to management*. Clin Orthop Relat Res, 1980(149): p. 90-7.
47. Marsh, J.L., et al., *Fracture and dislocation classification compendium - 2007: Orthopaedic Trauma Association classification, database and outcomes committee*. J Orthop Trauma, 2007. 21(10 Suppl): p. S1-133.
48. Bohler, L., et al., *The results of treatment of 734 fresh, simple fractures of the scaphoid.* J Hand Surg Br, 2003. 28(4): p. 319-31.
49. Russe, O., *Fracture of the carpal navicular. Diagnosis, non-operative treatment and operative treatment*. J Bone Joint Surg Am, 1960. 42-a: p. 759-68.

50. McLaughlin, H.L. and Parkes, J.C., *Fracture of the carpal navicular (scaphoid) bone: gradations in therapy based upon pathology.* J Trauma, 1969. 9(4): p. 311-9.
51. Weber, E.R., *Biomechanical implications of scaphoid waist fractures.* Clin Orthop Relat Res, 1980(149): p. 83-9.
52. Herbert, T.J. and Fisher W.E., *Management of the fractured scaphoid using a new bone screw.* J Bone Joint Surg Br, 1984. 66(1): p. 114-23.
53. Lozano-Calderon, S., et al., *Diagnosis of scaphoid fracture displacement with radiography and computed tomography.* J Bone Joint Surg Am, 2006. 88(12): p. 2695-703.
54. Desai, V.V., et al., *The prognostic value and reproducibility of the radiological features of the fractured scaphoid.* J Hand Surg Br, 1999. 24(5): p. 586-90.
55. Wieschollek, S., et al., Handchir Mikrochir Plast Chir, 2018. 50(3): p. 169-173.
56. Temple, C.L., et al., *Comparison of sagittal computed tomography and plain film radiography in a scaphoid fracture model.* J Hand Surg Am, 2005. 30(3): p. 534-42.
57. Buijze, G.A., et al., *Training improves interobserver reliability for the diagnosis of scaphoid fracture displacement.* Clin Orthop Relat Res, 2012. 470(7): p. 2029-34.
58. Tiel-van Buul, M.M., et al., *Radiography and scintigraphy of suspected scaphoid fracture. A long-term study in 160 patients.* J Bone Joint Surg Br, 1993. 75(1): p. 61-5.
59. Divelbiss, B.J. and Adams, B.D., *Electrical and ultrasound stimulation for scaphoid fractures.* Hand Clin, 2001. 17(4): p. 697-701, x-xi.
60. Rajagopalan, B.M., et al., *Results of Herbert-screw fixation with bone-grafting for the treatment of nonunion of the scaphoid*. J Bone Joint Surg Am, 1999. 81(1): p. 48-52.
61. Dias, J.J. and Singh H.P., *Displaced fracture of the waist of the scaphoid*. J Bone Joint Surg Br, 2011. 93(11): p. 1433-9.
62. Jenkins, P.J., et al., *A comparative analysis of the accuracy, diagnostic uncertainty and cost of imaging modalities in suspected scaphoid fractures*. Injury, 2008. 39(7): p. 768-74.
63. Cheung, G.C., et al., *X-ray diagnosis of acute scaphoid fractures.* J Hand Surg Br, 2006. 31(1): p. 104-9.
64. Berger, R.A., *The anatomy of the scaphoid.* Hand Clin, 2001. 17(4): p. 525-32.
65. Bearcroft, P.W.P. and Hopper, M.A., *Imaging Techniques and Fundamental Observations for The Musculoskeletal System*. Grainger & Allison's Diagnostic Radiology, 2015.
66. Dorsay, T.A., et al., *Cost-effectiveness of immediate MR imaging versus traditional follow-up for revealing radiographically occult scaphoid fractures*. AJR Am J Roentgenol, 2001. 177(6): p. 1257-63.
67. Breitenseher, M.J., et al., *Radiographically occult scaphoid fractures: value of MR imaging in detection.* Radiology, 1997. 203(1): p. 245-50.

68. Harness, N.G., et al., *The influence of three-dimensional computed tomography reconstructions on the characterization and treatment of distal radial fractures.* J Bone Joint Surg Am, 2006. 88(6): p. 1315-1323.
69. Rozental, T.D., et al., *Evaluation of the sigmoid notch with computed tomography following intra-articular distal radius fracture.* The Journal of hand surgery, 2001. 26(2): p. 244-251.
70. Radon, J., *Uber die bestimmung von funktionen durch ihre integralwerte langs gewisser mannigfaltigkeiten.* Journal of Mathematical Physics, 1917. 69;262-277.
71. Hounsfield, G.N., *Computed Medical Imaging.* Science, 1980(7): p. 277-282.
72. Ilica, A.T., et al., *Diagnostic accuracy of multidetector computed tomography for patients with suspected scaphoid fractures and negative radiographic examinations*. Jpn J Radiol, 2011. 29(2): p. 98-103.
73. Buijze, G.A., et al., *Diagnostic performance of radiographs and computed tomography for displacement and instability of acute scaphoid waist fractures*. J Bone Joint Surg Am, 2012. 94(21): p. 1967-74.
74. Mallee, W.H., et al*., Computed tomography versus magnetic resonance imaging versus bone scintigraphy for clinically suspected scaphoid fractures in patients with negative plain radiographs.* Cochrane Database Syst Rev, 2015(6): p. Cd010023.
75. Rhemrev, S.J., et al*., Early computed tomography compared with bone scintigraphy in suspected scaphoid fractures.* Clin Nucl Med, 2010. 35(12): p. 931-4.
76. Panfili, E., et al., *Magnetic resonance imaging (MRI) artefacts in hip prostheses: a comparison of different prosthetic compositions.* Radiol Med, 2014. 119(2): p. 113-20.
77. Beeres, F.J., et al., *Early magnetic resonance imaging compared with bone scintigraphy in suspected scaphoid fractures.* J Bone Joint Surg Br, 2008. 90(9): p. 1205-9.
78. Buijze, G.A., et al., *Diagnostic performance tests for suspected scaphoid fractures differ with conventional and latent class analysis.* Clin Orthop Relat Res, 2011. 469(12): p. 3400-7.
79. de Zwart, A.D., et al., *Comparison of MRI, CT and bone scintigraphy for suspected scaphoid fractures.* Eur J Trauma Emerg Surg, 2016. 42(6): p. 725-731.
80. De Zwart, A.D., et al., *MRI as a reference standard for suspected scaphoid fractures*. Br J Radiol, 2012. 85(1016): p. 1098-101.
81. Yin, Z.G., et al., *Diagnosing suspected scaphoid fractures: a systematic review and meta-analysis.* Clin Orthop Relat Res, 2010. 468(3): p. 723-34.
82. McCready, R., Gnanasegaran, G. and Bomanji, J.B., *Bone Radionuclide Imaging, Quantitation and Bone Densitometry*. A History of Radionuclide Studies in the UK: 50th Anniversary of the British Nuclear Medicine Society, 2016.

83. Fogelman, I. and Boyle, I.T., *The bone scan in clinical practice.* Scott Med J, 1980. 25(1): p. 45-9.
84. Beeres, F.J., et al., *Observer variation in MRI for suspected scaphoid fractures*. Br J Radiol, 2008. 81(972): p. 950-4.
85. McCollough, C.H., et al., *Strategies for reducing radiation dose in CT*. Radiol Clin North Am, 2009. 47(1): p. 27-40.
86. MacNeil, J.A. and Boyd S.K., *Accuracy of high-resolution peripheral quantitative computed tomography for measurement of bone quality.* Med Eng Phys, 2007. 29(10): p. 1096-105.
87. Boutroy, S., et al., *In vivo assessment of trabecular bone microarchitecture by high-resolution peripheral quantitative computed tomography.* J Clin Endocrinol Metab, 2005. 90(12): p. 6508-15.
88. Macneil, J.A. and Boyd, S.K., *Bone strength at the distal radius can be estimated from high-resolution peripheral quantitative computed tomography and the finite element method.* Bone, 2008. 42(6): p. 1203-13.
89. Schneider, P., et al., *Bone quality parameters of the distal radius as assessed by pQCT in normal and fractured women.* Osteoporos Int, 2001. 12(8): p. 639-46.
90. Nickolas, T.L., et al., *High-resolution computed tomography imaging: a virtual bone biopsy.* Kidney Int, 2010. 77(11): p. 1046.
91. Krause, M., et al., *Accuracy of trabecular structure by HR-pQCT compared to gold standard muCT in the radius and tibia of patients with osteoporosis and long-term bisphosphonate therapy.* Osteoporos Int, 2014. 25(5): p. 1595-606.
92. Dalzell, N., et al., *Bone micro-architecture and determinants of strength in the radius and tibia: age-related changes in a population-based study of normal adults measured with high-resolution pQCT.* Osteoporos Int, 2009. 20(10): p. 1683-94.
93. Chapurlat, R.D. and Genant H.K., *Osteoporosis*. Endocrinology: Adult and Pediatric, 2016.
94. Pistoia, W., et al., *Estimation of distal radius failure load with micro-finite element analysis models based on three-dimensional peripheral quantitative computed tomography images.* Bone, 2002. 30(6): p. 842-8.
95. Pistoia, W., et al., *Image-based micro-finite-element modeling for improved distal radius strength diagnosis: moving from bench to bedside*. J Clin Densitom, 2004. 7(2): p. 153-60.
96. Varga, P., et al., *HR-pQCT based FE analysis of the most distal radius section provides an improved prediction of Colles' fracture load in vitro.* Bone, 2010. 47(5): p. 982-8.
97. Mueller, T.L., et al., *Computational finite element bone mechanics accurately predicts mechanical competence in the human radius of an elderly population.* Bone, 2011. 48(6): p. 1232-8.

98. Mueller, T.L., et al., *Non-invasive bone competence analysis by high-resolution pQCT: an in vitro reproducibility study on structural and mechanical properties at the human radius.* Bone, 2009. 44(2): p. 364-71.
99. van Rietbergen, B. and Ito K., *A survey of micro-finite element analysis for clinical assessment of bone strength: the first decade*. J Biomech, 2015. 48(5): p. 832-41.
100. Samelson, E.J., et al., *Cortical and trabecular bone microarchitecture as an independent predictor of incident fracture risk in older women and men in the Bone Microarchitecture International Consortium (BoMIC): a prospective study.* Lancet Diabetes Endocrinol, 2019. 7(1): p. 34-43.
101. Burghardt, A.J., et al., *A longitudinal HR-pQCT study of alendronate treatment in postmenopausal women with low bone density: Relations among density, cortical and trabecular microarchitecture, biomechanics and bone turnover.* J Bone Miner Res, 2010. 25(12): p. 2558-71.
102. Folkesson, J., et al., *Longitudinal evaluation of the effects of alendronate on MRI bone microarchitecture in postmenopausal osteopenic women.* Bone, 2011. 48(3): p. 611-21.
103. de Jong, J.J., et al*., Assessment of the healing process in distal radius fractures by high resolution peripheral quantitative computed tomography.* Bone, 2014. 64: p. 65-74.
104. de Jong, J.J.A., et al*., Fracture Repair in the Distal Radius in Postmenopausal Women: A Follow-Up 2 Years Postfracture Using HRpQCT.* J Bone Miner Res, 2016. 31(5): p. 1114-22.
105. Heyer, F.L., et al., *Long-term functional outcome of distal radius fractures is associated with early post-fracture bone stiffness of the fracture region: An HR-pQCT exploratory study.* Bone, 2019. 127: p. 510-516.
106. Burghardt, A.J., et al., *Quantitative in vivo HR-pQCT imaging of 3D wrist and metacarpophalangeal joint space width in rheumatoid arthritis.* Ann Biomed Eng, 2013. 41(12): p. 2553-64.
107. Fouque-Aubert, A., et al., *Assessment of hand bone loss in rheumatoid arthritis by high-resolution peripheral quantitative CT*. Ann Rheum Dis, 2010. 69(9): p. 1671-6.
108. Peters, M., et al*., Assessment of Cortical Interruptions in the Finger Joints of Patients With Rheumatoid Arthritis Using HR-pQCT, Radiography and MRI*. J Bone Miner Res, 2018. 33(9): p. 1676-1685.
109. Stach, C.M., et al., *Periarticular bone structure in rheumatoid arthritis patients and healthy individuals assessed by high-resolution computed tomography.* Arthritis Rheum, 2010. 62(2): p. 330-9.
110. Lee, C.H., et al., *Correlation of structural abnormalities of the wrist and metacarpophalangeal joints evaluated by high-resolution peripheral quantitative computed tomography, 3 Tesla magnetic resonance imaging and conventional radiographs in rheumatoid arthritis*. Int J Rheum Dis, 2015. 18(6): p. 628-39.

111. Finzel, S., et al., *A detailed comparative study of high-resolution ultrasound and micro-computed tomography for detection of arthritic bone erosions.* Arthritis Rheum, 2011. 63(5): p. 1231-6.
112. Albrecht, A., et al., *The structural basis of MRI bone erosions: an assessment by microCT*. Ann Rheum Dis, 2013. 72(8): p. 1351-7.
113. Scharmga, A., et al., *Visual detection of cortical breaks in hand joints: reliability and validity of high-resolution peripheral quantitative CT compared to microCT.* BMC Musculoskelet Disord, 2016. 17: p. 271.
114. Peters, M., et al., *An automated algorithm for the detection of cortical interruptions on high resolution peripheral quantitative computed tomography images of finger joints.* PLoS One, 2017. 12(4): p. e0175829.
115. Clayton, R.A., et al*., Association between decreased bone mineral density and severity of distal radial fractures*. J Bone Joint Surg Am, 2009. 91(3): p. 613-9.
116. Dhainaut, A., et al., *Exploring the relationship between bone density and severity of distal radius fragility fracture in women.* J Orthop Surg Res, 2014. 9: p. 57.
117. de Klerk, G., J. et al., *The relation between AO-classification of distal radial fractures and bone mineral density.* Injury, 2013. 44(11): p. 1657-8.
118. Bleibler, F., et al., *The health burden and costs of incident fractures attributable to osteoporosis from 2010 to 2050 in Germany--a demographic simulation model.* Osteoporos Int, 2013. 24(3): p. 835-47.
119. Robin, B.N., et al., *Relationship of bone mineral density of spine and femoral neck to distal radius fracture stability in patients over 65.* J Hand Surg Am, 2014. 39(5): p. 861-6.e3.
120. Adey, L., et al., *Computed tomography of suspected scaphoid fractures.* J Hand Surg Am, 2007. 32(1): p. 61-6.
121. Ring, D. and Lozano-Calderon S., *Imaging for suspected scaphoid fracture*. J Hand Surg Am, 2008. 33(6): p. 954-7.
122. Rhemrev, S.J., et al., *Clinical prediction rule for suspected scaphoid fractures: A prospective cohort study*. Injury, 2010. 41(10): p. 1026-30.
123. Carpenter, C.R., et al., *Adult scaphoid fracture.* Acad Emerg Med, 2014. 21(2): p. 101-21.
124. Mallee, W.H., et al., *Clinical diagnostic evaluation for scaphoid fractures: a systematic review and meta-analysis.* J Hand Surg Am, 2014. 39(9): p. 1683-1691.e2.
125. Karl, J.W., et al., *Diagnosis of Occult Scaphoid Fractures: A Cost-Effectiveness Analysis.* J Bone Joint Surg Am, 2015. 97(22): p. 1860-8.
126. Memarsadeghi, M., et al., *Occult scaphoid fractures: comparison of multidetector CT and MR imaging--initial experience*. Radiology, 2006. 240(1): p. 169-76.
127. Rhemrev, S.J., et al., *Current methods of diagnosis and treatment of scaphoid fractures.* Int J Emerg Med, 2011. 4: p. 4.

128. Gemme, S. and Tubbs R., *What physical examination findings and diagnostic imaging modalities are most useful in the diagnosis of scaphoid fractures?* Ann Emerg Med, 2015. 65(3): p. 308-9.
129. Groves, A.M., et al., *An international survey of hospital practice in the imaging of acute scaphoid trauma.* AJR Am J Roentgenol, 2006. 187(6): p. 1453-6.

Bone microarchitecture and distal radius fracture pattern complexity

A.M. Daniels, L.M.A. Theelen, C.E. Wyers, H.M.J. Janzing, B. van Rietbergen, L. Vranken, R.Y. van der Velde, P.P.M.M. Geusens, S. Kaarsemaker, M. Poeze, J.P. van den Bergh

J Orthop Res. 2019; 37(8):1690–1697

Abstract

Background
Distal radius fractures (DRFs) occur in various complexity patterns among patients differing in age, gender and bone mineral density (BMD). Our aim was to investigate the association of patient characteristics, BMD, bone microarchitecture and bone strength with the pattern complexity of DRFs.

Methods
In this study, 251 patients aged 50-90 years with a radiologically confirmed DRF who attended the Fracture Liaison Service of VieCuri Medical Centre, the Netherlands, between November 2013 and June 2016 were included. In all patients fracture risk factors and underlying metabolic disorders were evaluated and BMD measurement with vertebral fractures assessment by dual-energy X-ray absorptiometry was performed. Radiographs of all DRFs were reviewed by two independent investigators to assess fracture pattern complexity according to the AO/OTA classification in extra-articular (A), partially articular (B) and complete articular (C) fractures. For this study, patients with A and C fractures were compared. Seventy-one patients were additionally assessed by high-resolution peripheral quantitative CT.

Results
Compared to group A, the mean age, proportion of males and current smokers were higher in group C, but BMD and prevalent vertebral fractures were not different. In univariate analyses, age, male gender, trabecular area and volumetric BMD (vBMD) and stiffness were associated with type C fractures. In multivariate analyses, only male gender (OR 8.48 [95% CI 1.75-41.18, p=0.008]) and age (OR 1.11 [95% CI 1.03-1.19, p=0.007]) were significantly associated with DRF pattern complexity.

Conclusion
In conclusion, our data demonstrate that age and gender, but not BMI, BMD, bone microarchitecture or strength were associated with pattern complexity of DRFs.

Introduction

Fracture patterns of the distal radius are commonly complex in middle-aged and elderly women, which is related to worse functional outcome. Pattern complexity of DRFs can be assessed using a classification system such as the AO/OTA classification. It is hypothesized that bone microarchitecture and strength are associated with the pattern complexity of the fracture[1-8]. Decreased bone mineral density (BMD) has been described as a contributor to the peak in incidence rates of distal radius fractures (DRFs) at the age of 50-60 years [3,4,7,9-11]. Clayton et al. (2009) found a non-significant trend towards a higher BMD in partially articular (B) and complete articular (C) fractures compared to complete extra-articular (A) fractures [6]. Several other studies reported no significant difference in mean BMD between extra-articular and complete articular fractures [3,7,8]. However, assessment of bone microarchitecture and separate assessment of trabecular and cortical bone is not feasible with bone densitometry. Computed tomography (CT) has been used to assess trabecular and cortical bone, but visualization of trabecular and cortical bone requires spatial resolutions of less than 200 µm [12-14]. More recently, a non-invasive method for the assessment of bone microarchitecture at the distal radius and tibia using high resolution peripheral quantitative CT (HR-pQCT) has become available [15-18].

To the best of our knowledge, there are no previous studies regarding the association of DRF pattern complexity with bone microarchitecture and strength assessed by HR-pQCT at the distal radius and tibia. In addition, since most studies on DRF pattern complexity contain only female patients, the impact of gender is not yet extensively examined [3,6]. The aim of this study was to investigate the associations of patient characteristics, BMD (measured by DXA and HR-pQCT), bone microarchitecture and calculated bone strength (by HR-pQCT) with the pattern complexity of DRFs.

Methods

Study population

A cross-sectional cohort study (level of evidence: III) was conducted among patients with a recent DRF. All men and women aged 50-90 years with a clinical fracture who attended the Fracture Liaison Service (FLS) of VieCuri Medical Centre, Venlo, The Netherlands between November 2013 and June 2016 were identified. Patients with fractures as result of high energy trauma, patients with open fractures, osteomyelitis and bone metastasis were excluded. A total of 251 patients with a radiologically confirmed DRF were included for this study. At the FLS, patients received a detailed evaluation according to the Dutch guideline for treatment of osteoporosis. The evaluation consisted of a questionnaire assessing risk factors for falls, fracture risk, medical history including medication use and daily dietary calcium intake. Additionally, blood samples were collected to identify metabolic disorders and a DXA measurement with vertebral fracture assessment (VFA) was performed. If indicated, anti-osteoporosis treatment or treatment of newly diagnosed metabolic bone disorders was initiated according to current guidelines [19].

Of the 251 patients with a DRF included in this study, 71 participated in an observational three-year follow-up study at the FLS ("Prospective evaluation of bone strength, physical activity, falls, subsequent fractures and mortality in patients presenting with a recent clinical fracture"). This study is approved by the Medical Ethics Committee (NL 45707.072.13) of Maastricht University. In that study patients consented with HR-pQCT measurements of the distal radius and tibia and the baseline data are used for the HR-pQCT part of the current study.

Assessment of fracture pattern complexity

DRFs were classified based on severity of comminution, displacement, involvement of the radioulnar or radiocarpal joint and associated lesions (for example ulnar styloid fracture) according the AO/OTA classification system, which has a strong intra-observer reliability [20-22]. DRFs were classified into three main types and each main type was then divided into nine subtypes [Figure 1].

Figure 1. AO/OTA classification for distal radius fractures. Copyright by AO/OTA Foundation, Switzerland

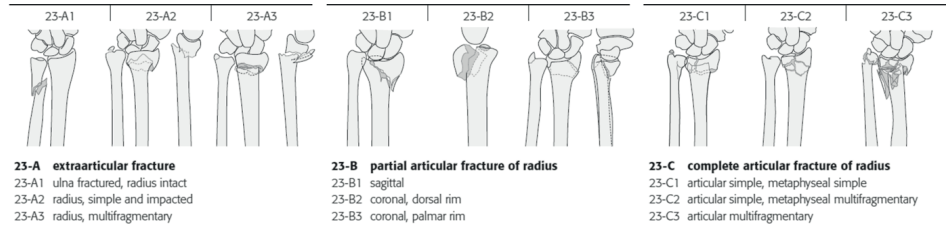

Plain radiographs were used to classify the fractures. Two investigators independently classified all fractures by type and subtype according to the AO/OTA classification [23]. In 200 patients, there was agreement between the investigators. Assessment by a third independent investigator resulted in agreement on another 47 fractures. For the remaining four fractures conformity was reached by all three investigators in a consensus meeting. For this study, type B fractures were not included in the analysis because we aimed to compare the complete extra-articular fractures (type A) to the complete articular fractures (type C).

DXA

Two-dimensional BMD was measured at the lumbar spine (LS; L1-L4), total hip (TH) and femoral neck (FN) using DXA (Hologic QDR 4500, Hologic Inc., Bedford, MA, USA). BMD measurements were categorized according to the WHO criteria [24] based on the lowest T-score at the LS, TH or FN into normal BMD (T-score ≥ -1), osteopenia (T-score between -1 and -2.5) and osteoporosis (T-score ≤ -2.5).

VFA

Vertebral fractures assessment was performed on the DXA lateral spine images using quantitative morphometric assessment of vertebral height. The method described by Genant et al. was used to classify the severity of vertebral fractures (VF); grade 1 (mild fracture, with vertebral height loss of 20-25%), grade 2 (moderate fracture with height loss of 25-40%) and grade 3 (severe fracture with height loss > 40%) [25].

HR-pQCTThe non-fractured radius and ipsilateral tibia of the patients were scanned using the second generation HR-pQCT (XtremeCT II; Scanco Medical AG, Brüttisellen, Switzerland). Images were evaluated using the standard manufacturer protocol (effective energy of 68 kVp, tube current of 1470 µA and 43 ms integration time) [26]. A standard phantom was scanned daily for quality control. The patients' forearm and lower leg were placed into an anatomically

formed fiber cast to obtain a standardized position. Based on a scout view of the forearm and lower leg, the region of interest was determined and a reference line was placed on the joint surface of the distal radius and tibia. The area to be scanned starts 9.0 mm proximally to the reference line and ends 1.2 mm distally to the reference line. Images were reconstructed using an isotropic voxel size of 61 µm, resulting in 168 consecutive slices. Motion-induced degradation of the images was graded according to the manufacturer protocol and the method of Pialat et al. [27]. Scans with grade 1-3, referring to high to moderate quality, were accepted for analysis, scans with grade 4-5 (bad quality) had to be repeated with a maximum of two extra scans.Images were processed according to the manufacturer's standard protocol [26]. The following parameters were analyzed: total, trabecular and cortical bone area [cm^2], volumetric bone mineral density for the total [$mgHA/cm^3$], trabecular [$mgHA/cm^3$] and cortical [$mgHA/cm^3$] compartment, trabecular bone volume fraction, trabecular number [mm-1], trabecular thickness [mm], trabecular separation [mm], cortical thickness [mm], cortical perimeter [mm], cortical porosity [%] and cortical pore diameter [mm]. In addition, micro-finite element (micro-FE) analyses were generated by directly converting bone voxels in the segmented image to brick elements [28-30]. Elements were assigned a Young's modulus of 10 GPa and a Poisson's ratio of 0.3 and for each model, four tests were simulated [31].The first load case represented a 'high friction' compression test with a prescribed displacement in the axial direction of 1% of the total length, from which the compression stiffness [kN/mm] as well as the estimated strength was calculated [32-34]. The second load case represented a prescribed rotation of 0.01 rad around the longitudinal axis from which the torsional stiffness [kNmm/rad] was calculated. A third and fourth load case represented a prescribed rotation of 0.01 radian applied around the sagittal and transversal axes respectively, thus inducing a state of pure bending in two directions, from which the bending stiffness in each direction was calculated. These 4 load cases were included to test if the fracture type is associated with a reduced stiffness in a specific loading direction.

Statistical analysis

Data analysis was performed using IBM SPSS Statistics, version 24 (IBM Corporation 1989, 2016). Normal distribution was tested using Q-Q plots and the Kolmogorov-Smirnov test. Data are presented as mean with standard deviations (SD) or as median and interquartile range, depending on their distribution. Chi-square tests and ANOVA were used to analyze differences between the main types AO/OTA (A/B/C). In further analysis complete extra-articular fractures (type A) and complete articular fractures (type C) were compared. Independent samples t-tests were used to compare bone microarchitecture and strength assessed by HR-pQCT between both groups. Logistic regression analysis was used to investigate the independent association between the fracture pattern complexity (type C vs type A) and baseline characteristics. Univariate analyses were conducted for gender, age, osteopenia, osteoporosis, vertebral fractures (grade 2/3), smoking, alcohol use and all standardized scores (z-scores) of the HR-pQCT variables for both the HR-pQCT radius group (N=55) and HR-pQCT tibia group (N=63). Multivariate analyses were conducted with adjustment for age and gender for HR-pQCT variables at the distal tibia and radius. The significance level was set as α=0.05.

Results

Patient characteristics

In this cohort study 251 patients with a DRF visited the FLS. In total 38 men (15%) and 213 women (85%) with a mean age of 67 years (SD ± 9). According to the AO/OTA classification 131 fractures (52%) were classified as extra-articular (type A) fractures, 36 as partial articular (type B) fractures (14%) and 84 as complete articular (type C) fractures (34%). Overall, there was no difference in patient characteristics between the three groups except for age (p=0.034). Based on the T-scores, 93 patients (37%) had osteoporosis, 120 (48%) osteopenia and 38 patients (15%) had a normal BMD [Table 1]. Patients in the group with type C fractures (N=84) were older (median age 68.0 [IQR 14] versus 66.0 [IQR 16] years, p=0.043) and the proportion of males and was higher (18 (21%) versus 14 (11%), p=0.031) compared to patients with type A fractures (N=131). There were no differences for BMI, BMD, number and severity of vertebral fractures, smoking, alcohol intake and 25(OH)vitamin D.

Table 1. Characteristics of 251 patients with type A, B and C distal radius fractures according to the AO/OTA classification

	AO/OTA A	AO/OTA B	AO/OTA C	p-value
	N=131	N=36	N=84	
Female	117 (89)	30 (83)	66 (79)	*NS*
Age (y)*	66.0 [16]	70.5 [14]	68.0 [14]	0.034
Weight (kg)*	69.9 [23.9]	75.4 [21.7]	72.3 [19.6]	*NS*
Height (m)	1.63 ± 0.07	1.64 ± 0.09	1.64 ± 0.08	*NS*
BMI (kg/m^2)*	25.5 [6.8]	28.0 [7.9]	27.1 [7.3]	*NS*
BMI category				*NS*
<30 kg/m^2 (non-obese)	95 (77.9)	21 (63.6)	49 (71.0)	
>30 kg/m^2 (obese)	27 (22.1)	12 (36.4)	20 (29.0)	
Bone mineral density				*NS*
Normal BMD	18 (13.7)	4 (11.1)	16 (19.0)	
Osteopenia	66 (50.4)	15 (41.7)	39 (46.4)	
Osteoporosis	47 (35.9)	17 (47.2)	29 (34.5)	
Vertebral fracture assessment				*NS*
No Grade 2/3 Fx	116 (88.5)	29 (80.6)	76 (90.5)	
1Grade 2/3 Fx	15 (11.5)	7 (19.4)	8 (9.5)	
Smoking				*NS*
Never	49 (38.6)	20 (55.6)	38 (46.3)	
Past smoker	57 (44.9)	12 (33.3)	35 (42.7)	
Current smoker	21 (16.5)	4 (11.1)	9 (11.0)	
Alcohol intake				*NS*
< 1 unit /day	98 (77.2)	30 (85.7)	59 (73.8)	
≥ 1 unit / day	29 (22.8)	5 (14.3)	21 (26.3)	
Calcium intake (mg/day)*	780.0 [320]	785.5 [557]	844.5 [473]	*NS*
25-OH Vitamin D(nmol/l)				*NS*
<30 (deficiency)	14 (10.7)	3 (8.3)	9 (10.7)	
30-50 (insufficiency)	37 (28.2)	10 (27.8)	27 (32.1)	
>50 (sufficiency)	80 (61.1)	23 (63.9)	48 (57.1)	

BMI=body mass index | BMD=bone mineral density | Fx=fracture | NS=not significantData missing: length (26), weight (26), calcium intake (6), alcohol intake (9), smoking (6)Normally distributed data are presented as mean (SD) | Non-normally distributed data * as median [IQR]

HR-pQCT analyses

In a subset of 71 patients, HR-pQCT scans were performed. HR-pQCT of the distal radius was conducted in 63 out of 71 patients; eight patients could not undergo HR-pQCT due to a current or previous bilateral DRF. Of those scans, 61 were graded as high to moderate quality (grade 1-3). Two scans had a poor quality (grade 4/5) and therefore not included in the analysis. HR-pQCT of the tibia was conducted in 71 patients; all scans were graded as high to moderate quality and included in the analysis. Eight patients had a type B DRF and were therefore not included in this analysis. This resulted in a subset of 63 patients with type A or C DRFs assessed with HR-pQCT. Patients with type C DRFs (N=22) were significantly older (69 vs. 64 years, p=0.009) and more frequent of male gender (36% vs. 10%, p=0.017) compared to patients with type A DRF (N=41). Exploration of men and women separately revealed that both women (N=14) and men (N=8) with type C DRF were older than those (women N=37, men N=4) with type A DRF (mean difference of seven years for women and eight years for men). All other parameters were not different between groups, except for a higher proportion of past smokers in patients with type C DRF [Table S-1].

Univariate analyses in the HR-pQCT group are presented in table 2 and 3, for distal tibia (N=63) and radius (N=55) respectively. There was a significant association of age, male gender, total area, trabecular area and vBMD, trabecular bone volume fraction, trabecular thickness (only at the distal radius) and cortical perimeter at the distal radius and tibia with DRF type C versus A. In addition, compression and torsion stiffness at the distal tibia and bending stiffness at the distal radius and tibia were also significantly associated with DRF pattern complexity. After adjustment for age alone, almost all univariate associations for HR-pQCT parameters at the distal tibia and radius remained significant, while after adjustment for gender alone, none of the HR-pQCT parameters was associated with DRF pattern complexity anymore [Table 2 and Table 3]. Results of the age adjusted analysis of the female subgroup are analogous to the analyses for the total cohort, with no association of HR-pQCT parameters at the distal tibia (N=51) and distal radius (N=43) [Table S-5 and S-6]. In the model with adjustment for gender and age, both male gender (OR 8.48 [95% CI 1.75-41.18, p=0.008]) and age (OR per year 1.11 [95% CI 1.03-1.19, p=0.007]) were significantly associated with DRF type C vs A, but no significant associations were found for any HR-pQCT parameters at the tibia or radius.

Table 2. Associations with fracture pattern complexity (type C vs type A) in 63 patients with a HR-pQCT at the distal tibia

	Odds ratio Unadjusted	**p-value**	**Odds ratio** Age adjusted	**p-value**	**Odds ratio** Gender adjusted	**p-value**	**Odds ratio** Age & gender adjusted	**p-value**
Gender (M vs F)	5.29 (1.37-20.36)	**0.016**	-	-	-	-	8.48 (1.75-41.18)	**0.008**
Age (per year)	1.09 (1.02-1.16)	**0.014**	-	-	-	-	1.11 (1.03-1.19)	**0.007**
Osteopenia	0.38 (0.10-1.50)	0.168	-	-	-	-	-	-
Osteoporosis	0.69 (0.19-2.54)	0.572	-	-	-	-	-	-
Vfx (grade 2/3 vs no Vfx)	0.60 (0.06-6.17)	0.670	-	-	-	-	-	-
Smoking past	1.75 (0.58-5.32)	0.324	-	-	-	-	-	-
Alcohol (≥1 vs 0/1)	2.40 (0.59-9.76)	0.220	-	-	-	-	-	-
Total area	1.87 (1.07-3.29)	**0.028**	1.85 (1.02-3.35)	**0.042**	1.40 (0.70-2.81)	0.344	1.20 (0.56-2.56)	0.637
Trabecular area	1.85 (1.05-3.27)	**0.034**	1.71 (0.95-3.10)	0.074	1.42 (0.74-2.74)	0.293	1.45 (0.56-2.34)	0.711
Cortical area	1.28 (0.74-2.20)	0.383	1.99 (0.99-4.03)	0.054	0.71 (0.34-1.48)	0.359	1.18 (0.49-2.84)	0.711
Total vBMD	1.09 (0.64-1.86)	0.758	1.40 (0.76-2.56)	0.277	0.88 (0.48-1.59)	0.660	1.14 (0.59-2.20)	0.699
Trabecular vBMD	1.78 (1.01-3.13)	**0.047**	1.81 (1.00-3.27)	0.050	1.47 (0.80-2.71)	0.212	1.47 (0.76-2.80)	0.237
Cortical vBMD	0.81 (0.47-1.40)	0.452	1.23 (0.63-2.42)	0.549	0.66 (0.36-1.20)	0.170	0.99 (0.49-2.02)	0.993
Trabecular BV fraction	1.80 (1.03-3.14)	**0.039**	1.80 (1.00-3.22)	**0.048**	1.51 (0.83-2.74)	0.177	1.48 (0.79-2.77)	0.223
Trabecular thickness	1.15 (0.68-1.95)	0.602	1.13 (0.64-2.00)	0.677	1.23 (0.70-2.15)	0.478	1.22 (0.66-2.27)	0.533
Trabecular separation	0.55 (0.24-1.24)	0.148	0.51 (0.22-1.18)	0.116	0.69 (0.30-1.57)	0.375	0.63 (0.26-1.50)	0.292
Cortical perimeter	1.98 (1.10-3.57)	**0.022**	1.92 (1.04-3.57)	**0.039**	1.49 (0.73-3.08)	0.277	1,23 (0.57-2.67)	0.596
Cortical porosity	0.85 (0.48-1.51)	0.583	0.73 (0.38-1.42)	0.353	0.94 (0.51-1.71)	0.828	0.81 (0.40-1.62)	0.547
Cortical thickness	0.93 (0.53-1.60)	0.784	1.33 (0.70-2.50)	0.386	0.70 (0.38-1.31)	0.262	1.02 (0.50-2.05)	0.964
Cortical pore diameter	0.54 (0.27-1.06)	0.073	0.64 (0.32-1.30)	0.214	0.47 (0.22-1.02)	0.056	0.60 (0.28-1.31)	0.199
Torsion stiffness	1.94 (1.11-3.38)	**0.020**	2.55 (1.27-5.15)	**0.009**	1.39 (0.55-3.53)	0.490	1.84 (0.65-5.25)	0.252
	Odds ratio Unadjusted	**p-value**	**Odds ratio** Age adjusted	**p-value**	**Odds ratio** Gender adjusted	**p-value**	**Odds ratio** Age & gender adjusted	**p-value**
Compression stiffness	1.78 (1.03-3.09)	**0.039**	2.29 (1.20-4.39)	**0.013**	1.23 (0.58-2.61)	0.585	1.60 (0.71-3.60)	0.259
Compression ultimate force	0.52 (0.30-0.89)	**0.017**	0.54 (0.31-0.96)	**0.034**	0.68 (0.34-1.36)	0.272	0.89 (0.42-1.91)	0.767
Bending stiffness horizontal	2.08 (1.17-3.70)	**0.013**	2.60 (1.29-5.24)	**0.007**	1.66 (0.71-3.87)	0.243	1.96 (0.76-5.01)	0.162
Bending stiffness vertical	1.79 (1.05-3.07)	**0.034**	2.21 (1.15-4.21)	**0.017**	1.13 (0.44-2.86)	0.803	1.34 (0.49-3.67)	0.563

Odds ratio for DRF type C versus type A are presented per standard deviation with confidence interval (CI) | Vfx=vertebral fracture | vBMD=volumetric bone mineral density

Table 3. Associations with fracture pattern complexity (type C vs type A) in 55 patients with a HR-pQCT at the distal radius

	Odds ratio Unadjusted	**p-value**	**Odds ratio** Age adjusted	**p-value**	**Odds ratio** Gender adjusted	**p-value**	**Odds ratio** Age & gender adjusted	**p-value**
Gender (M vs F)	5.17 (1.31-20.40)	**0.019**	-	-	-	-	8.84 (1.72-45.42)	**0.009**
Age (per year)	1.08 (1.01-1.16)	**0.019**	-	-	-	-	1.11 (1.03-1.19)	**0.008**
Osteopenia	0.49 (0.12-0.20)	0.316	-	-	-	-	-	-
Osteoporosis	0.62 (0.18-2.42)	0.487	-	-	-	-	-	-
Vfx grade 2/3 vs no Vfx	0.87 (0.07-10.23)	0.911	-	-	-	-	-	-
Smoking past	1.86 (0.55-6.33)	0.316	-	-	-	-	-	-
Alcohol (≥1 vs 0/1)	1.47 (0.33-6.47)	0.611	-	-	-	-	-	-
Total area	1.88 (1.07-3.31)	**0.029**	2.03 (1.10-3.76)	**0.025**	1.26 (0.48-3.35)	0.638	1.04 (0.36-2.97)	0.949
Trabecular area	1.98 (1.11-3.56)	**0.022**	1.99 (1.09-3.65)	**0.026**	1.48 (0.63-3.52)	0.371	1.12 (0.45-2.81)	0.804
Cortical area	1.48 (0.84-2.60)	0.178	1.92 (0.98-3.75)	0.057	0.85 (0.39-1.86)	0.690	1.06 (0.46-2.47)	0.890
Total vBMD	1.06 (0.60-1.85)	0.850	1.34 (0.72-2.49)	0.363	0.88 (0.48-1.63)	0.682	1.12 (0.58-2.18)	0.731
Trabecular vBMD	1.95 (1.05-3.63)	**0.036**	2.18 (1.12-4.25)	**0.021**	1.47 (0.71-3.04)	0.295	1.59 (0.75-3.38)	0.226
Cortical vBMD	0.68 (0.37-1.22)	0.197	0.83 (0.43-1.59)	0.573	0.73 (0.39-1.38)	0.333	0.97 (0.49-1.93)	0.937
Trabecular BV fraction	2.15 (1.14-4.04)	**0.018**	2.33 (1.19-4.59)	**0.014**	1.68 (0.78-3.54)	0.171	1.69 (0.78-3.67)	0.188
Trabecular thickness	1.98 (1.08-3.62)	**0.027**	1.77 (0.94-3.34)	0.080	1.65 (0.86-3.15)	0.133	1.28 (0.63-2.61)	0.500
Trabecular separation	0.82 (0.46-1.46)	0.490	0.65 (0.36-1.19)	0.164	1.09 (0.60-2.00)	0.772	0.82 (0.43-1.58)	0.557
Cortical perimeter	1.99 (1.11-3.57)	**0.020**	1.95 (1.05-3.62)	**0.034**	1.49 (0.66-3.39)	0.342	1.07 (0.44-2.61)	0.882
Cortical porosity	1.13 (0.63-2.04)	0.683	1.16 (0.60-2.24)	0.663	0.99 (0.52-1.89)	0.978	0.98 (0.46-2.10)	0.958
Cortical thickness	1.12 (0.64-1.95)	0.700	1.49 (0.78-2.86)	0.229	0.86 (0.46-1.61)	0.639	1.11 (0.57-2.19)	0.758
Cortical pore diameter	0.79 (0.40-1.53)	0.474	0.74 (0.34-1.60)	0.443	0.87 (0.43-1.74)	0.686	0.84 (0.36-2.01)	0.701
	Odds ratio Unadjusted	**p-value**	**Odds ratio** Age adjusted	**p-value**	**Odds ratio** Gender adjusted	**p-value**	**Odds ratio** Age & gender adjusted	**p-value**
Torsion stiffness	1.79 (0.99-3.25)	0.056	2.50 (1.19-5.24)	**0.015**	0.99 (0.36-2.77)	0.998	1.47 (0.41-5.21)	0.552
Compression stiffness	1.50 (0.85-2.64)	0.162	2.11 (1.04-4.29)	0.039	0.91 (0.42-1.96)	0.804	1.24 (0.49-3.13)	0.654
Compression ultimate force	1.55 (0.87-2.74)	0.134	2.22 (1.08-4.56)	**0.031**	0.95 (0.44-2.07)	0.905	1.33 (0.52-3.46)	0.553
Bending stiffness horizontal	1.54 (0.88-2.69)	0.130	2.08 (1.05-4.10)	**0.036**	0.74 (0.29-1.91)	0.534	0.96 (0.31-2.98)	0.946
Bending stiffness vertical	2.19 (1.13-4.25)	**0.020**	3.01 (1.32-6.87)	**0.009**	1.69 (0.56-5.05)	0.349	2.37 (0.60-9.26)	0.216

Odds ratio for DRF type C versus type A are presented per standard deviation with confidence interval (CI) | Vfx=vertebral fracture | vBMD=volumetric bone mineral density

Discussion

We observed that patients with type C (complete articular) DRFs were significantly older and more frequently of male gender compared to patients with a type A (extra-articular) DRF, but there was no difference in BMI, BMD, number and severity of prevalent vertebral fractures, smoking, alcohol intake and 25(OH) vitamin D levels.

In the unadjusted HR-pQCT analyses, fracture pattern complexity (type C versus A fractures) was significantly associated with age, male gender, total trabecular area and vBMD and stiffness parameters. However, in the fully adjusted model DRF pattern complexity was significantly associated with age and male gender, but not with any of the other parameters. These findings imply that bone characteristics, such as BMD, VF status, bone microarchitecture and strength are not independently associated with DRF pattern complexity.

In previous studies, it was reported that the prevalence of osteoporosis in patients with DRFs was high compared with prevalence in control subjects and that osteoporosis was a risk factor for DRFs in in both men and women [4,5]. With regard to the severity or complexity of DRFs, literature is sparse and the methods applied varied. Dhainaut et al. reported a weak association between cortical hand BMD by digital X-ray radiogrammetry and increased ulnar variance and dorsal angle, but no association of BMD with the AO scoring system for fracture type [3]. Itoh et al. reported no significant difference in the mean BMD, measured by DXA at the distal radius and the fracture pattern, which was classified according to a modification of Frykman's system [7]. Although the findings in these studies are in line with our study, it is difficult to compare studies due to differences in BMD measurement techniques, location of measurement and DRF classification system.

Clayton et al. found a trend towards a higher BMD in patients with AO/OTA type B and C fractures compared to type A fractures [6], which is in contrast to our study. However, they did not directly compare group C versus A and BMD was only measured at the total hip, not at the femoral neck and lumbar spine as we did in our study. In a limited report, de Klerk et al. found no correlation between the AO-classification of DRFs and BMD, measured at the hip and lumbar spine, which is in line with our findings [8]. Rozental et al. (2013) reported a significantly lower total and trabecular vBMD and trabecular separation, measured by HR-pQCT, at the distal radius and tibia in premenopausal women with a DRF compared to those without a fracture [2]. However, the association of other characteristics, such as prevalent vertebral fractures, vitamin D levels and bone microarchitecture and strength assessed by HR-pQCT, with DRF pattern complexity was not studied up till now.

Based on the findings in this study, it is important to note that risk factors known to be associated with fracture risk, such as BMI, osteoporosis, number and severity of prevalent vertebral fractures, smoking and alcohol use are not associated with DRF pattern complexity. In the univariate model age, male gender and mainly trabecular microarchitectural parameters as well as compression, torsion and bending stiffness especially at the distal tibia were associated with DRF pattern complexity. The finding that bone microarchitectural and stiffness parameters were univariate associated with the more complex (type C) DRFs, but not after adjustment for age and gender can be explained by the fact that men and older patients have larger bones, with greater cortical perimeter, trabecular and total area and trabecular vBMD and higher stiffness [35-38].

Our study has limitations. First, we used the AO/OTA classification, which is only one of many fracture classification systems such as the universal system, the Fernandez classification, the Frykman classification and the Melone classification [20,22,39-41]. Unfortunately, none of these classification methods has perfect reproducibility [10,21,39,40]. In contrast to the other classification systems; a strong intra- and inter-observer reliability was reported for the AO/OTA classification when focusing on the main type only (A – extra-articular, B – partly articular, C – complete articular) [20-22]. In line with this, we had a consensus rate of 79.7% after classification by two independent investigators and the distribution of the main types of DRFs correlates with previous published papers [3,9,42]. Second, we studied a selection of patients that presented at the emergency department (ED) of our hospital with a DRF because assessment of BMD, VFA and HR-pQCT was only possible in FLS attenders. Third, not all of the patients in our study had a HR-pQCT measurement due to the retrospective design of our study. However, there was no difference between the HR-pQCT group and non-HR-pQCT group (except for alcohol intake) [Table S-2], hence we believe that the results in this study are representative for the total cohort of patients with a DRF. Fourth, the number of patients with type C fractures in the HR-pQCT analyses was relatively low, resulting in large confidence intervals in some of the analyses. In addition, we could only adjust for a limited number of determinants in the multivariate analyses. Fifth, we do not have information on the specific trauma mechanism.

In conclusion, our data demonstrate that age and gender were independently associated with the pattern complexity of DRFs. Other factors known to be associated with fracture risk, such as BMI, osteoporosis, number and severity of

prevalent vertebral fractures, smoking and alcohol use are not associated with DRF pattern complexity. This indicates that, besides age and gender, trauma mechanism may also be an important determinant for distal radius fracture pattern complexity.

References

1. Burghardt, A.J., et al., *Age- and gender-related differences in the geometric properties and biomechanical significance of intracortical porosity in the distal radius and tibia.* J Bone Miner Res, 2010. 25(5): p. 983-93.
2. Rozental, T.D., et al.*, Premenopausal women with a distal radial fracture have deteriorated trabecular bone density and morphology compared with controls without a fracture*. J Bone Joint Surg Am, 2013. 95(7): p. 633-42.
3. Dhainaut, A., et al., *Exploring the relationship between bone density and severity of distal radius fragility fracture in women*. J Orthop Surg Res, 2014. 9: p. 57.
4. Oyen, J., et al., *Osteoporosis as a risk factor for distal radial fractures: a case-control study*. J Bone Joint Surg Am, 2011. 93(4): p. 348-56.
5. Oyen, J., et al., *Low bone mineral density is a significant risk factor for low-energy distal radius fractures in middle-aged and elderly men: a case-control study*. BMC Musculoskelet Disord, 2011. 12: p. 67.
6. Clayton, R.A., et al., *Association between decreased bone mineral density and severity of distal radial fractures*. J Bone Joint Surg Am, 2009. 91(3): p. 613-9.
7. Itoh, S., et al., *Relationship between bone mineral density of the distal radius and ulna and fracture characteristics*. J Hand Surg Am, 2004. 29(1): p. 123-30.
8. de Klerk, G.J., et al., *The relation between AO-classification of distal radial fractures and bone mineral density*. Injury, 2013. 44(11): p. 1657-8.
9. Koo, O.T., et al., *Distal radius fractures: an epidemiological review*. Orthop Surg, 2013. 5(3): p. 209-13.
10. Porrino, J.A., et al., *Fracture of the distal radius: epidemiology and premanagement radiographic characterization.* AJR Am J Roentgenol, 2014. 203(3): p. 551-9.
11. Lotters. F.J., et al., *Current and Future Incidence and Costs of Osteoporosis-Related Fractures in The Netherlands: Combining Claims Data with BMD Measurements*. Calcif Tissue Int, 2016. 98(3): p. 235-43.
12. Prevrhal, S., et al., *Accuracy limits for the determination of cortical width and density: the influence of object size and CT imaging parameters.* Phys Med Biol, 1999. 44(3): p. 751-64.
13. Riggs, B.L., et al., *Population-based study of age and sex differences in bone volumetric density, size, geometry and structure at different skeletal sites.* J Bone Miner Res, 2004. 19(12): p. 1945-54.
14. Laib, A., et al., *In vivo high resolution 3D-QCT of the human forearm*. Technol Health Care, 1998. 6(5-6): p. 329-37.
15. Petit MA, Beck TJ, Kontulainen SA. 2005. Examining the developing bone: What do we measure and how do we do it? J Musculoskelet Neuronal Interact 5(3): p. 213-24.

16. D'Elia G, Caracchini G, Cavalli L, Innocenti P. 2009. Bone fragility and imaging techniques. Clin Cases Miner Bone Metab 6(3): p. 234-46.
17. Schneider P, Reiners C, Cointry GR, et al. 2001. Bone quality parameters of the distal radius as assessed by pQCT in normal and fractured women. Osteoporos Int 12(8): p. 639-46.
18. Engelke K, Libanati C, Fuerst T, et al. 2013. Advanced CT based in vivo methods for the assessment of bone density, structure and strength. Curr Osteoporos Rep 11(3): p. 246-55.
19. Dutch Institute for Healthcare Improvement CBO. *Richtlijn Osteoporose Fractuurpreventie*, 2011.
20. Lill, C.A., et al., *Impact of bone density on distal radius fracture patterns and comparison between five different fracture classifications.* J Orthop Trauma, 2003. 17(4): p. 271-8.
21. Belloti, J.C., et al. *Are distal radius fracture classifications reproducible? Intra and interobserver agreement.* Sao Paulo Med, 2008. J 126(3): p. 180-5.
22. Plant, C.E., et al. *Is it time to revisit the AO classification of fractures of the distal radius? Inter- and intra-observer reliability of the AO classification.* Bone Joint J, 2015. 97-b(6): p. 818-23.
23. Marsh, J.L., et al. *Fracture and dislocation classification compendium: Orthopaedic Trauma Association classification, database and outcomes committee*. J Orthop Trauma, 2007. 21(10 Suppl): p. S1-133.
24. Kanis, J.A., et al. *The diagnosis of osteoporosis.* J Bone Miner Res, 1994. 9(8): p. 1137-41.
25. Genant, H.K., et al., *Vertebral fracture assessment using a semiquantitative technique*. J Bone Miner Res, 1993. 8(9): p. 1137-48.
26. Manske, S.L., et al., *Human trabecular bone microarchitecture can be assessed independently of density with second generation HR-pQCT.* Bone, 2015. 79: p. 213-21.
27. Pialat, J.B., et al., *Visual grading of motion induced image degradation in high resolution peripheral computed tomography: impact of image quality on measures of bone density and micro-architecture*. Bone, 2012. 50(1): p. 111-8.
28. Agarwal, S., et al., *In vivo assessment of bone structure and estimated bone strength by first- and second-generation HR-pQCT.* Osteoporos Int, 2016. 27(10): p. 2955-66.
29. van Rietbergen, B., et al., *A new method to determine trabecular bone elastic properties and loading using micromechanical finite-element models.* J Biomech, 1995. 28(1): p. 69-81.
30. Vranken, L., et al. *Comorbidities and medication use in patients with a recent clinical fracture at the Fracture Liaison Service.* Osteoporos Int, 2018. 29(2): p. 397-407.

31. de Jong, J.J., et al., *Assessment of the healing process in distal radius fractures by high resolution peripheral quantitative computed tomography*. Bone, 2014. 64: p. 65-74.
32. Pistoia, W., et al. *Image-based micro-finite-element modeling for improved distal radius strength diagnosis: moving from bench to bedside*. J Clin Densitom, 2004. 7(2): p. 153-60.
33. Mueller, T.L., et al., *Computational finite element bone mechanics accurately predicts mechanical competence in the human radius of an elderly population.* Bone, 2011. 48(6): p. 1232-8.
34. Hosseini, H.S., et al. *Fast estimation of Colles' fracture load of the distal section of the radius by homogenized finite element analysis based on HR-pQCT.* Bone, 2017. 97: p. 65-75.
35. Seeman, E., *Bone quality: the material and structural basis of bone strength.* J Bone Miner Metab, 2008. 26(1): p. 1-8.
36. Ruff, C.B. and Hayes, W.C., Sex differences in age-related remodeling of the femur and tibia. J Orthop Res, 1988. 6(6): p. 886-96.
37. Duan, Y. et al.,, Seeman E., *Sexual dimorphism in vertebral fragility is more the result of gender differences in age-related bone gain than bone loss.* J Bone Miner Res, 2001. 16(12): p. 2267-75.
38. Wang, X.F., et al., *Varying contributions of growth and ageing to racial and sex differences in femoral neck structure and strength in old age.* Bone, 2005. 36(6): p. 978-86.
39. Arealis, G., et al., *Does the CT improve inter- and intra-observer agreement for the AO, Fernandez and Universal classification systems for distal radius fractures?* Injury, 2014. 45(10): p. 1579-84.
40. Andersen, D.J., et al., *Classification of distal radius fractures: an analysis of interobserver reliability and intraobserver reproducibility*. J Hand Surg Am, 1996. 21(4): p. 574-82.
41. Ferrero, A., et al., *Analysis of the inter- and intra-observer agreement in radiographic evaluation of wrist fractures using the multimedia messaging service.* Hand (N Y), 2011. 6(4): p. 384-9.
42. Jayakumar, P., et al., *AO Distal Radius Fracture Classification: Global Perspective on Observer Agreement*. J Wrist Surg, 2017. 6(1): p. 46-53

Supplemental tables

Table S-1. Characteristics of patients with type A and type C fractures in the subset of 63 patients with HR-pQCT measurements

	AO/OTA A	**AO/OTA C**	**p-value**
	N= 41	N= 22	
Female	37 (90)	14 (64)	0.017
Age (y)*	64 [11]	69 [13]	0.009
Weight (kg)*	72.0 [18.7]	77.6 [21.5]	*NS*
Height (m)	1.65 ± 0.06	1.68 ± 0.07	*NS*
BMI(kg/m^2)*	25.5 [5.2]	28.4 [7.1]	*NS*
BMI category			*NS*
< 30 kg/m^2 (non-obese)	30 (81.1)	11 (61.1)	
>30 kg/m^2 (obese)	7 (18.9)	7 (38.9)	
Bone mineral density			*NS*
Normal BMD	8 (19.5)	7 (31.8)	
Osteopenia	18 (43.9)	6 (27.3)	
Osteoporosis	15 (36.6)	9 (40.9)	
Vertebral fracture ass			*NS*
No Grade 2/3 Fx	38 (92.7)	21 (95.5)	
≥1 Grade 2/3 Fx	3 (7.3)	1 (4.5)	
Smoking			0.026
Never	16 (39.0)	8 (36.4)	
Past smoker	16 (39.0)	14 (63.6)	
Current smoker	9 (22.0)	0 (0.0)	
Alcohol intake			*NS*
< 1 unit / day	11 (27.5)	3 (13.6)	
≥ 1 unit / day	29 (72.5)	19 85.4)	
Calcium intake (mg/day)*	791 [351]	877 [503]	*NS*
25-OH Vitamin D(nmol/l)			*NS*
<30 (deficiency)	3 (7.3)	1 (4.5)	
30-50 (insufficiency)	9 (22.0)	6 (27.3)	
>50 (sufficiency)	29 (70.7)	15 (68.2)	

BMI=body mass index | BMD=bone mineral density | Fx=fracture
Normally distributed data are presented as mean (SD) | Non-normally distributed data * as median [IQR]
Data missing: HR-pQCT radius (8 – due to bilateral or previous DRF), length/weight/BMI A (4) C (4), alcohol (1)

Table S-2. Characteristics of patients with and without HR-pQCT measurement

	HR-pQCT	**No HR-pQCT**	**p-value**
	N=71	N=180	
Female	58 (82)	155 (86)	*NS*
Age (y)*	67.5 [14]	68.0 [14]	*NS*
Weight (kg)*	72.2 [21.6]	70.0 [22.1]	*NS*
Height (m)	1.65 ± 0.07	1.63 ± 0.08	*NS*
BMI(kg/m^2)*	26.3 [6.2]	26.5 [8.3]	*NS*
BMI category			*NS*
< 30 kg/m^2 (non-obese)	47 (75.8)	118 (72.8)	
>30 kg/m^2 (obese)	15 (24.2)	44 (27.2)	
AO classification			*NS*
A	41 (57.7)	90 (50.0)	
B	8 (11.3)	28 (15.6)	
C	22 (31.0)	62 (34.4)	
Bone mineral density			*NS*
Normal BMD	16 (22.5)	22 (12.2)	
Osteopenia	29 (40.8)	91 (50.6)	
Osteoporosis	26 (36.6)	67 (37.2)	
Vertebral fracture ass			*NS*
No Grade 2/3 Fx	65 (91.5)	156 (86.7)	
≥1 Grade 2/3 Fx	6 (9.5)	24 (13.3)	
Smoking			*NS*
Never	29 (40.8)	78 (44.8)	
Past smoker	32 (45.1)	72 (41.4)	
Current smoker	10 (14.1)	24 (13.8)	
Alcohol intake			0.008
< 1 unit / day	47 (66.2)	140 (81.9)	
≥ 1 unit / day	24 (33.8)	31 (18.1)	
Calcium intake (mg/day)*	831 [398]	780 [436]	*NS*
25-OH Vitamin D(nmol/l)			*NS*
<30 (deficiency)	3 (4.2)	9 (5.0)	
30-50 (insufficiency)	21 (29.6)	67 (37.2)	
>50 (sufficiency)	47 (66.2)	104 (57.7)	

BMI=body mass index | BMD=bone mineral density | Fx=fracture
Normally distributed data are presented as mean (SD) | Non-normally distributed data * as median [IQR]
Data missing: length (26), weight (26), calcium intake (6), alcohol intake (9), smoking (6).

Table S-3. Microarchitectural parameters and micro-FEA analyses of HR-pQCT scan at the distal tibia in 63 patients with type A or C DRF

	AO/OTA A N=41	**AO/OTA C** N=22	**p-value**
Total area (mm^2)	716.3 [207.8]	794.1 [174.1]	0.022
Trabecular area (mm^2)	614.3 [216.0]	672.7 [214.3]	0.028
Cortical area (mm^2) *	105.5 [24.9]	103.1 [45.7]	*NS*
Total vBMD ($mgHA/mm^3$)	226.0 [64.0]	231.7 [84.1]	*N.S*
Trabecular vBMD ($mgHA/mm^3$)	116.6 [47.1]	140.2 [116.3]	0.042
Cortical vBMD ($mgHA/mm^3$) *	855.8 [116.3]	825.1 [109.1]	*NS*
Trabecular bone volume fraction	0.19 [0.06]	0.22 [0.08]	0.034
Trabecular thickness (mm)	0.25 [0.03]	0.25 [0.03]	*NS*
Trabecular separation (mm) *	0.90 [0.47]	0.84 [0.29]	*NS*
Cortical perimeter (mm)	103.1 [14.7]	109.1 [11.9]	0.017
Cortical porosity (%)	3.0 [1.6]	3.2 [1.1]	*NS*
Cortical thickness (mm)	1.22 [0.37]	1.12 [0.30]	*NS*
Cortical pore diameter (mm) *	0.22 [0.03]	0.21 [0.02]	0.034
Torsion stiffness (kNmm/rad) *	7821 [2866]	9697 [8023]	0.033
Compression stiffness (kN/mm) *	133.8 [38.0]	145.1 [89.4]	*NS*
Compression ultimate force (kN) *	7.17 [6.29]	6.26 [6.29]	0.029
Bending stiffness horizontal axis (kNmm/rad) *	10884 [4708]	13480 [8352]	0.007
Bending stiffness vertical axis (kNmm/rad) *	13438 [4664]	15956 [14461]	*NS*

All data are presented as median [IQR] | *= non-normally distributed data | NS = not significant

Table S-4. Micro-architectural parameters and micro-FEA analyses of HR-pQCT scan at the distal radius in 55 patients with type A or C DRF

	AO/OTA A N=35	**AO/OTA C** N=20	**p-value**
Total area (mm^2) *	265.6 [76.5]	316.9 [140.4]	0.023
Trabecular area (mm^2) *	213.7 [57.6]	272.2 [111.4]	0.015
Cortical area (mm^2)	52.4 [13.8]	55.9 [23.6]	*NS*
Total vBMD ($mgHA/mm^3$)	257.2 [93.6]	247.6 [91.3]	*NS*
Trabecular vBMD ($mgHA/mm^3$)	96.0 [48.0]	125.4 [65.8]	0.030
Cortical vBMD ($mgHA/mm^3$) *	896.4 [75.4]	866.3 [78.7]	*NS*
Trabecular bone volume fraction *	0.14 [0.05]	0.18 [0.08]	0.012
Trabecular thickness (mm)	0.22 [0.02]	0.23 [0.02]	0.019
Trabecular separation (mm) *	0.98 [0.41]	0.79 [0.29]	*NS*
Cortical perimeter (mm) *	68.6 [7.4]	75.9 [17.6]	0.015
Cortical porosity (%)	0.7 [0.7]	0.9 [0.5]	*NS*
Cortical thickness (mm)	0.95 [0.23]	0.87 [0.28]	*NS*
Cortical pore diameter (mm) *	0.19 [0.03]	0.19 [0.02]	*NS*
Torsion stiffness (kNmm/rad) *	1032 [606]	1184 [1393]	*NS*
Compression stiffness (kN/mm) *	48.6 [13.9]	46.8 [33.2]	*NS*
Compression ultimate force (kN) *	2.53 [0.75]	2.55 [1.79]	*NS*
Bending stiffness horizontal axis (kNmm/rad) *	2330 [1163]	2339 [2751]	*NS*
Bending stiffness vertical axis (kNmm/rad) *	1257 [693]	1482 [1525]	0.029

All data are presented as median [IQR] | *= non-normally distributed data | NS = not significant

Table S-5. Associations with fracture pattern complexity (type C vs type A) in 51 women with a HR-pQCT at the distal tibia

	AO type A N=37	**AO type C** N=14	**p-value**	**Odds ratio** Unadjusted	**p-value**	**Odds ratio** Age adjusted	**p-value**
Age	64 [11]	73 [16]	**0.007**	1.12 (1.02-1.22)	**0.013**	-	-
Total area	697.8 [153.4]	745.5 [132.4]	0.256	1.58 (0.72-3.45)	0.254	1.41 (0.61-3.26)	0.429
Trabecular area	587.0 [180.0]	652.4 [108.3]	0.165	1.71 (0.80-3.64)	0.167	1.43 (0.64-3.22)	0.385
Cortical area	103.2 [25.0]	89.9 [23.7]	**0.021**	0.293 (0.10-0.88)	**0.029**	0.47 (0.14-1.55)	0.212
Total vBMD	219.1 [73.9]	214.1 [70.1]	0.260	0.67 (0.33-1.34)	0.256	0.87 (0.41-1.84)	0.717
Trabecular vBMD	109.5 [50.1]	128.2 [62.5]	0.358	1.37 (0.71-2.65)	0.352	1.46 (0.71-2.97)	0.303
Cortical vBMD	855.8 [114.7]	765.4 [107.9]	0.084	0.56 (0.29-1.09)	0.089	0.84 (0.38-1.85)	0.655
Trabecular BV fraction	0.18 [0.06]	0.20 [0.09]	0.305	1.42 (0.73-2.75)	0.301	1.48 (0.73-3.03)	0.279
Trabecular thickness	0.25 [0.03]	0.25 [0.03]	0.560	1.20 (0.66-2.21)	0.553	1.16 (0.58-2.31)	0.673
Trabecular separation	0.96 [0.47]	0.85 [0.21]	0.153	0.60 (0.24-1.54)	0.292	0.53 (0.19-1.46)	0.220
Cortical perimeter	102.0 [11.8]	106.2 [8.7]	0.224	1.64 (0.74-3.60)	0.222	1.37 (0.59-3.17)	0.468
Cortical porosity	3.0 [1.6]	3.2 [1.4]	0.656	0.86 (0.44-1.66)	0.649	0.79 (0.37-1.69)	0.548
Cortical thickness	1.22 [0.39]	1.03 [0.22]	**0.017**	0.32 (0.12-0.87)	**0.026**	0.48 (0.18-1.33)	0.158
Cortical pore diameter	0.22 [0.03]	0.21 [0.02]	**0.010**	0.40 (0.16-0.98)	**0.045**	0.53 (0.21-1.31)	0.169
Torsion stiffness	7600 [2580]	8143 [3138]	0.921	1.06 (0.33-3.40)	0.919	1.56 (0.43-5.64)	0.494
Compression stiffness	130.1 [31.9]	136.1 [45.3]	0.694	0.82 (0.31-2.17)	0.688	1.30 (0.45-3.73)	0.631
Compression ultimate force	7.17 [1.86]	7.38 [2.38]	0.905	1.07 (0.36-3.16)	0.903	1.87 (0.46-7.61)	0.384
Bending stiffness horizontal	10702 [4063]	50281 [14401]	0.375	1.60 (0.57-4.46)	0.369	2.03 (0.65-6.34)	0.225
Bending stiffness vertical	12945 [4586]	12127 [5953]	0.651	0.75 (0.22-2.58)	0.644	1.05 (0.28-3.87)	0.943

Data are presented as median [IQR] and OR (CI) | OR for age = per year | OR for HR-pQCT parameters = per SD

Table S-6. Associations with fracture complexity (type C vs type A) in 43 women with a HR-pQCT at the distal radius

	AO type A N=31	**AO type C** N=12	**p-value**	**Odds ratio** Unadjusted	**p-value**	**Odds ratio** Age adjusted	**p-value**
Age	64 [10]	74 [16]	**0.009**	1.12 (1.02-1.22)	**0.017**	-	-
Total area	259.6 [49.2]	252.5 [79.2]	0.452	1.55 (0.51-4.72)	0.443	1.32 (0.39-4.49)	0.653
Trabecular area	211.2 [43.4]	222.4 [79.6]	0.148	2.13 (0.76-5.97)	0.151	1.64 (0.55-4.93)	0.379
Cortical area	51.9 [13.0]	48.3 [11.9]	0.227	0.51 (0.17-1.51)	0.224	0.74 (0.22-2.45)	0.620
Total vBMD	247.6 [99.8]	212.2 [72.2]	0.365	0.73 (0.37-1.44)	0.357	0.97 (0.46-2.06)	0.943
Trabecular vBMD	91.5 [47.5]	102.2 [47.5]	0.554	1.27 (0.59-2.72)	0.545	1.48 (0.65-3.33)	0.350
Cortical vBMD	896.4 [65.5]	859.8 [64.4]	0.141	0.57 (0.27-1.21)	0.144	0.82 (0.34-1.98)	0.665
Trabecular BV fraction	0.14 [0.05]	0.14 [0.05]	0.424	1.40 (0.62-3.16)	0.416	1.50 (0.63-3.55)	0.360
Trabecular thickness	0.22 [0.02]	0.22 [0.02]	0.242	1.55 (0.74-3.22)	0.242	1.11 (0.48-2.56)	0.809
Trabecular separation	1.03 [0.49]	0.88 [0.36]	0.747	1.11 (0.61-2.03)	0.741	0.78 (0.39-1.56)	0.486
Cortical perimeter	68.1 [6.9]	68.8 [9.3]	0.297	1.60 (0.66-3.84)	0.298	1.20 (0.47-3.08)	0.710
Cortical porosity	0.7 [0.7]	0.9 [0.5]	0.742	0.88 (0.41-1.86)	0.735	0.88 (0.34-2.30)	0.799
Cortical thickness	0.92 [0.23]	0.79 [0.11]	0.201	0.59 (0.27-1.32)	0.200	0.85 (0.35-2.02)	0.706
Cortical pore diameter	0.19 [0.02]	0.19 [0.02]	0.399	0.71 (0.32-1.57)	0.392	0.73 (0.27-2.00)	0.541
Torsion stiffness	1022 [481]	1073 [395]	0.835	0.84 (0.16-4.33)	0.830	1.21 (0.18-8.03)	0.845
Compression stiffness	48.4 [11.9]	43.0 [8.7]	0.257	0.49 (0.14-1.67)	0.253	0.68 (0.18-2.61)	0.574
Compression ultimate force	2.52 [0.58]	2.32 [0.51]	0.374	0.57 (0.17-1.95)	0.366	0.76 (0.19-3.01)	0.761
Bending stiffness horizontal	2284 [1078]	2090 [776]	0.321	0.44 (0.09-2.16)	0.315	0.57 (0.10-3.41)	0.537
Bending stiffness vertical	1150 [573]	1333 [460]	0.639	1.55 (0.26-9.09)	0.630	2.05 (0.26-16.10)	0.495

Data are presented as median [IQR] and OR (CI) | OR for age = per year | OR for HR-pQCT parameters = per SD

Chapter 3

Association of secondary displacement of distal radius fractures with cortical bone quality at the distal radius

A.M. Daniels, H.M.J. Janzing, C.E. Wyers, B. van Rietbergen, L. Vranken, R.Y. van der Velde,P.P.M.M. Geusens, S. Kaarsemaker, M. Poeze, J.P. van den Bergh

Arch Orthop Trauma Surg. 2021; 141(11):1909-1918

Abstract

Introduction
The aim of this study was to investigate the associations of patient characteristics, bone mineral density (BMD), bone microarchitecture and calculated bone strength with secondary displacement of a DRF based on radiographic alignment parameters.

Materials and methods
Dorsal angulation, radial inclination and ulnar variance were assessed on conventional radiographs of a cohort of 251 patients, 38 men and 213 women, to determine the anatomic position of the DRF at presentation (primary position) and during follow-up. Secondary fracture displacement was assessed in the non-operatively treated patients (N=154) with an acceptable position, preceded (N=97) or not preceded (N=57) by primary reduction (baseline position). Additionally, bone microarchitecture and calculated bone strength at the contralateral distal radius and tibia were assessed by HR-pQCT in a subset of respectively 63 and 71 patients.

Outcome
Characteristics of patients with and without secondary fracture displacement did not differ. In the model with adjustment for primary reduction (OR 22.00 [2.27-212.86], p=0.008), total (OR 0.16 [95%CI 0.04-0.68], p=0.013) and cortical (OR 0.19 [95%CI 0.05-0.80], p=0.024) volumetric BMD (vBMD) and cortical thickness (OR 0.13 [95%CI 0.02-0.74], p=0.021) at the distal radius were associated with secondary DRF displacement. No associations were found for other patient characteristics, such as age gender, BMD or prevalent vertebral fractures.

Conclusions
In conclusion, our study indicates that besides primary reduction, cortical bone quality may be important for the risk of secondary displacement of DRFs.

Introduction

Standard initial management for distal radius fractures (DRFs) at the emergency department (ED) is cast immobilization preceded by closed reduction in the case of a dislocated fracture. Further management depends on the anatomic position, DRFs with acceptable position can be managed non-operatively [1]. Dislocated intra-articular DRFs often require surgical fixation to restore and retain correct fracture position. Patient characteristics, such as age and comorbidities, must be taken into account when making this decision [2-4]. It is of great importance to identify fractures at risk for displacement to achieve the most adequate treatment. By being able to anticipate early stage instability, unnecessary manipulation can be prevented, surgical treatment options can be discussed timely and a reduction in complications such as mal-union might be accomplished.

In 1989, five risk factors for DRF instability were identified by Lafontaine et al., namely primary dorsal angulation exceeding 20 degrees, dorsal comminution, involvement of the radio-carpal joint, styloid ulnae fracture and patients aged over 60 years [5]. From that time on, many prediction rules for instability have been developed, some previous risk factors could not be confirmed by new studies and new risk factors for secondary displacement, such as radial shortening, have been identified [6-11]. In this debate, little attention was paid to the influence of bone properties such as bone mineral density (BMD), bone microarchitecture and calculated bone strength. BMD can be assessed using bone densitometry whereas bone microarchitecture and separate assessment of trabecular and cortical bone requires spatial resolution of less than 200 μm. Recently, a non-invasive method for the assessment of bone microarchitecture at the distal radius and tibia using high resolution peripheral quantitative CT (HR-pQCT) has become available.

The aim of this study was to investigate the associations of patient characteristics, BMD (measured by dual-energy X-ray absorptiometry (DXA) and High Resolution peripheral Quantitative CT (HR-pQCT)), bone microarchitecture and calculated bone strength with secondary displacement of a DRF based on radiographic alignment parameters.

Methods

Study population

This cohort comprised patients aged 50-90 years presenting with a radiologically confirmed DRF, between November 2013 and June 2016. All consecutive patients were referred to the Fracture Liaison Service (FLS) and included in this study if they attended the FLS. After exclusion of patients with high energy trauma (as this study focuses on fall-related fractures), osteomyelitis and bone metastasis, 251 patients with a recent DRF were included in this cross-sectional cohort study.

At the FLS, patients received a detailed evaluation according to the Dutch guideline for treatment of osteoporosis. The evaluation consisted of a questionnaire assessing risk factors for falls, fracture risk, medical history including medication use and daily dietary calcium intake. Additionally, blood samples were collected to identify metabolic disorders and a DXA measurement with vertebral fractures assessment (VFA) was performed 3-4 months after trauma [Figure 1]. If indicated, anti-osteoporosis treatment or treatment of newly diagnosed metabolic bone disorders was initiated according to current guidelines [12].

Of the 251 patients with a DRF included in this study, 71 participated in an observational three-year follow-up study at the FLS ("Prospective evaluation of bone strength, physical activity, falls, subsequent fractures and mortality in patients presenting with a recent clinical fracture"). Approval was obtained from an institutional Review Board prior to performing the study (METC NL 45707.072.13). In that study patients consented with HR-pQCT measurements of the distal radius (N=63) and tibia (N=71) and the baseline data were used for the HR-pQCT part of this study. HR-pQCT measurements were conducted approximately three weeks after the DXA scan was performed [Figure 1].

DRF position and classification

All conventional radiographs (antero-posterior and lateral) were used for assessment of alignment parameters, comprising angulation (dorsal=DA, volar/palmar=VA), radial inclination (RI) and ulnar variance (UV). DA/VA is measured on the lateral radiograph and represents the angle between a line perpendicular to the longitudinal axis of the radius and a line along the articular surface of the distal radius. RI is measured on the antero-posterior radiograph and represents the angle between a line connecting the tip of the radial styloid and the most ulnar point of the distal radius and a second line perpendicular to the longitudinal axis of the radius. UV represents the length of the ulna compared to the radius. According to the Dutch Guideline, DRFs were classified as fractures with an 'unacceptable position' when at least one of the following criteria was met; DA > 15°, VA >20°, RI ≤ 15° and UV >5mm [Figure 2 A/B/C] [13]. Position at presentation, referred to as primary position, was assessed on the first radiographs of every patient. If reduction was applied, the position was reassessed on radiographs following reduction. This position is referred to as baseline position. Adequate reduction was defined as regaining an acceptable position according to the criteria. In unreduced fractures with repeated radiographs immediately after cast immobilization, baseline position is the position as measured on the repeated radiographs. In unreduced fractures without repeated radiographs, baseline position was equivalent to primary position. All subsequent radiographs were assessed individually and used for secondary fracture displacement assessment, starting at baseline position. Patients with primary surgical intervention, an unacceptable baseline position or without follow-up radiographs were excluded from secondary fracture displacement assessment [Figure 3]. Secondary fracture displacement was defined as a displacement of the DRF that resulted in an unacceptable position, after an adequate baseline position in non-operatively treated patients.

Figure 1. Flowchart of patients included in this study and corresponding investigations

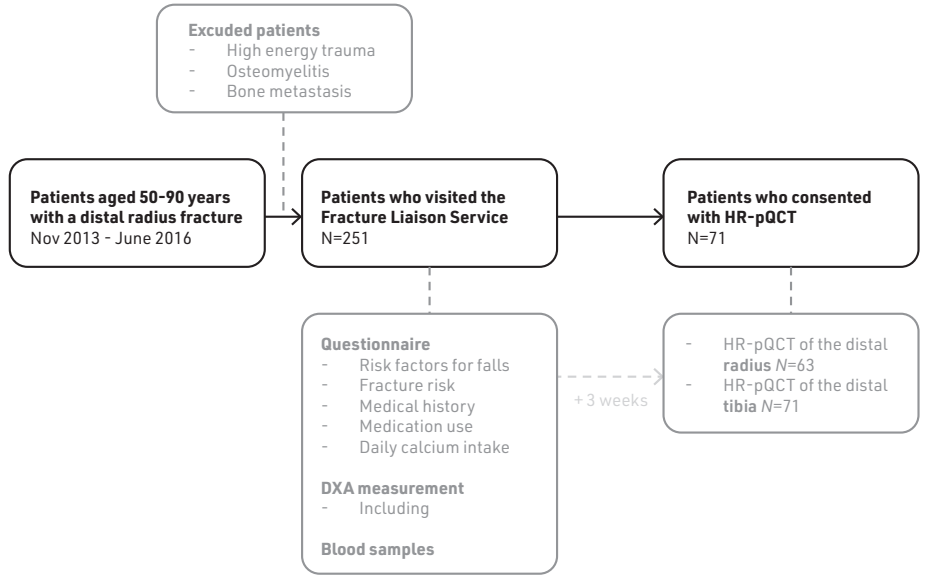

Figure 2 A/B/C. Radiographic alignment parameters (RI/UV/DA/VA) to assess the distal radius

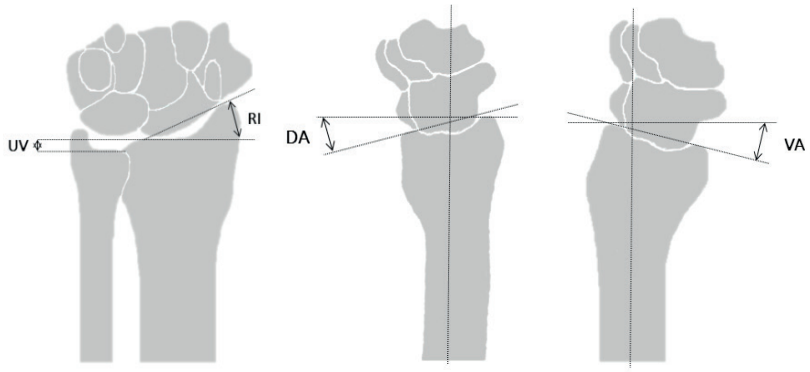

Figure 3. Flowchart of patient distribution and (eligibility for) secondary fracture displacementassessment

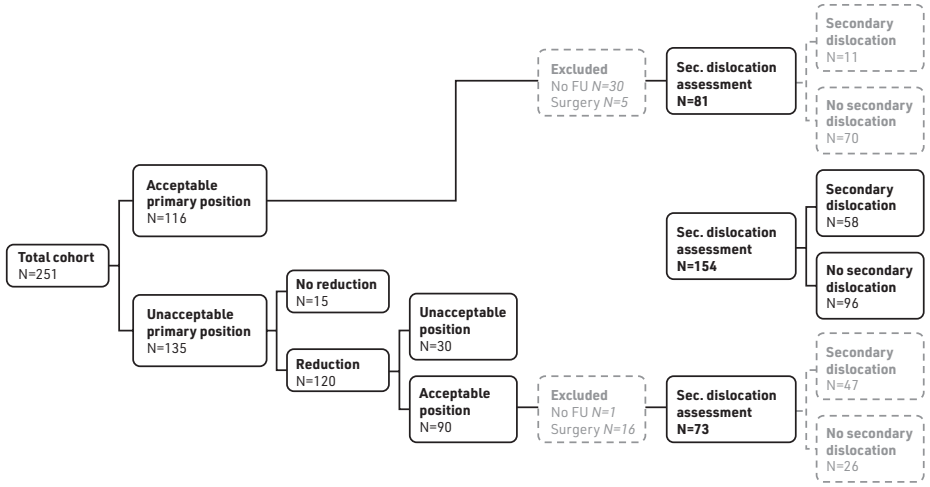

All fractures were classified based on the AO/OTA classification on baseline plain radiographs by two independent investigators. DRFs were classified into three main types, namely type A (extra-articular), type B (partial articular) and type C (complete articular). Assessment by a third independent investigator was necessary for 51 patients with discrepant initial classification and resulted in agreement on another 47 fractures. For the remaining four fractures, conformity was reached by all three investigators in a consensus meeting.

DXA and VFA

Two-dimensional BMD was measured at the lumbar spine (LS; L1-L4), total hip (TH) and femoral neck (FN) using DXA (Hologic QDR 4500, Hologic Inc., Bedford, MA, USA). Areal BMD measurements (g/cm^2), were categorized according to the WHO criteria based on the lowest T-score at the LS, TH or FN into normal BMD (T-score ≥ -1), osteopenia (T-score between -1 and -2.5) and osteoporosis (T-score ≤ -2.5) [14].

VFA was performed on the DXA lateral spine images using quantitative morphometric assessment of vertebral height. The method described by Genant et al. was used to classify the severity of vertebral fractures (VFs); grade 1 (mild fracture, with vertebral height loss of 20-25%), grade 2 (moderate fracture with height loss of 25-40%) and grade 3 (severe fracture with height loss > 40%) [15].

HR-pQCT

The second generation HR-pQCT (XtremeCT II; Scanco Medical AG, Brüttisellen, Switzerland) was used to scan the contralateral radius and ipsilateral tibia. Scans were conducted and evaluated according to the standard protocol of the manufacturer (effective energy of 68 kVp, tube current of 1470 µA and 43 ms integration time) [16,17]. The reference line was placed on the joint surface of the distal radius and tibia. The area to be scanned starts 9.0 mm proximally to the reference line and ends 1.2 mm distally to the reference line. Motion-induced degradation of the images was graded according to the method of Pialat et al. [17]. Images were processed according to the manufacturer's standard protocol. The following parameters were analyzed: total, trabecular and cortical bone area [cm^2], volumetric bone mineral density (vBMD) for the total, trabecular and cortical compartment [mgHA/cm^3], trabecular bone volume fraction, trabecular number [mm^{-1}], trabecular thickness [mm], trabecular separation [mm], cortical thickness [mm], cortical perimeter [mm], cortical porosity [%] and cortical pore diameter [mm]. In addition, micro-finite element analyses (micro-FEA) were generated by directly converting bone voxels in the segmented image to brick elements [18,19]. Elements were assigned a Young's modulus of 10 GPa and Poisson's ratio of 0.3 and for each model, four tests were simulated [20]. The first load case represented a 'high friction' compression test with a prescribed displacement in the axial direction of 1% of the total length, from which the compression stiffness [kN/mm] as well as the estimated strength was calculated [21-23]. The second load case represented a prescribed rotation of 0.01 rad around the longitudinal axis from which the torsional stiffness [kNmm/rad] was calculated. A third and fourth load case represented a prescribed rotation of 0.01 rad applied around the sagittal and transversal axes respectively, thus inducing a state of pure bending in

two directions, from which the bending stiffness in each direction was calculated. These four load cases were included to test if the fracture type is associated with a reduced stiffness in a specific loading direction.

Statistical analysis

Data were analyzed using IBM SPSS Statistics, version 24 (IBM Corporation 1989, 2016). Normal distribution was tested with Q-Q plots and Kolmogorov-Smirnov analysis. Depending on the distribution, data are presented as mean with standard deviation (SD) or median with interquartile range (IQR). Chi-square tests were used to analyze differences in patient characteristics between the groups. Independent samples t-tests were used to compare HR-pQCT parameters between patients with an acceptable and unacceptable primary position and between patients with and without secondary fracture displacement.

Logistic regression analysis was used to investigate the independent association between secondary fracture displacement (yes vs no) and HR-pQCT parameters. Bivariate analyses were conducted for primary reduction and all standardized scores (z-scores) of the HR-pQCT parameters for both the HR-pQCT radius group (N=30) and HR-pQCT tibia group (N=36). The cutoff value for significance to assess parameters in a multivariable model was defined as p≤0.10. Due to the small sample size, multivariable analyses with adjustment for age and primary reduction were conducted separately for each significant HR-pQCT parameter in bivariate analysis. Receiver operating characteristic (ROC) analyses with area under the curve (AUC) measurements were conducted for all significant variables in the HR-pQCT analyses. Adjustment for age was conducted because of the potential effect on bone microarchitecture and strength. Significance level was set as α=0.05.

Results

Primary position

Of 251 patients, 38 men (15%) and 213 women (85%) with a mean age of 67 years (SD ±9), 116 (46%) had an acceptable and 135 (54%) an unacceptable primary position. One patient had a fracture with 20 degrees volar angulation and was therefore subjected to surgery. None of the fractures with volar angulation exceeded the range of 20 degrees. Patients with a DRF with primary unacceptable position were significantly older (69 vs. 66 years, p=0.015) and had a lower body weight (68.6 vs. 73.5 kg, p=0.035) and BMI (25.5 vs. 27.7 kg/m2, p=0.048) than DRF patients with acceptable position [Table S-1]. The proportion of AO/OTA type A and B fractures was higher and type C fractures was lower in patients with an acceptable primary position compared to patients with an unacceptable primary position (p<0.001). There was no difference in gender, BMD, number and severity of previous VFs, alcohol intake, smoking, calcium intake and vitamin D levels. Neither was there a difference in bone microarchitecture and strength measured by HR-pQCT between patients with a DRF with primary acceptable (tibia N=31, radius N=26) and unacceptable position (tibia N=40, radius N=35) [data not shown]. HR-pQCT scans of the distal tibia were conducted in all patients (N=71), while distal radius scans could not be conducted in eight of these patients due to the presence of a bilateral DRF at the time of the study or a prior DRF at the contralateral side. Furthermore two patients with unacceptable primary position had a bad quality HR-pQCT of the distal radius and were therefore not included in HR-pQCT analysis.

Secondary fracture displacement

Reduction was conducted in 120/135 patients with a primary unacceptable position with a success rate of 75%. This resulted in 206 patients with an acceptable baseline position. In 20 patients, surgery was conducted because of comminution of the fracture or patients' preference. One patient had a fracture with 20 degrees volar angulation and therefore underwent surgery. After exclusion of these 21 patients and 31 patients without follow up, 154 were eligible and assessed for secondary fracture displacement. Median follow-up with radiographs was 35 days (interquartile range 45 days), with numerous follow-up visits in this time range [Figure 3]. Secondary displacement occurred within the first two weeks in 39 patients (67%), in the third week in 12 patients (21%) and seven patients (12%) had a DRF displacement after one month. When comparing patients with secondary fracture displacement (N=58) to those without (N=96), we found no differences for age, gender distribution, BMI, BMD, number and severity of previous VFs, smoking, alcohol intake, calcium intake and vitamin D levels [Table 1]. Primary reduction was significantly associated with secondary DRF displacement (OR 12.53 [95% CI 4.60-34.09, p<0.001] in 154 patients.

HR-pQCT tibia and radius scans were available in 36 (23%) respectively 30 (20%) patients for evaluation of secondary fracture displacement. Characteristics of patients with HR-pQCT measurement (N=36) were not different compared to those without HR-pQCT (N=118). Neither was there a difference in the proportion of secondary vs. non secondary dislocated fractures [Table 2]. At the distal radius (measured in 30 patients), total (OR 0.27 [95% CI 0.10-0.73], p=0.010) and cortical (OR 0.31 [95% CI 0.12-0.80], p=0.016) vBMD and cortical thickness (0.32 [95% CI 0.13-0.80], p=0.015) were significantly lower in patients with secondary

dislocated fractures. There were no differences for trabecular parameters and micro-FEA. The strongest determinant for secondary fracture displacement was primary reduction (OR 22.00 [95% CI 2.27-212.86], p=0.008). After adjustment for primary reduction, total (0.16 [95% CI 0.04-0.68], p=0.013) and cortical (0.19 [95% CI 0.05-0.80], p=0.024) vBMD and cortical thickness (0.13 [95% CI 0.02-0.74], p=0.021) were significantly associated with secondary fracture displacement. Adjustment for age did not change the association of HR-pQCT parameters with secondary displacement of a DRF [Table S-2].

At the distal tibia (measured in 36 patients), total vBMD (OR 0.35 [95% CI 0.13-0.92], p=0.034) and cortical pore diameter (OR 0.37 [95% CI 0.14-0.94], p=0.036) were significantly lower in patients with secondary dislocated fractures, while there were no differences for trabecular parameters and micro-FEA. After adjustment for primary reduction, both total vBMD (OR 0.06 [95% CI 0.01-0.64], p=0.020) and cortical thickness (OR 0.22 [95% CI 0.06-0.84], p=0.027) were significantly associated with secondary fracture displacement. After adjustment for age, none of the HR-pQCT parameters at the distal tibia was significantly associated with secondary displacement of a DRF [Table S-3].

Table 1. Characteristics of 154 patients with and without secondary fracture displacement

	No secondary displacement N= 96	**Secondary displacement** N= 58	**p-value**
Female	83 (87)	54 (93)	0.202
Age (y)*	66 [14]	68.5 [13]	0.054
Weight (kg)*	73.3 [22.8]	66.6 [22.0]	0.101
Height (m)	1.63 ± 0.08	1.62 ± 0.06	0.340
BMI (kg/m2)*	26.4 [6.9]	25.4 [7.4]	0.174
AO			0.334
A	57 (59.4)	36 (62.1)	
B	14 (14.6)	4 (6.9)	
C	25 (26.0)	18 (31.0)	
BMI category			0.557
<30 (non obees)	63 (72.4)	40 (76.9)	
≥30 (obees)	24 (27.6)	12 (23.1)	
Bone densitometry			0.710
Normal BMD	16 (16.7)	8 (13.8)	
Osteopenia	48 (50.0)	27 (46.6)	
Osteoporosis	32 (33.4)	23 (39.7)	
VFA			0.595
No VF	87 (90.6)	51 (87.9)	
1Grade 2/3 VF	9 (9.4)	7 (12.1)	
Smoking			0.689
Never	40 (42.6)	23 (41.1)	
Past smoker	42 (44.7)	23 (41.1)	
Current smoker	12 (12.8)	10 (17.9)	
Alcohol intake			0.260
< 1 unit/day	28 (30.4)	21 (39.6)	
≥ 1 unit/day	64 (69.6)	32 (60.4)	
Calcium intake (mg/day)*	797 [396]	843 [428]	0.968
25-OH Vitamin D(nmol/l)			0.308
<30 (deficiency)	8 (8.3)	9 (15.5)	
30-50 (insufficiency)	32 (33.3)	15 (25.9)	
>50 (sufficiency)	56 (58.3)	34 (58.6)	

BMI = body mass index | BMD = bone mineral density | VF= vertebral fracture
Data missing: length (14), weight (14), calcium intake (4), alcohol use (9), smoking (4)
Normally distributed data are presented as mean (SD) | Non normally distributed data* as median [IQR]

Table 2. Characteristics of patients assessed for secondary displacement with and without HR-pQCT measurement (N=154)

	With HR-pQCT N= 36	**Without HR-pQCT** N= 118	**p-value**
Secondary displacement	12 (33)	24 (24)	0.540
Female	32 (89)	105 (89)	0.597
Age (y)*	68 [12]	67 [16]	0.673
Weight (kg)*	71.5 [21]	69.3 [21]	0.981
Height (m)	1.65 ± 0.06	1.63 ± 0.07	0.118
BMI*	25.4 [5.0]	26.4 [8.4]	0.476
AO			0.648
A	24 (66.7)	69 (58.5)	
B	4 (11.1)	14 (11.9)	
C	8 (22.2)	35 (29.7)	
BMI category			0.247
<30 (non obees)	27 (81.8)	76 (71.7)	
≥30 (obees)	6 (18.2)	30 (28.3)	
Bone densitometry			0.939
Normal BMD	6 (16.7)	18 (15.3)	
Osteopenia	18 (50.0)	57 (48.3)	
Osteoporosis	12 (33.3)	43 (36.3)	
VFA			0.532
No VF	31 (86.1)	107 (90.7)	
1Grade 2/3 VF	5 (13.9)	11 (9.3)	
Smoking			0.863
Never	14 (38.9)	49 (43.0)	
Past smoker	17 (47.2)	48 (42.1)	
Current smoker	5 (13.9)	17 (14.9)	
Alcohol use			0.090
< 1 unit/day	8 (22.2)	41 (37.6)	
≥ 1 unit/day	28 (77.8)	68 (62.4)	
Calcium intake (mg/day)*	855 [379]	780 [404]	0.205
25-OH Vitamin D(nmol/l)			0.256
<30 (deficiency)	2 (5.6)	15 (12.7)	
30-50 (insufficiency)	9 (25.0)	38 (32.2)	
>50 (sufficiency)	25 (69.4)	65 (55.1)	

BMI = body mass index | BMD = bone mineral density | VF= vertebral fracture
Data missing: length (14), weight (14), calcium intake (4), alcohol use (9), smoking (4)
Normally distributed data are presented as mean (SD) | Non normally distributed data * as median [IQR]

Discussion

DRFs with an unacceptable position are generally reduced at the ED as the first step of treatment. Recovery of alignment is thought to be important to preserve adequate function [1,24]. Our study showed that fractures with an unacceptable position at need for reduction are, after adequate reduction, at high risk for secondary displacement. In addition, this study shows for the first time, that secondary fracture displacement is independently associated with lower total and cortical vBMD and lower cortical thickness at the distal radius, measured by HR-pQCT, after adjustment for primary reduction while no other clinical parameter including BMD and previous vertebral fractures are associated with secondary fracture displacement. The HR-pQCT results are clinically relevant as the odds of secondary fracture displacement are 81-87% higher in patients with lower total and cortical vBMD and cortical thickness at the distal radius.

Previous data regarding timing of displacement are controversial. Some studies reported that all DRFs dislocate in the first two weeks, whereas others describe it as a gradual process [6,25,26]. Our data indicate that 88% of all displacements occur in the first three weeks. Although nearly significant (p=0.054), our data did not confirm previous findings that secondary fracture displacement was associated with age [5-8]. This might be due to the age limit of 50-90 years in our study, whereas Abbaszadegan et al. included patients from the age of 18 years. Gender, BMI, VFA, smoking/alcohol status, calcium intake and vitamin D levels were not associated with secondary displacement of a DRF in our study.

The association between BMD, measured by DXA and the ability to maintain adequate position of a DRF has previously been investigated. Clayton et al. (2009) concluded that osteoporosis (T-score <-2,5) was associated with secondary DRF displacement in a cohort of 137 patients aged over fifty-five [27]. On the contrary, Robin et al. (2014) studied patients aged over 65 years with a displaced DRF and concluded that there was no relationship between BMD, measured by DXA and the ability to maintain position after adequate reduction [28]. These findings are in line with our study where we observed no difference in or association with BMD, measured by DXA, between patients with and without secondary fracture displacement.

Although cortical integrity is widely suggested to play a role in DRF stability [5,6,29,30], assessment of cortical comminution is frequently conducted without a clear definition [5,9]. For example, dorsal comminution is assessed on conventional radiographs, but exact measurement is not possible due to limited resolution.

A non-invasive method recently available for the assessment of bone microarchitecture at the extremities is HR-pQCT [23,31,32]. In our study, secondary fracture displacement was independently associated with lower total and cortical vBMD and lower cortical thickness at the distal radius, measured by HR-pQCT. At the distal tibia, lower total vBMD and lower cortical thickness appeared to be determinants for secondary DRF displacement, however after adjustment for age these HR-pQCT parameters were no longer associated with secondary DRF displacement. Although the HR-pQCT measurements were performed in a limited number of patients we found significant associations with total and cortical vBMD and cortical thickness at the distal radius. We believe that the comparison of the affected with the unaffected distal radius is the most appropriate way to study the associations of skeletal parameters with secondary fracture displacement. To best of our knowledge, this is the first study demonstrating the association of bone microarchitecture with secondary DRF displacement.

Some issues were limiting in our study. Firstly, closed reduction was performed by the treating physician at the ED by which some variability might exist in the decision, the technique and quality (as result of experience level) of reduction. Secondly, due to the retrospective design of our study, radiographic alignment parameters were only assessed at the fractured radius. Since both wrists of one individual can be considered as symmetrical [33], van Eerten et al. [34] assessed the implementation of a technique comparing the fractured site with the unaffected side. They conclude that only reproducibility of radial inclination measurement and not of radial length or dorsal/volar angulation, improved after implementation of the new template technique. Thirdly, fracture assessment in this study was conducted using radiographs since previous literature shows no significant increase of inter and intra observer agreement of the AO classification of DRFs when using CT [35]. However, recent studies suggests that additional CT scanning may be of importance for the accuracy of scoring the fracture types [36,37]. Fourth, for classification of the complexity of DRFs, the AO/OTA classification was used. This is one of many available classification systems being the Frykman, Fernandez, Melone and universal classification system [35,38,39], unfortunately none of these systems has perfect reproducibility rates [35,40-42]. In contrast to other classification systems, the AO/OTA classification has a strong intra- and inter-observer reliability for assessment of the main type (A - extra articular, B - partially articular, C - complete articular). Classifying the AO subtype is not recommended based on the poor intra- and inter- observer reliability [43]. In concordance with this, consensus rate in our study for two independent investigators was 79.7%. Furthermore, classification of main type was in line with previous published papers [44,45]. Fifth, since assessment of BMD and VFs was only possible in FLS attenders, we studied a selected cohort of patients presenting at the ED with a DRF. Due to the retrospective design of our study, not all patients underwent HR-pQCT. However, there was no difference between patients with and without HR-pQCT measurement and no difference in secondary fracture displacement distribution between the total cohort and the subgroup with HR-pQCT measurement. Accordingly, the study results of the subset of patients with HR-pQCT are representative for and can be extrapolated to our total cohort of patients with a DRF. Finally, as described in the result section, fourteen patients with an unacceptable position were treated non-operatively. This was due to the fact that they were not willing or suitable, as judged by their treating physician, to undergo surgery. It is well founded not to subject older patients with multiple comorbidities to manipulation/surgery since it is proven to be of minimal value [46,47], however this might have caused bias in our study.

In conclusion, our data demonstrate that the most important determinant for secondary displacement of a DRF was primary reduction. However, while other patient characteristics, BMD and VF status were not associated with secondary fracture displacement, lower total and cortical vBMD and lower cortical thickness at the distal radius were independently associated with secondary displacement of a DRF. This indicates that besides primary reduction, cortical bone quality may be important for the risk of secondary displacement of DRFs.

References

1. Mauck, B.M. and Swigler, C.W., *Evidence-Based Review of Distal Radius Fractures.* Orthop Clin North Am, 2018. 49(2): p. 211-222.
2. Orbay, J.L. and Fernandez, D.L., *Volar fixed-angle plate fixation for unstable distal radius fractures in the elderly patient.* J Hand Surg Am, 2004. 29(1): p. 96-102.
3. Rozental, T.D. and Blazar, P.E., *Functional outcome and complications after volar plating for dorsally displaced, unstable fractures of the distal radius.* J Hand Surg Am, 2006. 31(3): p. 359-65.
4. Diaz-Garcia, R.J., et al., *A systematic review of outcomes and complications of treating unstable distal radius fractures in the elderly.* J Hand Surg Am, 2011. 36(5): p. 824-35.e2.
5. Lafontaine, M., et al., *Stability assessment of distal radius fractures.* Injury, 1989. 20(4): p. 208-10.
6. Abbaszadegan, H., et al., *Prediction of instability of Colles' fractures.* Acta Orthop Scand, 1989. 60(6): p. 646-50.
7. Adolphson, P., et al., *Computer-assisted prediction of the instability of Colles' fractures.* Int Orthop, 1993. 17(1): p. 13-5.
8. Hove, L.M., et al., *Prediction of secondary displacement in Colles' fracture.* J Hand Surg Br, 1994. 19(6): p. 731-6.
9. Mackenney, P.J., et al., *Prediction of instability in distal radial fractures.* J Bone Joint Surg Am, 2006. 88(9): p. 1944-51.
10. Nesbitt, K.S., et al., *Assessment of instability factors in adult distal radius fractures.* J Hand Surg Am, 2004. 29(6): p. 1128-38.
11. Walenkamp, M.M., et al., *Predictors of unstable distal radius fractures: a systematic review and meta-analysis.* J Hand Surg Eur Vol, 2016. 41(5): p. 501-15.
12. Dutch Institute for Healthcare Improvement CBO. *Richtlijn Osteoporose en Fractuurpreventie*, 2011.
13. Nederlandse Vereniging voor Heelkunde, *Richtlijn distale radius fracturen: diagnostiek en behandeling*. Richlijnendatabase, 2010.
14. Kanis, J.A., et al., *A reference standard for the description of osteoporosis.* Bone, 2008. 42(3): p. 467-75.
15. Genant, H.K., et al., *Vertebral fracture assessment using a semiquantitative technique.* J Bone Miner Res, 1993. 8(9): p. 1137-48.
16. Manske, S.L., et al., *Human trabecular bone microarchitecture can be assessed independently of density with second generation HR-pQCT.* Bone, 2015. 79: p. 213-21.
17. Pialat, J.B., et al., *Visual grading of motion induced image degradation in high resolution peripheral computed tomography: impact of image quality on measures of bone density and micro-architecture.* Bone, 2012. 50(1): p. 111-8.
18. Agarwal, S., et al., *In vivo assessment of bone structure and estimated bone strength by first- and second-generation HR-pQCT.* Osteoporos Int, 2016. 27(10): p. 2955-66.
19. van Rietbergen, B., et al., *A new method to determine trabecular bone elastic properties and loading using micromechanical finite-element models.* J Biomech, 1995. 28(1): p. 69-81.
20. de Jong, J.J., et al., *Assessment of the healing process in distal radius fractures by high resolution peripheral quantitative computed tomography.* Bone, 2014. 64: p. 65-74.
21. Pistoia, W., et al., *Image-based micro-finite-element modeling for improved distal radius strength diagnosis: moving from bench to bedside.* J Clin Densitom, 2004. 7(2): p. 153-60.
22. Mueller, T.L., et al., *Computational finite element bone mechanics accurately predicts mechanical competence in the human radius of an elderly population.* Bone, 2011. 48(6): p. 1232-8.
23. Hosseini, H.S., et al., *Fast estimation of Colles' fracture load of the distal section of the radius by homogenized finite element analysis based on HR-pQCT.* Bone, 2017. 97: p. 65-75.
24. Batra, S. and Gupta, A., *The effect of fracture-related factors on the functional outcome at 1 year in distal radius fractures.* Injury, 2002. 33(6): p. 499-502.
25. Abbaszadegan, H., et al., *Late displacement of Colles' fractures.* Int Orthop, 1988. 12(3): p. 197-9.
26. Altissimi, M., et al., *Early and late displacement of fractures of the distal radius. The prediction of instability.* Int Orthop, 1994. 18(2): p. 61-5.
27. Clayton, R.A., et al., *Association between decreased bone mineral density and severity of distal radial fractures.* J Bone Joint Surg Am, 2009. 91(3): p. 613-9.
28. Robin, B.N., et al., *Relationship of bone mineral density of spine and femoral neck to distal radius fracture stability in patients over 65.* J Hand Surg Am, 2014. 39(5): p. 861-6.e3.
29. Alemdaroglu, K.B., et al., *Three-point index in predicting redisplacement of extra-articular distal radial fractures in adults.* Injury, 2010. 41(2): p. 197-203.
30. LaMartina, J., et al., *Predicting alignment after closed reduction and casting of distal radius fractures.* J Hand Surg Am, 2015. 40(5): p. 934-9.
31. D'Elia, G., et al., *Bone fragility and imaging techniques.* Clin Cases Miner Bone Metab, 2009. 6(3): p. 234-46.

32. de Jong, J.J.A., et al., *Fracture Repair in the Distal Radius in Postmenopausal Women: A Follow-Up 2 Years Postfracture Using HRpQCT.* J Bone Miner Res, 2016. 31(5): p. 1114-22.
33. Hollevoet, N., et al., *Comparison of palmar tilt, radial inclination and ulnar variance in left and right wrists.* J Hand Surg Br, 2000. 25(5): p. 431-3.
34. van Eerten, P.V., et al., *An X-ray template assessment for distal radial fractures.* Arch Orthop Trauma Surg, 2008. 128(2): p. 217-21.
35. Arealis, G., et al., *Does the CT improve inter- and intra-observer agreement for the AO, Fernandez and Universal classification systems for distal radius fractures?* Injury, 2014. 45(10): p. 1579-84.
36. Kleinlugtenbelt, Y.V., et al., *Classification systems for distal radius fractures.* Acta Orthop, 2017. 88(6): p. 681-687.
37. Li, S.L., et al., *Diagnostic value of CT scan for AO B3 fracture of distal radius.* Beijing Da Xue Xue Bao Yi Xue Ban, 2017. 49(4): p. 675-679.
38. Lill, C.A., et al., *Impact of bone density on distal radius fracture patterns and comparison between five different fracture classifications.* J Orthop Trauma, 2003. 17(4): p. 271-8.
39. Plant, C.E., et al., *Is it time to revisit the AO classification of fractures of the distal radius? Inter- and intra-observer reliability of the AO classification.* Bone Joint J, 2015. 97-b(6): p. 818-23.
40. Yinjie, Y., et al., *A retrospective evaluation of reliability and reproducibility of Arbeitsgemeinschaftfur Osteosynthesefragen classification and Fernandez classification for distal radius fracture.* Medicine (Baltimore), 2020. 99(2): p. e18508.
41. Porrino, J.A., et al., *Fracture of the distal radius: epidemiology and premanagement radiographic characterization.* AJR Am J Roentgenol, 2014. 203(3): p. 551-9.
42. Belloti, J.C., et al., *Are distal radius fracture classifications reproducible? Intra and interobserver agreement.* Sao Paulo Med J, 2008. 126(3): p. 180-5.
43. Wæver, D., et al., *Distal radius fractures are difficult to classify.* Injury, 2018. 49 Suppl 1: p. S29-s32.
44. Dhainaut, A., et al., *Exploring the relationship between bone density and severity of distal radius fragility fracture in women.* J Orthop Surg Res, 2014. 9: p. 57.
45. Jayakumar, P., et al., *AO Distal Radius Fracture Classification: Global Perspective on Observer Agreement.* J Wrist Surg, 2017. 6(1): p. 46-53.
46. Beumer, A. and McQueen M.M., *Fractures of the distal radius in low-demand elderly patients: closed reduction of no value in 53 of 60 wrists.* Acta Orthop Scand, 2003. 74(1): p. 98-100.
47. Levin, L.S., et al., *Distal Radius Fractures in the Elderly.* J Am Acad Orthop Surg, 2017. 25(3): p. 179-187.
48. Meinberg, E.G., et al., *Fracture and Dislocation Classification Compendium-2018.* J Orthop Trauma, 2018. 32 Suppl 1: p. S1-s170.

Supplemental tables

Table S-1. Characteristics of 251 patients with an acceptable and unacceptable primary DRF position

	Primary position unacceptable N = 135	**Primary position acceptable** N = 116	**p-value**
Female	117 (87)	96 (83)	*NS*
Age (y)*	69 [13]	66 [14]	0.015
Weight (kg)*	68.6 [19.1]	73.5 [23.7]	0.035
Height (m)	1.63 ± 0.10	1.63 ± 0.09	*NS*
BMI (kg/m2)*	25.5 [6.2]	27.7 [7.7]	0.048
AO			<0.001
A	61 (45.2)	70 (60.3)	
B	12 (8.9)	24 (20.7)	
C	62 (45.9)	22 (19.0)	
BMI category			*NS*
<30 (non obees)	95 (80.5)	70 (66.0)	
≥30 (obees)	23 (19.5)	36 (34.0)	
Bone densitometry			*NS*
Normal BMD	18 (13.3)	20 (17.2)	
Osteopenia	64 (47.4)	56 (48.3)	
Osteoporosis	53 (39.3)	40 (34.5)	
VFA			*NS*
No VF	116 (85.9)	105 (90.5)	
1Grade 2/3 VF	19 (14.1)	11 (9.5)	
Smoking			*NS*
Never	58 (43.9)	49 (43.3)	
Past smoker	54 (40.9)	50 (44.2)	
Current smoker	20 (15.2)	14 (12.4)	
Alcohol use			*NS*
< 1 unit/day	41 (32.5)	35 (32.4)	
≥ 1 unit/day	85 (67.5)	73 (67.6)	
Calcium intake (mg/day)*	813 [390]	770 [420]	*NS*
25-OH Vitamin D(nmol/l)			*NS*
<30 (deficiency)	13 (9.6)	13 (11.2)	
30-50 (insufficiency)	43 (31.9)	31 (26.7)	
>50 (sufficiency)	79 (58.5)	72 (62.1)	

BMI = body mass index | BMD = bone mineral density | VF= vertebral fracture
Data missing: length (26), weight (26), calcium intake (6), alcohol use (9), smoking (6)
Normally distributed data are presented as mean (SD) | Non normally distributed data * as median [IQR]

Table S-2. Associations of bone microarchitecture and strength with secondary fracture displacement (vs. no secondary fracture displacement) in 30 patients with HR-pQCT at the distal radius

	Odds ratio Unadjusted	**p-value**	**Odds ratio** Age adjusted	**p-value**	**Odds ratio** Primary reduction adjusted	**p-value**
Primary reduction	22.00 [2.27-212.86]	0.008	-	-	-	-
Total area	1.44 [0.65-3.15]	0.376	-	*NS*	-	*NS*
Trabecular area	2.06 [0.89-4.77]	0.092	1.96 [0.81-4.79]	*NS*	3.97 [1.00-15.69]	*NS*
Cortical area	0.46 [0.18-1.18]	0.108	-	*NS*	-	*NS*
Total vBMD	0.27 [0.10-0.73]	0.010	0.31 [0.11-0.85]	0.023	0.16 [0.04-0.68]*^	0.013
Trabecular vBMD	0.55 [0.22-1.33]	0.182	-	*NS*	-	*NS*
Cortical vBMD	0.31 [0.12-0.80]	0.016	0.37 [0.13-0.99]	0.049	0.19 [0.05-0.80]*^	0.024
Trabecular BV fraction	0.61 [0.24-1.53]	0.291	-	*NS*	-	*NS*
Trabecular thickness	1.70 [0.69-4.21]	0.248	-	*NS*	-	*NS*
Trabecular separation	1.90 [0.89-4.06]	0.100	1.75 [0.71-4.32]	*NS*	1.92 [0.70-5.27]	*NS*
Cortical perimeter	1.80 [0.77-4.17]	0.173	-	*NS*	-	*NS*
Cortical porosity	0.63 [0.26-1.54]	0.309	-	*NS*	-	*NS*
Cortical thickness	0.32 [0.13-0.80]	0.015	0.39 [0.15-0.99]	0.050	0.13 [0.02-0.74]*^	0.021
Cortical pore diameter	0.54 [0.20-1.44]	0.215	-	*NS*	-	*NS*
Torsion stiffness	0.82 [0.33-2.06]	0.679	-	*NS*	-	*NS*
Compression stiffness	0.39 [0.13-1.16]	0.090	0.48 [0.16-1.42]	*NS*	0.32 [0.09-1.18]	*NS*
Compression ultimate force	0.39 [0.13-1.19]	0.098	0.48 [0.16-1.46]	*NS*	0.32 [0.09-1.18]	*NS*
Bending stiffness horizontal	0.67 [0.26-1.72]	0.409	-	*NS*	-	*NS*
Bending stiffness vertical	0.95 [0.36-2.50]	0.913	-	*NS*	-	*NS*

OR=odds ratio for secondary fracture dislocation vs no secondary fracture dislocation | ORs for HR-pQCT parameters are presented per standard deviation (SD)

vBMD = volumetric bone mineral density | BV = bone volume | NS = not significant.

* OR of primary reduction in multivariable model:

With total vBMD: OR 71.96 [2.80-1848.20], p 0.010 | With cortical vBMD: OR 62.92 [2.20-1803.45], p 0.016 | With cortical thickness: OR 123.29 [2.82-5388.05], p 0.012

^ AUC of significant HR-pQCT parameters in primary reduction adjusted model:

Total vBMD; AUC = 0.824, 95% CI 0.67-0.98, p 0.003 | Cortical vBMD; AUC = 0.819, 95% CI 0.67-0.97, p 0.003 | Cortical thickness; AUC = 0.787, 95 % CI 0.61-0.96, p 0.009

Table S-3. Associations of bone microarchitecture and strength with secondary fracture displacement (vs. no secondary fracture displacement) in 36 patients with HR-pQCT at the distal tibia

	Odds ratio Unadjusted	**p-value**	**Odds ratio** Age adjusted	**p-value**	**Odds ratio** Primary reduction adjusted	**p-value**
Primary reduction	18.33 [2.02-166.73]	0.010	-	-	-	-
Total area	1.20 [0.62-2.31]	0.585	-	*NS*	-	*NS*
Trabecular area	1.32 [0.69-2.55]	0.406	-	*NS*	-	*NS*
Cortical area	0.48 [0.18-1.27]	0.137	-	*NS*	-	*NS*
Total vBMD	0.35 [0.13-0.92]	0.034	0.40 [0.15-1.05]	0.063	0.06 [0.01-0.64]*	0.020
Trabecular vBMD	0.54 [0.24-1.23]	0.141	-	*NS*	-	*NS*
Cortical vBMD	0.52 [0.24-1.09]	0.085	0.64 [0.28-1.45]	0.286	0.41 [0.16-1.04]	*NS*
Trabecular BV fraction	0.55 [0.24-1.26]	0.157	-	*NS*	-	*NS*
Trabecular thickness	1.03 [0.51-2.10]	0.926	-	*NS*	-	*NS*
Trabecular separation	1.00 [0.54-1.86]	0.990	-	*NS*	-	*NS*
Cortical perimeter	1.32 [0.67-2.61]	0.424	-	*NS*	-	*NS*
Cortical porosity	0.96 [0.49-1.91]	0.918	-	*NS*	-	*NS*
Cortical thickness	0.44 [0.18-1.12]	0.085	0.58 [0.23-1.46]	0.248	0.22 [0.06-0.84]*	0.027
Cortical pore diameter	0.37 [0.14-0.94]	0.036	0.48 [0.20-1.20]	0.117	0.38 [0.14-1.09]	*NS*
Torsion stiffness	0.82 [0.36-1.86]	0.630	-	*NS*	-	*NS*
Compression stiffness	0.55 [0.22-1.37]	0.196	-	*NS*	-	*NS*
Compression ultimate force	0.68 [0.30-1.53]	0.345	-	*NS*	-	*N.S*
Bending stiffness horizontal	0.91 [0.43-1.93]	0.813	-	*NS*	-	*NS*
Bending stiffness vertical	0.79 [0.35-1.81]	0.578	-	*NS*	-	*NS*

OR=odds ratio for secondary fracture dislocation vs no secondary fracture dislocation | ORs for HR-pQCT parameters are presented per standard deviation (SD).

vBMD = volumetric bone mineral density | BV = bone volume | NS = not significant.

* OR of primary reduction in multivariable model:

With total vBMD: 251.94 [3.90-16274.94], p 0.009 | With cortical thickness: OR 46.34 [3.10-692.30], p 0.005

^ AUC of significant HR-pQCT parameters in primary reduction adjusted model:

Total vBMD; AUC = 0.731, 95% CI 0.55-0.91, p 0.026 | Cortical thickness; AUC = 0.719, 95% CI 0.53-0.90, p 0.035

Chapter 4

The feasibility of High Resolution peripheral Quantitative CT in patients with suspected scaphoid fractures

M.S.A.M. Bevers, A.M. Daniels, C.E. Wyers, B. van Rietbergen, P.P.M.M. Geusens, S. Kaarsemaker, H.M.J. Janzing, P.F.W. Hannemann, M. Poeze, J.P. van den Bergh

J Clin Densitom. 2020; 23(3):432-442

Abstract

Introduction
Diagnosing scaphoid fractures remains challenging. High-resolution peripheral quantitative computed tomography (HR-pQCT) might be a potential imaging technique, but no data are available on its feasibility to scan the scaphoid bone in vivo.

Methodology
Patients (≥18 years) with a clinically suspected scaphoid fracture received an HR-pQCT scan of the scaphoid bone (three 10.2-mm stacks, 61-mm voxel size) with their wrist immobilized with a cast. Scan quality assessment and bone contouring were performed using methods originally developed for HR-pQCT scans of radius and tibia. The contouring algorithm was applied on coarse hand drawn pre-contours of the scaphoid bone and the resulting contours (AUTO) were manually corrected (sAUTO) when visually deviating from bone margins. Standard morphologic analyses were performed on the AUTO- and sAUTO-contoured bones.

Results
Ninety-one patients were scanned. Two out of the first five scans were repeated due to poor scan quality (40%) based on standard quality assessment during scanning, which decreased to three out of the next 86 scans (3.5%) when using an additional thumb cast. Nevertheless, after excluding one scan with an incompletely scanned scaphoid bone, post hoc grading revealed a poor quality in 14.9% of the stacks and 32.9% of the scans in the remaining 85 patients. After excluding two scans with contouring problems due to scan quality, bone indices obtained by AUTO- and sAUTO-contouring were compared in 83 scans. All AUTO contours were manually corrected, resulting in significant but small differences in densitometric and trabecular indices (<1.0%).

Conclusions
In vivo HR-pQCT scanning of the scaphoid bone is feasible in patients with a clinically suspected scaphoid fracture when using a cast with thumb part. The proportion of poor quality stacks is similar to radius scans and AUTO-contouring appears appropriate in good- and poor-quality scans . Thus, HR-pQCT may be promising for diagnosis of and microarchitectural evaluations in suspected scaphoid fractures.

Introduction

Scaphoid fractures account for approximately 60%-75% of all carpal fractures [1-4] and can have long-term complications when they are not immediately treated. The treatment is usually conservative (i.e. cast) for stable and nondisplaced fractures and operative (e.g. screw fixation) for unstable or displaced fractures [5]. A delay in treatment may cause healing complications, increased healing time and an increased risk for a scaphoid nonunion [6,7]. A scaphoid nonunion, in turn, is challenging to treat successfully and can cause carpal instability and osteoarthritis [8].

Early diagnosis and adequate treatment of scaphoid fractures is thus important, but immediate diagnosis remains challenging. Plain radiography is typically used at initial presentation, but misses up to 25% of scaphoid fractures compared to magnetic resonance imaging, computed tomography and bone scintigraphy [9]. While these advanced imaging techniques have a better sensitivity and specificity than radiography [10,11], they lack good positive predictive values and their improved sensitivity is generally associated with a reduced specificity and vice versa [12,13]. Consequently, there is no consensus today on a gold standard imaging technique for scaphoid fractures [14,15]. High-resolution peripheral quantitative CT (HR-pQCT) may be a potential alternative imaging technique. It is a noninvasive technique that provides 3-dimensional images of peripheral bones at a low radiation dose and with a spatial resolution higher than currently used imaging techniques [16]. Its high resolution may enable recognizing more and smaller scaphoid fractures than currently used techniques and enables microarchitectural bone evaluations of (fractured) scaphoid bones, which have already provided new insights into fracture mechanism, nonunion etiology and optimal screw fixation and design in cadaveric bones [17-21].

Although the use of HR-pQCT in scaphoid fractures may thus be interesting for diagnostic and research purposes, the feasibility of in vivo HR-pQCT scanning of the scaphoid bone is not yet fully explored. To our knowledge, Reina et al performed the only in vivo HR-pQCT study on the scaphoid bone thus far, investigating the patterns in trabecular bone between normal dominant and nondominant radial carpal bones [22]. In that study, nothing was reported about motion artefacts or image quality of the HR-pQCT scans. However, it is unknown whether subject motion is comparable or worse in scaphoid bone scans compared to radius or tibia scans as three stacks rather than one are needed to capture the entire scaphoid bone [23] and whether image quality is adequate for application in clinical practice. This study, therefore, explored the feasibility of in vivo HR-

pQCT scanning of the scaphoid bone in patients with a clinically suspected scaphoid fracture. Scan-quality assessment and scaphoid bone contouring were performed using methods originally developed for HR-pQCT scans of radius and tibia and differences in bone indices were determined between contours with and without manual correction.

Methodology

Study design and population

All consecutive patients (aged ≥18 years) presenting between December 2017 and October 2018 at the emergency department of VieCuri Medical Centre Venlo (The Netherlands) within one week after trauma with a clinically suspected scaphoid fracture were eligible for study participation. Patients were excluded in case of pregnancy or a previous ipsilateral scaphoid fracture in medical history. All included patients gave written consent prior to participation. The study protocol (METC registration number NL62476.068.17) was approved by an independent Medical Ethics Committee and complied with the Declaration of Helsinki of 1975, revised in 2000.

The included patients followed the standard diagnostic protocol for suspected scaphoid fractures. They were subjected to standard plain radiography at initial presentation followed by immobilization of the wrist with a synthetic nonfiberglass cast. Within 10 days after initial presentation, a clinical reassessment was performed to determine treatment strategy. In addition to this standard protocol and independent of the outcome of the clinical reassessment, all included patients received an HR-pQCT scan.

HR-pQCT imaging

HR-pQCT (XtremeCTII, Scanco Medical, Switzerland) scans of the scaphoid bone were performed on a 30.6-mm region of the wrist (3 consecutive 10.2-mm stacks) with the reference line at the longitudinal sagittal ridge between the scaphoid bone and lunate fossa at the articular surface of the distal radius [Figure 1]. During scanning, the wrist was immobilized with a synthetic nonfiberglass cast and standard motion restraining holders for HR-pQCT scanning were used. Synthetic casts have been found to affect scan quality and bone parameters only marginally [24]. Total scan time was 6.0 min, subjecting the patients to an effective radiation dose of approx 15 mSv. X-ray tube voltage and intensity were 68 kV and 1460 mA respectively and integration time was 43 ms. The images were reconstructed using an isotropic voxel size of 61 mm, resulting in 504 consecutive slices [25].

Figure 1. Scout view showing the reference line used to scan the scaphoid bone (left) and a 3-dimensional view of the scanned region of the wrist (right top) and scaphoid bone (right bottom)

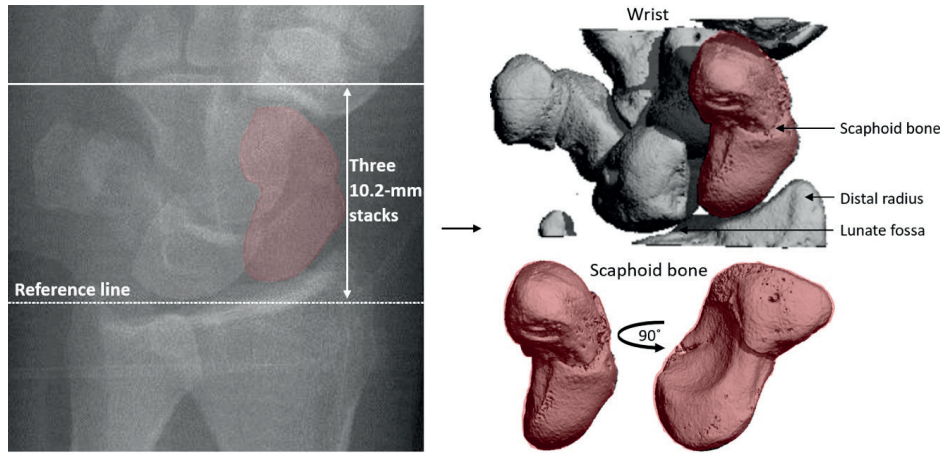

Scan-quality assessment

Scan quality was graded using the grading system used by Pialat et al. to grade HR-pQCT scans of radius and tibia [26]. A single low-resolution slice of each stack of the scans was graded by the operator during scan acquisition (standard grading). Scans were completely repeated once when the quality of at least one stack had a grade >3. The scan with the best quality in the 3 stacks was included for further analyses. Additionally, scan quality was post hoc graded by one researcher using the same grading system on multiple full-resolution slices of each stack (post hoc grading). More specifically, the first slice in which the scaphoid bone appeared was determined and from that slice on every tenth slice was graded. Based on these gradings, an overall grade was determined for each stack. The scan was assigned a good quality when each of the three stacks had a grade 1-3 and a poor quality when at least one stack had a grade >3.

Scaphoid fracture assessment

All HR-pQCT scans were evaluated by an experienced radiologist to assess fractures.

Scaphoid bone contouring

To investigate the quantitative potential of HR-pQCT in scaphoid bones, the scaphoid bones were contoured in the scans. Initially, the automatic contouring algorithm, originally developed to contour radius and tibia and similar to the algorithm for automatic contouring of the periosteal and endosteal margins of radius and tibia [27], was used to contour the scaphoid bone. However, its application on the scaphoid bone scans resulted in severe contouring problems, including contouring the wrong bone [Figure 2A] and multiple bones [Figure 2B].

Therefore, its application was changed from the entire scan of the scaphoid bone to coarse hand-drawn precontours of the bone. Moreover, the lower threshold for binarization was changed from the default 120-105 per 1000 as the cortex of the scaphoid bone is thinner and less mineralized than that of radius and tibia. The resulting contouring algorithm (AUTO) thus comprised manual drawing of coarse precontours of the scaphoid bone followed by application of the automatic contouring algorithm with adjusted settings on these coarse contours, which solved the problems of applying the contouring algorithm on entire scans [Figure 2C, Figure 2D]. As a separate study procedure, the obtained AUTO contours were manually corrected (sAUTO) by one researcher when visually deviating from the margins of the scaphoid bone.

Figure 2. Problems of the automatic contouring algorithm originally developed for radius and tibia in contouring the correct bone (A) and only one bone (B). These problems were solved when applying the algorithm on coarse hand-drawn pre-contours of the scaphoid bone (C, D).

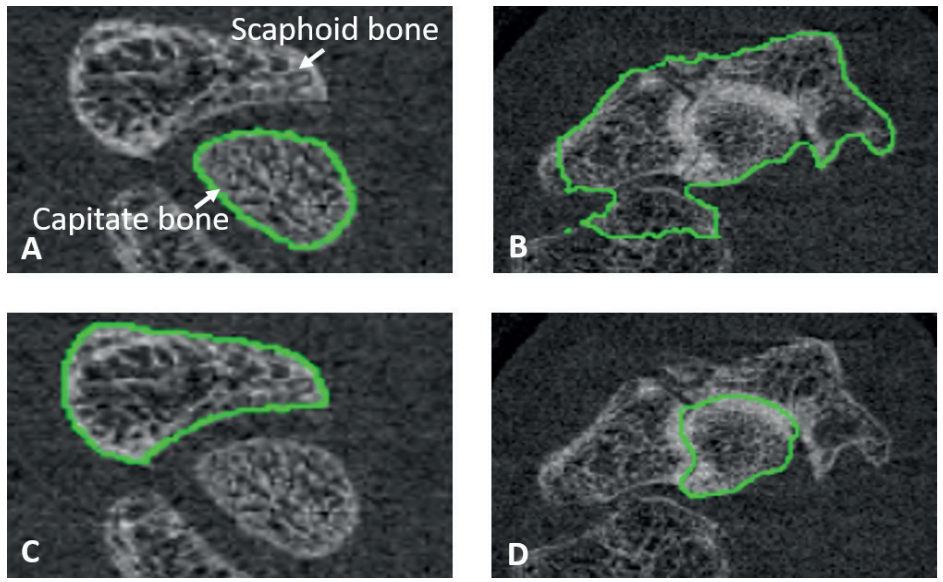

Quantitative analysis

Standard morphologic analyses were performed on the AUTO- and sAUTO-contoured scaphoid bones. Bone and tissue mineral density (BMD and TMD, respectively) were determined, as were the ratio of bone volume to total bone volume (BV/TV) and trabecular number (Tb.N), thickness (Tb.Th) and separation (Tb.Sp). The trabecular indices were calculated using distance transformation [28]. Cortical indices were not determined because of the lack of a clear cortical layer in the scaphoid bone.

Statistical analysis

The quantitative measures obtained were statistically analyzed (IBM SPSS Statistics for Windows, Version 25.0. Armonk, NY: IBM Corp). Normality of the distribution of the data was analyzed using Shapiro-Wilk tests. Differences in patient characteristics between poor-and good-quality scans were analyzed using Mann-Whitney U and chi-square tests and determinants of scan quality using uni- and multivariate binomial logistic regression models with covariates age, gender and the presence of a scaphoid fracture. Differences in bone indices between the AUTO- and sAUTO-contoured scaphoid bones were analyzed using paired-sample t tests or related-samples Wilcoxon signed rank tests and performed on the entire dataset and on subgroups with either good-quality scans (grade 1-3 for all three stacks of a scan), poor-quality scans (grade 4-5 for at least one of the three stacks), scans with a scaphoid fracture, or scans without a scaphoid fracture. Additionally, the differences in bone indices between both contouring methods were compared between the good- and poor-quality scans and between the scans with and without a scaphoid fracture within the subgroups of poor- and good-quality scans using Mann-Whitney U tests. All tests were 2-sided and the significance level was set at 0.05.

Results

Patient characteristics

Ninety-one patients were included in the study, 45 men (49.5%) and 46 women with a median age of 37 ± 32 and 62 ± 24 yr, respectively. Twenty-four patients (26.4%) were diagnosed with a scaphoid fracture (15 men and 9 women) based on the HR-pQCT scans. Median time between initial presentation at the emergency department and HR-pQCT scanning was nine days (range 2-13 days).

The scans of six patients were excluded from further analyses [Figure 3A]. The scans of the first five patients were excluded: the scans of two out of these first patients (40%) had to be repeated due to a poor quality based on the standard grading. In an attempt to reduce this proportion, the next patients received the original cast [Figure 4A] extended with a temporary thumb part [Figure 4B]. This adaptation lowered the proportion of rescanning due to poor quality to 3.5% (three out of 86 scans). Only these 86 scans were included in further analyses to keep uniformity in casting procedure among patients. Of these scans, one scan was excluded because the scaphoid bone was not entirely scanned due to a wrong positioning of the wrist in the scanner, resulting in a total of 85 included scans [Figure 3A].

Figure 3. Flow-chart of the included scans for the determination of patient characteristics of poor- and good-quality scans based on the standard grading and post hoc grading (A) and scaphoid bone contouring (B).

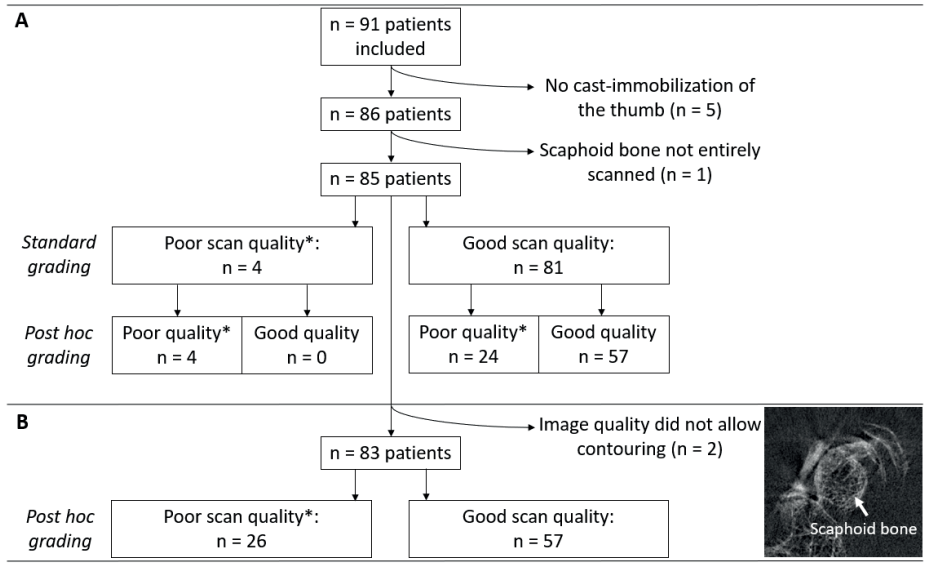

*A scan with at least one of the three stacks having a grade >3 due to motion artifacts

Scan-quality assessment

Based on the standard grading, four out of the 85 scans (4.7%) were assessed as poor quality, while 28 scans (32.9%) were assessed as poor quality based on the post hoc grading [Figure 3A, Table 1]. Although the standard grading assessed scans as poor quality that were also assessed as poor quality during the post hoc grading, it missed 24 poor-quality scans compared to the post hoc grading [Figure 3A]. Patients with poor-quality scans based on the post hoc grading were significantly older than those with good-quality scans [Table 1] and logistic regression models showed age to be significantly associated with scan quality in a univariate model (OR_{10yrs} = 1.47, 95% CI = 1.13-1.92) and in multivariate models with gender and/or the presence of a scaphoid fracture as other covariates [Table S-1]. More than half of the poor-quality scans had only one poor-quality stack (75.0% and 64.3% for standard grading and post hoc grading, respectively) [Table 1]. Stated differently, the post hoc grading revealed 18 of 85 scans (21.2%) to have a poor quality in only one stack (21.2%) and 38 of 255 stacks (14.9%) to be of poor quality, which was the middle stack in 50% of the scans (Table 1). Scans with multiple poor quality stacks had a poor-quality proximal and distal stack in 50% of the cases [post hoc grading; Table 1].

Scaphoid bone contouring

The scans of two patients out of the 85 included scans were excluded from quantitative analyses because their scan quality did not allow contouring, resulting in 83 scans [Figure 3B].

The AUTO-algorithm solved the problems of the automatic algorithm [Figure 2], but incorrectly contoured the scaphoid bone in the first and last few slices due to its anatomy, which required manual contour corrections (sAUTO) in all 83 scans [Figure 5A], as well as scaphoid bones with (displaced) fractures [Figure 5B], small joint spaces due to rheumatoid arthritis or osteoarthritis [Figure 5C] or thin subchondral bone layers [Figure 5D] and scaphoid bones in poor-quality scans [Figure 5E]. The sAUTO-contours resulted in significant, but small differences in bone indices [Table 2, Figure 6A]. In the subgroups of good- and poor-quality scans (post hoc grading), all indices were significantly different between the AUTO and sAUTO-contoured scaphoid bones except for Tb.N and BV/TV, respectively [Table 3]. Nevertheless, all differences were <0.5% (except Tb.Th <1.0%) [Figure 6A].

Percentage differences between both contouring methods were in general larger in the poor-quality scans and reached statistical significance for TMD and the trabecular indices [Figure 6A]. Within the subgroup of poor-quality scans, differences between the AUTO- and sAUTO-contoured bones were in general larger in scans with multiple poor-quality stacks or a poor-quality middle stack than in those with one poor-quality stack or a poor-quality proximal or distal stack [Figure S-1]. In the subgroups of scans with and without a scaphoid fracture, all indices were significantly different between the AUTO- and sAUTO-contoured bones except for Tb.N in the former and BV/TV in the latter subgroup [Table 4]. Percentage differences disseminated significantly between scans with and without a scaphoid fracture for TMD within the subgroup of good-quality scans

(post hoc grading) and for BV/TV, BMD and Tb.N within the subgroup of poor-quality scans [Figure 5B].

Table 1. Patient characteristics according to scan quality

	Standard grading			*Post hoc* grading		
	Good quality Grade 1-3	**Poor quality** Grade >3	**p-value**	**Good quality** Grade 1-3	**Poor quality** Grade >3*	**p-value**
Scaphoid fracture	21 (100.0)	0 (0.0)	0.241	16 (76.2)	5 (23.8)	0.305
No scaphoid fracture	60 (93.8)	4 (6.3)		41 (64.1)	23 (35.9)	
Male gender	41 (50.6)	1 (25.0)	0.317	29 (50.9)	13 (46.4)	0.700
Age (years)	52 [38]	59.5 [29]	0.328	47 [37]	64.5 [64]	0.003
Quality distribution over stacks						
One stack	-	3 (75.0)		-	18 (64.3)	
Proximal stack		1 (33.3)			3 (16.7)	
Middle stack		0 (0.0)			9 (50.0)	
Distal stack		2 (66.7)			6 (33.3)	
Two stacks	-	1 (25.0)		-	10 (35.7)	
Proximal & middle stack		1 (100.0)			3 (30.0)	
Proximal & distal stack		0 (0.0)			5 (50.0)	
Middle & distal stack		0 (0.0)			2 (20.0)	
Three stacks	-	0** (0.0)		-	0** (0.0)	

**One scan had a scaphoid bone covering only two stacks that were both of poor quality, but is included in the 'Two stacks'-groupData are presented as number (%) | Age is presented as median [IQR]

Table 2. Difference in densitometric (BV/TV, BMD, TMD) and trabecular structural (Tb.N, Tb.Th, Tb.Sp) bone parameters between automatically contoured scaphoid bone (AUTO) and manually corrected contours (sAUTO)

	AUTO (n=83)	**sAUTO (n=83)**	**Difference**	**p-value**
BV/TV [%]	53.0 ± 7.85	53.0 ± 7.92	-0.0400 ± 0.130	0.004
BMD [mg HA/CC]	375 ± 59.7	375 ± 60.2	-0.574 ± 0.954	<0.001
TMD [mg HA/CC]	769 ± 29.4	770 ± 29.4	-0.834 ± 0.859	<0.001
Tb.N [mm-1]	1.75 ± 0.159	1.76 ± 0.160	-0.00120 ± 0.00340	0.002
Tb.Th [mm]	0.450 ± 0.0816	0.448 ± 0.0811	0.00220 ± 0.00260	<0.001
Tb.Sp [mm]	0.521 ± 0.0731	0.522 ± 0.0733	-0.000900 ± 0.00140	<0.001

Table 3. Difference in densitometric and trabecular structural bone parameters between automatically contoured scaphoid bone (AUTO) and manually corrected contours (sAUTO) for the subgroups of good- and poor-quality scans based on post hoc grading.

	Good quality N=57				**Poor quality N=26**			
	AUTO	**sAUTO**	**Difference**	**p-value**	**AUTO**	**sAUTO**	**Difference**	**p-value**
BV/TV [%]	53.5 ± 7.81	53.6 ± 7.84	-0.0400 ± 0.0700	<0.001	51.7 ± 7.93	51.8 ± 8.10	-0.0400 ± 0.220	0.304
BMD [mg HA/CC]	381 ± 61.4	381 ± 61.7	-0.464 ± 0.517	<0.001	362 ± 54.9	363 ± 56.1	-0.813 ± 1.52	0.011
TMD [mg HA/CC]	774 ± 30.7	775 ± 30.8	-0.447 ± 0.435	<0.001	757 ± 22.5	758 ± 22.6	-1.68 ± 0.949	<0.001
Tb.N [mm^{-1}]	1.73 ± 0.148	1.73 ± 0.148	-0.0002 ± 0.0020	0.516	1.81 ± 0.168	1.82 ± 0.172	-0.0034 ± 0.0047	0.001
Tb.Th [mm]	0.450 ± 0.0886	0.449 ± 0.0881	0.0011 ± 0.0014	<0.001	0.451 ± 0.0651	0.446 ± 0.0648	0.0047 ± 0.0027	<0.001
Tb.Sp [mm]	0.526 ± 0.0690	0.526 ± 0.0692	-0.00050 ± 0.0012	0.003	0.511 ± 0.0818	0.513 ± 0.0825	-0.0018 ± 0.0015	<0.001

Data are presented as mean ± SD

Table 4. Difference in densitometric and structural bone parameters between automatically contoured scaphoid bone (AUTO) and manually corrected contours (sAUTO) for the subgroups of scans with and without a scaphoid fracture based on the HR-pQCT scans

	Scans with scaphoid fracture N=21				**Scans without scaphoid fracture N=62**			
	AUTO	**sAUTO**	**Difference**	**p-value**	**AUTO**	**sAUTO**	**Difference**	**p-value**
BV/TV [%]	56.0 ± 6.03	56.1 ± 6.12	-0.0900 ± 0.130	0.004	51.9 ± 8.17	52.0 ± 8.23	-0.0300 ± 0.130	0.113
BMD [mg HA/CC]	395 ± 39.9	396 ± 40.5	-0.825 ± 1.09	0.002	368 ± 63.9	369 ± 64.4	-0.489 ± 0.899	<0.001
TMD [mg HA/CC]	762 ± 31.6	763 ± 31.4	-0.562 ± 0.833	0.006	771 ± 28.6	772 ± 28.5	-0.926 ± 0.854	<0.001
Tb.N [mm^{-1}]	1.80 ± 0.186	1.81 ± 0.189	-0.00190 ± 0.00490	0.086	1.74 ± 0.146	1.74 ± 0.147	-0.000900 ± 0.00270	0.011
Tb.Th [mm]	0.458 ± 0.0628	0.457 ± 0.0619	0.00150 ± 0.00200	0.003	0.447 ± 0.0873	0.445 ± 0.0869	0.00250 ± 0.00270	<0.001
Tb.Sp [mm]	0.495 ± 0.0832	0.495 ± 0.0830	-0.000600 ± 0.00110	0.010	0.530 ± 0.0677	0.531 ± 0.0681	-0.00100 ± 0.00150	<0.001

Data are presented as mean ± SD

Figure 4. Synthetic nonfiberglass cast used to immobilize the wrist during scanning; original cast (A) and the original cast (black) extended with an removable thumb cast (blue) seen from a dorsal (top) and volar (bottom) perspective (B)

Figure 5. The automatic contouring algorithm applied on coarse hand-drawn precontours (AUTO) incorrectly contoured the scaphoid bone at the first (A1) and last (A2) slices and in case of (displaced) fractures (B), small joint spaces (C), thin subchondral bone layers (D) and poor scan quality (E)

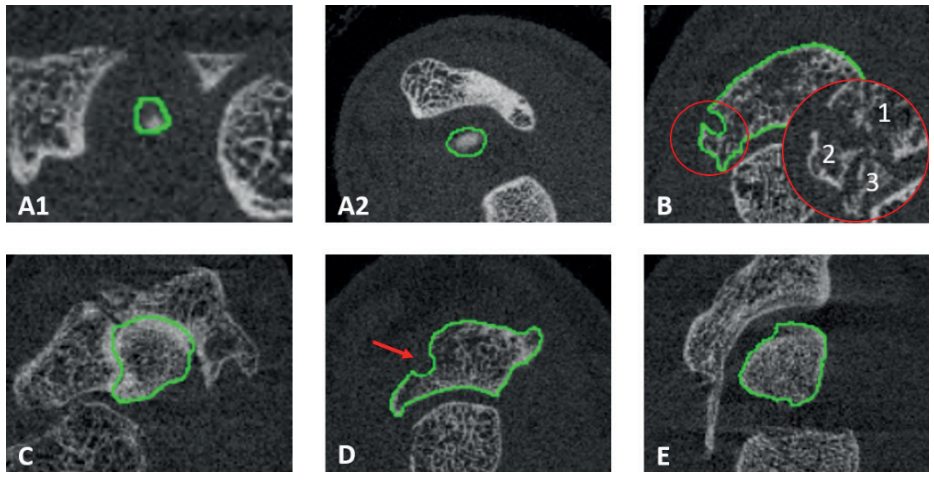

Figure 6. Difference in bone indices between the automatically contoured scaphoid bone without (AUTO) and with (sAUTO) manual corrections for all scans, good-quality scans and poor-quality scans (A) and for good- and poor-quality scans with and without fractured scaphoid bones (B)

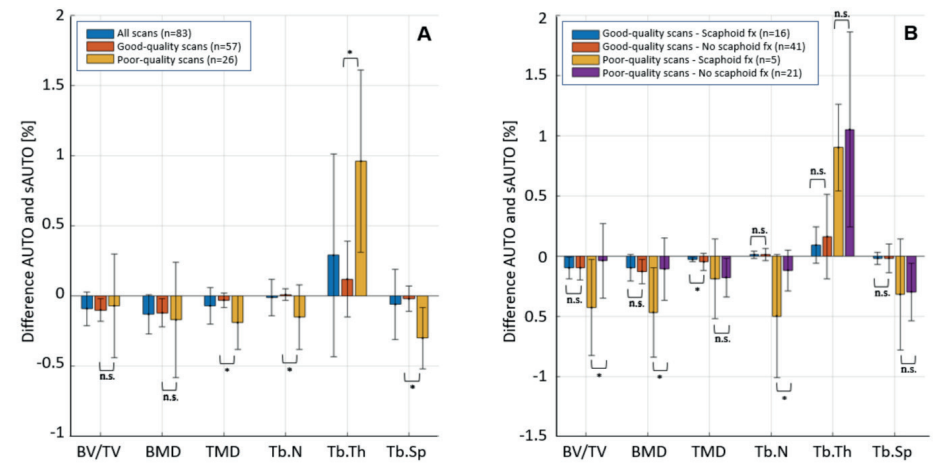

Data are presented as median percentage and IQR | Scan quality is based on *post hoc* grading

Discussion

This study showed that in vivo HR-pQCT scanning of the scaphoid bone is feasible in patients with a clinically suspected scaphoid fracture. The number of repeated scans considerably decreased by extending the wrist immobilizing cast, worn during scanning, with a temporary thumb part. The proportion of post hoc graded poor-quality stacks (14.9%) was considerably lower than of poor-quality scans (32.9%). Manual corrections were needed in the AUTO contours of all scans, but the resulting differences in bone indices were <1% for all bone indices in good- and poor-quality scans and scans with and without a scaphoid fracture.

A wrist- and thumb-immobilizing cast was necessary to reduce motion artifacts. While 40% of the first five scans had to be repeated due to motion artifacts using the original cast based on the standard grading during scan acquisition, extension of this cast with a thumb part lowered this proportion to 3.5%. An additional thumb cast is therefore recommended in future HR-pQCT studies scanning patients with a suspected scaphoid fracture.

Despite this adjusted cast, still 32.9% of the scans were post hoc assessed as poor quality, which is considerably higher than the poor-quality rate in 1-stack radius scans (3-19%) [29-32]. This relatively large poor-quality rate may have been caused by movement excursions due to the more distal scan region for scaphoid bone scans [29,31], which seemed to be more common in older patients considering the age dependency in scan quality. Also the necessity to scan three stacks to capture the entire scaphoid bone rather than one stack may explain the relatively large poor-quality rate as the proportion of poorquality stacks (14.9%) is in agreement with the poor-quality rates in the radius. This comparable poor-quality stack rate and the recent approved clinical use of HR-pQCT for osteoporosis assessment in adult patients may suggest that the image quality of HR-pQCT is sufficient for diagnosis of scaphoid fractures, but this needs to be further investigated.

Adequate image quality is also required for microarchitectural bone evaluations. Previous studies recommended to repeat or exclude poor-quality radius and tibia scans (i.e. 1-stack scans with grade >3) because of their influence on bone indices [33], but these recommendations might be different for scaphoid bone scans (i.e. 3-stack scans). Because bone indices are determined over the entire bone, the relative BV affected by subject motion likely influences the effect of subject motion on bone indices. This idea is reinforced by our finding that bone indices were more influenced by manual contour corrections in poor-quality scans with multiple poor-quality stacks or a poor-quality middle stack than in scans with one poor-quality stack or a poor-quality proximal or distal stack. Possibly, an additional distinction within 3-stack poor-quality scans based on relative motion affected BV might reduce the number of scaphoid bone scans that should be repeated or excluded from quantitative analyses, which requires a reproducibility study on the effects of subject motion on bone indices [26].

Microarchitectural evaluations require also proper bone contouring. Applied on coarse hand-drawn precontours, the standard algorithm for automatic radius and tibia contouring appeared to correctly contour the scaphoid bone. Although manual corrections were necessary in all scans, they caused differences in bone indices (<0.5%, except Tb.Th <1.0%) smaller than the voxel size of the scans and smaller than longitudinal bone changes in radius and tibia due to ageing, treatment, or repeated scans [26,32,34,35]. It is thus questionable whether manual corrections are needed, especially when taking into account time consumption (5-15 min for good-quality scans and 30-60 min for poor-quality scans) and expected interobserver variability and reduced reproducibility [36]. The ability to automatically contour the scaphoid bone on HR-pQCT scans allows for microarchitectural bone evaluations in suspected scaphoid fractures and possibly also for research into the healing process of these fractures [32].

Although this study was the first to explore the feasibility of in vivo HR-pQCT scanning of the scaphoid bone and used a uniform protocol and cast for every patient to allow between-patient comparison [24], it had several limitations. First, only one researcher post hoc graded scan quality and manually corrected contours, whereas both are known to be subjective in radius and tibia scans [26,36]. The subjectivity in grading may be even larger in scaphoid bone scans considering the discrepancy between standard and post hoc grading of 85.7% (i.e. the standard grading missed 85.7% of the scans that were post hoc assessed as poor quality), which is considerably higher than the 12% reported in literature on 1-stack radius and tibia scans (i.e. theoretically 36% in 3-stack scans) [26]. Our large discrepancy may possibly be caused by difficulties in applying the existing quality-grading criteria on scaphoid bone scans as one criteria is based on the continuity of the cortical layer, which is extremely thin in the scaphoid bone and which has small interruptions that could reflect transcortical vascular entries rather than cortical discontinuities due to motion artifacts [37]. Further research should therefore investigate inter- and intraobserver variability in grading and manually correcting contours and address the applicability of existing grading systems to scaphoid bone scans. Second, in this study the newest second-generation HR-pQCT scanner was used, whereas many first-generation systems are still in use. The use of the first-generation scanner would have likely resulted in a larger proportion of poor-quality scans because of a longer scanning time (8.4 min for a 27.1-mm scan using the first-generation 82 mm-resolution scanner and 6.0 min for a 30.6-mm scan using the second-generation 61 mm-resolution scanner [25]). The ability to automatically contour the scaphoid bone, on the other hand, would likely not have been different. Third, stack shifts were observed in the scans of some patients. Although these shifts could have influenced bone indices, they were not accounted for in the analyses because of their expected limited effect on bone indices. Fourth, although the comparable poor-quality stack rate and the recent approved clinical use of HR-pQCT for osteoporosis assessment in adult patients indicates that the image quality of HR-pQCT may be sufficient for diagnosis of scaphoid fractures, its diagnostic performance for scaphoid fractures is currently not known and it has to be further studied which quality of HR-pQCT scans is needed for adequate diagnosis of these fractures. Fifth, gender was not taken into account in the analyses despite the epidemiological differences between men and women with a fractured scaphoid bone.

In conclusion, in vivo HR-pQCT scanning of the scaphoid bone is feasible in patients with a clinically suspected scaphoid fracture when using a cast with thumb part during scanning. The proportion of poor-quality stacks is similar to radius and tibia scans and automatic contouring starting from coarse hand-drawn precontours is appropriate. HR-pQCT may be promising for diagnosis of scaphoid fractures, for microarchitectural bone evaluations in patients with a suspected scaphoid fracture and possibly also for research into the healing process of scaphoid fractures.

References

1. Hove, L.M., *Epidemiology of scaphoid fractures in Bergen, Norway*. Scand J Plast Reconstr Surg Hand Surg, 1999. 33:423–426.
2. Dennis, H.H.W., et al., *Prevalence of carpal fracture in Singapore*. J Hand Surg, 2011. 36:278–283.
3. Van Onselen, E.B.H., et al., *Prevalence and distribution of hand fractures*. J Hand Surg, 2003. 28:491–495.
4. Holloway, K.L., et al., *Carpal and scaphoid fracture incidence in south-eastern Australia: an epidemiologic study*. Arch Osteoporos, 2015. 10:10.
5. Arsalan-Werner, A., et al., *Current concepts for the treatment of acute scaphoid fractures.* Eur J Trauma Emerg Surg, 2016. 42:3–10.
6. Eddeland, A., et al.,*Fractures of the scaphoid.* Scand J Plast Reconstr Surg, 1975. 9:234–239.
7. Langhoff, O. and Andersen, J.L., *Consequences of late immobilization of scaphoid fractures*. J Hand Surg 1988. 13:77–79.
8. Mack, G.R., et al., *The natural history of scaphoid non-union*. J Bone Joint Surg Am, 1984. 66:504–509.
9. Brooks, S., et al., *The management of scaphoid fractures*. J Sci Med Sport, 2005. 8:181–189.
10. Carpenter, C.R., et al., *Adult scaphoid fracture*. Acad Emerg Med, 2014. 21:101–121.
11. Yin, Z.G., et al., *Diagnostic accuracy of imaging modalities for suspected scaphoid fractures*. J Bone Joint Surg, 2012. 94-B:1077–1085 British volume.
12. Groves, A.M., et al., *16 detector multislice CT versus skeletal scintigraphy in the diagnosis of wrist fractures: value of quantification of 99Tcm-MDP uptake.* Br J Radiol, 2005. 78:791–795.
13. Mallee, W., et al*., Comparison of CT and MRI for diagnosis of suspected scaphoid fractures*. JBJS, 2011. 93:20.
14. Groves, A.M., et al., *An international survey of hospital practice in the imaging of acute scaphoid trauma*. Am J Roentgenol, 2006. 187:1453–1456.
15. Smith, J.E., et al., *The management of suspected scaphoid fractures in English hospitals: a national survey.* Eur J Emerg Med, 2016. 23:190.
16. Burghardt, A.J., Krug, R. and Majumdar, S., *Highresolution imaging techniques for bone quality assessment*. Vitamin D, 2018.
17. Su-Bum, A.L., et al., *Osseous microarchitecture of the scaphoid: cadaveric study of regional variations and clinical implications*. Clin Anat, 2012. 25:203–211.
18. Qu, G. and von Schroeder, H.P., *Trabecular microstructure at the human scaphoid nonunion*. J Hand Surg. 2008. 33:650–655.
19. Leventhal, E.L., et al., *A computational approach to the "optimal" screw axis location and orientation in the scaphoid bone.* J Hand Surg, 2009. 34:677–684.

20. Varga P, Schefzig P, Unger E, et al. 2013 *Finite element based estimation of contact areas and pressures of the human scaphoid in various functional positions of the hand*. J Biomech 46:984–990.
21. Varga, P., et al., *A finite element analysis of two novel screw designs for scaphoid waist fractures.* Med Eng Phys, 2016. 38:131–139.
22. Reina, N., et al., *Laterality and grip strength influence hand bone micro-architecture in modern humans, an HRpQCT study.* J Anat, 2017. 230:796–804.
23. Pichler, W., et al., Computerassisted 3-dimensional anthropometry of the scaphoid. Orthopedics, 2010. 33.
24. de Jong, J.J.A., et al., *Effect of a cast on short-term reproducibility and bone parameters obtained from HR-pQCT measurements at the distal end of the radius.* J Bone Joint Surg, 2016. 98:356–362 American volume.
25. Vilayphiou, N., et al., *The 2nd generation of HR-pQCT: progresses in bone microstructure assessment with 61 um voxel size in vivo scans*. J Bone Miner Res, 2013.: 28.
26. Pialat, J., et al., *Visual grading of motion induced image degradation in high resolution peripheral computed tomography: impact of image quality on measures of bone density and micro-architecture.* Bone, 2012. 50:111–118.
27. Burghardt, A.J., et al., *Reproducibility of direct quantitative measures of cortical bone micro-architecture of the distal radius and Tibia by HR-pQCT.* Bone, 2010. 47:519–528.
28. Hildebrand, T. and Ruegsegger, P., *A new method for the model-independent assessment of thickness in three-dimensional images.* J Microsc, 1997. 185:67–75.
29. Macdonald, H.M., et al. *Agerelated patterns of trabecular and cortical bone loss differ between sexes and skeletal sites: a population-based HRpQCT study.* J Bone Miner Res, 2011. 26:50–62.
30. Dalzell. N., et al., *Bone microarchitecture and determinants of strength in the radius and tibia: age-related changes in a population-based study of normal adults measured with high-resolution pQCT.* Osteoporos Int, 2009. 20:1683–1694.
31. Engelke, K., et al., *Short-term in vivo precision of BMD and parameters of trabecular architecture at the distal forearm and tibia.* Osteoporos Int, 2012. 23:2151–2158.
32. de Jong, J.J.A., et al., *Assessment of the healing process in distal radius fractures by high resolution peripheral quantitative computed tomography.* Bone, 2014. 64:65–74.
33. Pauchard. Y., et al., *Quality control for bone quality parameters affected by subject motion in high-resolution peripheral quantitative computed tomography.* Bone, 2012. 50:1304–1310.
34. Gabel. L., et al., *Sex differences and growth-related adaptations in bone microarchitecture, geometry, density and strength from childhood to early adulthood: a mixed longitudinal HR-pQCT Study*. J Bone Miner Res, 2017. 32:250–263.
35. Khosla, S., et al., *Effects of sex and age on bone microstructure at the ultradistal radius: a population-based noninvasive in vivo assessment.* J Bone Miner Res, 2006. 21:124–131.
36. de Waard, E.A.C., et al., *Reliability of HR-pQCT derived cortical bone structural parameters when using uncorrected instead of corrected automatically generated endocortical contours in a crosssectional study: the Maastricht Study.* Calcif Tissue Int, 2018. 103:252–265.
37. van Alphen, N.A., et al., *A three-dimensional microcomputed tomographic study of the intraosseous lunate vasculature: implications for surgical intervention and the development of avascular necrosis.* Plast Reconstr Surg, 2016. 138:869e.

Supplemental figure

Figure S-1. Difference in bone indices between the automatically contoured scaphoid bone without (AUTO) and with (sAUTO) manual corrections for poor-quality scans subdivided into scans with one or multiple poor stacks (A) and one proximal, middle, or distal poor stack (B)

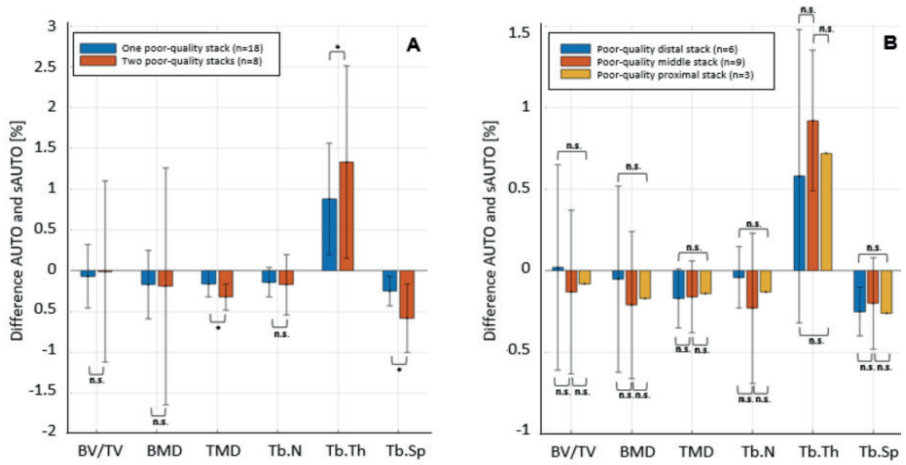

Data are presented as median percentage and IQR | Scan quality is based on *post hoc* grading

Supplemental table

Table S-1. Results of univariate and multivariate binominal logistic regression models that predict scan quality

	Standard grading	
	Odds ratio Univariate	**p-value**
Age (per year)	1.04 (0.97-1.10)	0.264
Age (per 10 years)	1.41 (0.77-2.59)	0.265
Gender (male)	0.33 (0.03-3.26)	0.339
Scaphoid fracture	0.00 (0.00-0.00)	0.998

	Post hoc grading							
	Odds ratio Univariate	**p-value**	**Odds ratio** Model 1	**p-value**	**Odds ratio** Model 2	**p-value**	**Odds ratio** Model 3	**p-value**
Age (per year)	1.04 (1.01-1.07)	0.005	1.05 (1.02-1.08)	0.003	1.04 (1.01-1.07)	0.008	1.05 (1.01-1.08)	0.005
Age (per 10 years)	1.47 (1.13-1.92)	0.005	-		-		-	
Gender (male)	0.84 (0.34-2.07)	0.700	1.81 (0.61-5.39)	0.284	-		1.83 (0.61-5.48)	0.280
Scaphoid fracture	0.56 (0.18-1.72)	0.309	-		0.98 (0.28-3.43)	0.978	0.91 (0.26-3.22)	0.880

	Post hoc grading							
	Odds ratio Univariate	**p-value**	**Odds ratio** Model 4	**p-value**	**Odds ratio** Model 5	**p-value**	**Odds ratio** Model 6	**p-value**
Age (per year)	1.04 (1.01-1.07)	0.005	-		-		-	
Age (per 10 years)	1.47 (1.13-1.92)	0.005	1.56 (1.16-2.10)	0.003	1.47 (1.11-1.94)	0.008	1.55 (1.14-2.10)	0.005
Gender (male)	0.84 (0.34-2.07)	0.700	1.68 (0.56-4.88)	0.342	-		1.71 (0.58-5.01)	0.332
Scaphoid fracture	0.56 (0.18-1.72)	0.309	-		0.95 (0.28-3.28)	0.949	0.87 (0.25-3.06)	0.829

Data are presented as odds ratio (OR) with 95% confidence interval (CI)

Chapter 5

The interobserver reliability of the diagnosis and classification of scaphoid fractures using High Resolution peripheral Quantitative CT

A.M. Daniels, C.E. Wyers, H.M.J. Janzing, S. Sassen, D. Loeffen, S. Kaarsemaker, B. van Rietbergen, P.F.W. Hannemann, M. Poeze, J.P. van den Bergh

Bone Joint J. 2020; 102-B(4):478-484

Abstract

Aims

Besides conventional radiographs, additional imaging techniques such as MRI, CT and BS are frequently used in diagnosing scaphoid fractures. However, no consensus has been reached regarding the optimal modality. Initiating a new imaging technique at first requires an analysis of precision. The primary aim of this study was therefore to determine the interobserver agreement of High Resolution peripheral Quantitative CT (HR-pQCT) for scaphoid fracture diagnosis. As secondary aim, interobserver agreement was examined for the presence of other fractures and for scaphoid fracture classification.

Methods

Two radiologists and two orthopaedic trauma surgeons evaluated HR-pQCT scans of 31 patients with a clinically suspected scaphoid fracture. The observers were asked to determine the presence of a scaphoid or other fracture and to classify the scaphoid fracture based on the Herbert classification system. Fleiss' kappa statistics were used to calculate the overall interobserver agreement for the presence of a fracture. Intraclass correlation coefficients were calculated to assess scaphoid fracture classification.

Results

Overall, nine (29%) scaphoid fractures and 12 (39%) other fractures were diagnosed in 20 patients (65%) with HR-pQCT by the four observers. The interobserver agreement for four observers was 91% for assessment of the presence of a scaphoid fracture (95% CI 0.76-1.00) and 80% for other fractures (95% CI 0.72-0.87). The mean ICC for the Herbert scaphoid fracture classification in the seven patients diagnosed with scaphoid fracture by all four observers was 73% (95%CI 0.42-0.94).

Conclusions

We conclude that diagnosis of scaphoid and other fractures is reliable with HR-pQCT in patients with a clinically suspected scaphoid fracture.

Introduction

Besides conventional radiographs, additional imaging techniques such as magnetic resonance imaging (MRI), computed tomography (CT) and bone scintigraphy are frequently used in diagnosing scaphoid fractures. Due to controversial diagnostic performance results, there is no consensus regarding the optimal modality to detect scaphoid fractures [1-14]. The lack of a reference standard toughens interpretation of diagnostic performance of the previous mentioned tests. The development of a novel low-dose radiation technique, High Resolution peripheral Quantitative CT (HR-pQCT), made it possible to visualize the cortical and trabecular bone microarchitecture [15,16]. Many in vivo studies have been conducted on its implementation in assessing microarchitectural changes due to ageing, osteoporosis, rheumatoid arthritis, metabolic disease and medication [17-30]. Several papers have been published assessing the failure load and healing process of distal radius fractures by HR-pQCT [31,32]. No previous studies have been conducted on scaphoid fracture detection using HR-pQCT. Initiating a new imaging technique to achieve superior detection of scaphoid fractures requires an analysis of precision to appreciate the diagnostic value of this technique and to assess its place in the diagnostic process of scaphoid fracture detection. Therefore, this study was conducted prior to the comparison of HR-pQCT with the current clinical diagnostics. In this study HR-pQCT scans of consecutive patients with a clinically suspected scaphoid fracture were analysed by four independent observers to assess interobserver reliability. The primary aim of this study was to determine the interobserver agreement for HR-pQCT diagnosis of scaphoid fractures. As secondary aim, the interobserver agreement was examined for other fractures and for scaphoid fracture classification.

Methods

Patient selection

Data for this feasibility study were extracted from our study approved by the Medical Ethics Committee ("SHOTGUN, Scaphoid fracture diagnosis with HR-pQCT", NL 62476.068.17) conducted between December 2017 and October 2018. This study was performed according to the principles of the Declaration of Helsinki and in accordance with the Medical Research Involving Human Subjects Act (WMO).

In this prospective study, all consecutive patients submitted to the Emergency Department (ED) within one week after trauma with a clinically suspected scaphoid fracture were screened for eligibility. Pregnant women and patients with a previous ipsilateral scaphoid fracture were not eligible. All patients received, conform current clinical practice, a cast until the day of reassessment and additional imaging. This resulted in 91 patients who consented with a HR-pQCT scan of the affected forearm around 10 days after presentation at the ED as additional imaging technique next to the regular clinical evaluation. An overview of the eligibility criteria and selection results is shown in Figure 1.

Figure 1. Overview of the eligibility criteria and selection results of patients with a clinically suspected scaphoid fracture

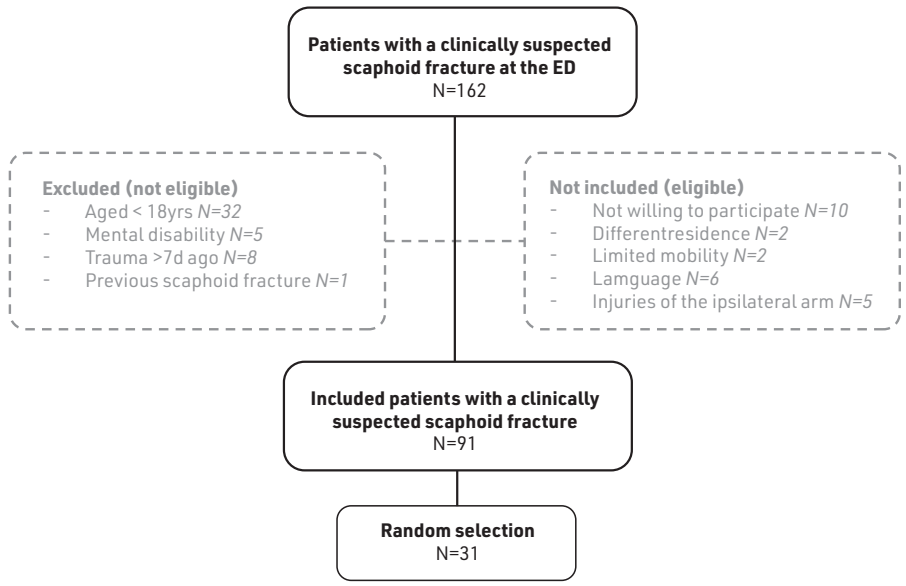

Sample size

The sample size for this study was determined based on the sample size requirements as published by Donner and Rotondi in 2010 [33]. We aimed to achieve an interobserver agreement of $\kappa_0 = 0.80$ according to Landis and Koch (1997) [34] between four independent observers. Based on the expected fracture detection with HR-pQCT, we estimated ϖ at 0.30 which is slightly higher than the current incidence appraised at 0.20 [2,6,7,35-37]. The minimal acceptable limit (lower bound of the 95% CI) was pre-specified as substantial agreement expressed by $\kappa_L = 0.60$, resulting in a sample size of 25 patients who had to be examined. To ensure a sufficient large cohort, we selected 31 patients with a computer based random number generator (being one-third of our cohort) out of the 91 eligible patients for this study. All thirty-one HR-pQCT scans were assessed by four independent observers.

HR-pQCT protocol and evaluation

All patients received a HR-pQCT scan which was conducted using the second-generation HR-pQCT (XtremeCT II; Scanco Medical AG, Brüttisellen, Zürich, Switzerland). The standard scan protocol of the distal radius, with an isotropic voxel size of 0.061 mm, was adapted to three consecutive stacks (30.6mm) to cover the entire scaphoid bone [38-40]. Consequently, surrounding bones in this scanned length, such as the proximal carpal row and a part of the distal carpal row, were displayed. This resulted in an effective radiation dose of 15 µSv which is compatible with 0.6%/0.5% of the annual background radiation exposure to an individual in The Netherlands/United States [41,42]. All scans were conducted with the wrist in a fiberglass cast with a detachable cast around the thumb, this latter was applied during the HR-pQCT procedure for added stability. The patients' forearm was placed into an anatomically shaped container to obtain a standardized position. Based on a scout view the region of interest was determined and a reference line was placed on the rim at the joint surface of the distal radius. Motion-induced degradation of the images was graded according to the manufacturer protocol and the method of Pialat et al. [40]. Scans with motion artefacts (grade 4-5) were repeated once. Scans of the HR-pQCT were exported in Digital Imaging and Communications in Medicine (DICOM) format. Source images were reconstructed into transversal, coronal and sagittal planes of the wrist. All HR-pQCT images and reconstructions were anonymized and uploaded into the local workstation.

Observers

Two radiologists, experienced in musculoskeletal trauma and two dedicated hand and wrist orthopaedic trauma surgeons independently evaluated each HR-pQCT. The observers were asked to determine the presence of a scaphoid or other fracture (distal radius or (meta)carpal) on HR-pQCT based on their expert opinion and to classify the scaphoid fracture, if present, according to the Herbert classification system [43][Figure 2]. The observers were aware of the fact that all patients were clinically suspected of having a scaphoid fracture based on physical examination at the ED. All observers were blinded for diagnosis on conventional radiographs and CT and were not aware of each other's assessment. The observers did not have access to any clinical data of the patients.

Figure 2. Scaphoid fracture classification system, according to Herbert.

Statistical analysis

Distribution of age was tested with Q-Q plots and the Kolmogorov-Smirnov test and chi-square and independent sample t-tests were used to analyse differences between the selected (N=31) and non-selected patients (N=60) using IBM SPSS Statistics. The Fleiss' kappa values for the, chance corrected, agreement of all four observers were calculated for the presence of a scaphoid fracture and for the presence of a fracture including scaphoid fractures and other fractures. These analyses were conducted using Microsoft Office Excel 2010. The intra class correlation coefficient (ICC) for the assessment of scaphoid fracture classification was calculated with the two-way mixed model in SPSS. The interpretation of the interobserver agreement values was based on the guidelines of Landis and Koch, with a value between 0.0 and 0.20 representing 'slight agreement', 0.21-0.40 'fair agreement', 0.41-0.60 'moderate agreement' and 0.61-0.80 'substantial agreement'. A value above 0.80 is considered to be an 'almost perfect agreement' [34,44].

Results

The 31 patients included in this study had a median age of 48 years and 16 (52%) were male. This was similar to the non-selected patients (N=60) [Table 3]. We decided to include all scans, irrespective of the presence of motion artefacts as this is comparable with using an imaging technique in a clinical situation. Moreover, the number of stacks (2/93) with grade 4 motion artefacts (grade 4) was low and no grade 5 stacks were present in this study. A total of nine patients (29%) were diagnosed with a scaphoid fracture by at least three out of four observers [Table 1]. This resulted in an interobserver agreement for the presence of a scaphoid fracture of κ=0.91 (95% CI 0.76-1.00) between the four observers. Figure 3 (A/B) presents an example of HR-pQCT images displaying a scaphoid fracture detected by all observers. Figure 4 (A/B) contains an example of HR-pQCT images with a scaphoid fracture detected by three out of four observers. Other fractures such as distal radius fractures and carpal fractures were diagnosed seven (23%) up to eleven (35%) times by the four respective observers [Table 1]. Diagnosing other fractures resulted in an interobserver agreement of κ=0.80 (95% CI 0.72-0.87) for four observers.

Seven patients (23%) were diagnosed with a scaphoid fracture by all four observers. The ICC for scaphoid fracture classification by the four observers in these seven patients was 0.73 (95%CI 0.42-0.94), indicating substantial agreement. Figure 5 (A/B/C) contains an example of HR-pQCT images with a scaphoid fracture detected by all four observers but classified differently according to the Herbert classification system.

Figure 3. Transversal (A) and sagittal (B) HR-pCT section of a patient with a scaphoid fracture (arrow) as diagnosed by all four observers

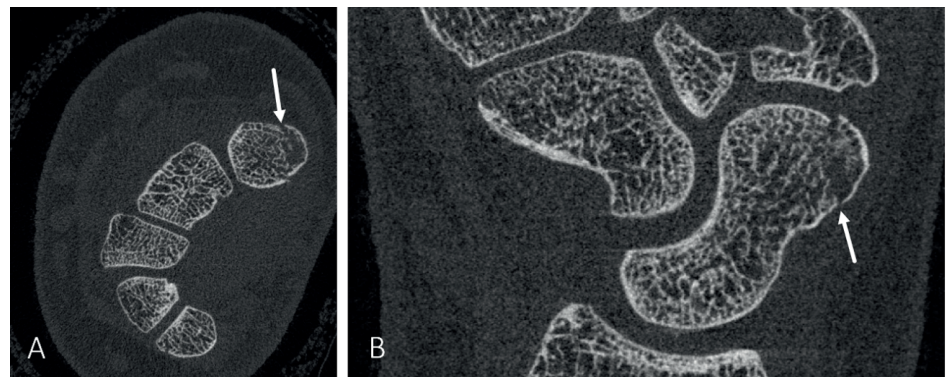

Figure 4. Transversal (A) and sagittal (B) HR-pCT section of a patient with a scaphoid fracture (arrow) as diagnosed by three out of four observers

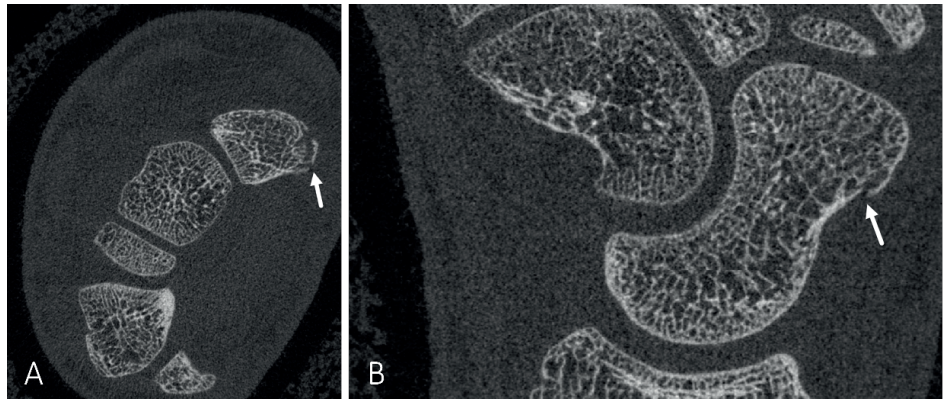

Figure 5. Transversal (A) and sagittal (B - radial, C-ulnar) HR-pCT section of a patient with a scaphoid fracture (arrow) with different classification (Herbert) by the four observers

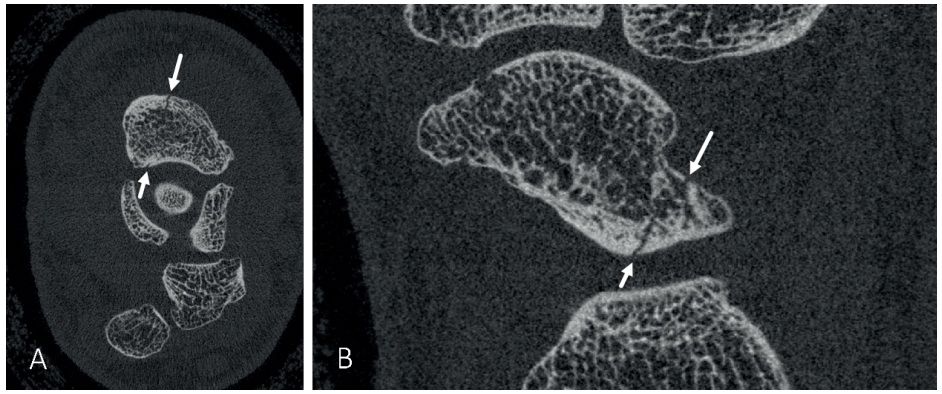

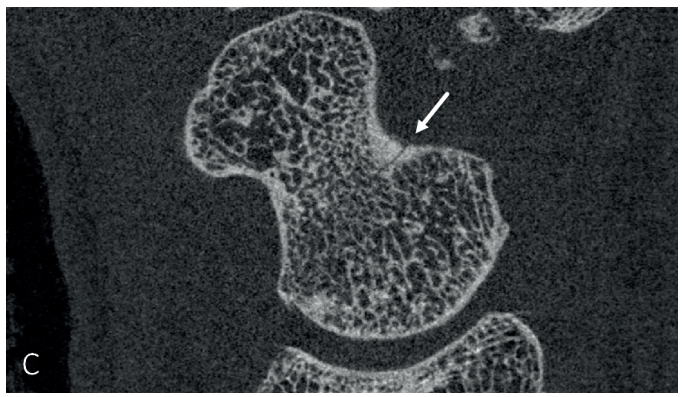

Table 1. Results of HR-pQCT fracture classification in 31 patients by 4 observers

Patients	Observers			
	I	II	III	IV
1	0	-	-	0
2	X	X	X	X
3	X	X	-	X
4	-	-	-	-
5	X	X	X	X
6	-	-	-	-
7	X	X	X	X
8	0	0	-	0
9	-	-	-	-
10	-	0	-	0
11	-	-	-	-
12	0	0	0	0
13	-	-	-	-
14	X	X	X	0
15	0	0	0	0
16	X	X	X	X
17	X	X	X	X
18	-	-	-	-
19	0	0	0	0
20	0	0	0	0
21	-	-	-	-
22	X	X	X	X
23	0	0	0	0
24	-	-	-	-
25	-	-	-	-
26	-	-	-	-
27	-	0	-	-
28	0	0	0	0
29	X	X	X	X
30	-	-	-	-
31	0	0	0	0
Total				
Scaphoid fractures (X)	9	9	8	8
Other fractures (0)	9	10	7	11
No fractures (-)	13	12	16	12

Scaphoid fractures κ=0.91 (95% CI 0.76-1.00)
Scaphoid and other fractures κ=0.84 (95% CI 0.73-0.94)

Table 2. Herbert scaphoid fracture classification with HR-pQCT in seven patients by four observers

Patients	Observers			IV
	I	II	III	
1	A1	A1	A1	A1
2	A1	A1	A1	A1
3	B1	B2	A2	B1
4	A2	B3	B3	B3
5	B1	B3	A2	B3
6	A1	A1	A1	A1
7	A1	A1	A1	A1
Total				
A1	4	4	4	4
A2	1	0	2	0
B1	2	0	0	1
B2	0	1	0	0
B3	0	2	1	2

ICC=0.73 (95%CI 0.42-0.94)

Table 3. Patient characteristics of selected (N=31) and non-selected (N=60) patients

	Selected patients N=31	Non-selected patients N=60	p-value
Age at trauma*	48 [29-71]	52 [28-65]	0.768
Male gender	16 (52)	29 (48)	0.767
Dominant hand affected	14 (45)	32 (53)	0.460

Normally distributed data are presented as mean (SD)
Non normally distributed data * as median [IQR]

Discussion

We demonstrated 90% agreement between four independent observers for HR-pQCT fracture diagnosis in 31 patients with a clinically suspected scaphoid fracture. Previous studies assessing interobserver variability of fracture diagnosis in patients suspected of a scaphoid fracture have been conducted for various imaging techniques. The κ-values for follow-up radiographs (2-6 weeks) were ranging from 0.14 to 0.37, representing slight to fair agreement between the observers [45,46]. These agreement rates can be explained by the poor sensitivity of conventional radiograph assessment of scaphoid fractures [47-49]. This, together with the large amount of false positives, implies that follow-up radiographs cannot be considered as reference in diagnosing scaphoid fractures [46,48,50,51]. Interobserver agreement for MRI assessment for scaphoid fracture presence by 4-5 raters in cohorts of 60-80 patients, with a similar percentage of scaphoid fractures among suspected ones compared to our study, does not transcend κ=0.67, representing moderate to substantial agreement [10,52]. Furthermore, Beeres et al. conducted a study on bone scintigraphy in which scans of both wrists of 100 patients with a clinically suspected scaphoid fracture on at least one side were analysed by three observers. They found a substantial agreement, κ=0.61-0.80 for scaphoid fracture diagnosis and for diagnosis of other fractures [53]. A study addressing the interobserver agreement of CT assessment of four raters in a large cohort of 150 patients with a clinically suspected scaphoid fracture reported a kappa value of 0.51 (moderate agreement) [54]. Additionally, in a study by Adey et al (2007) comparable to our study by means of cohort size, 30 CT scans were assessed by eight raters. Although they used a CT with lower resolution than the previous mentioned study, they found a kappa value of 0.66 [6]. As a higher number of observers should diminish the number of patients needed to assure a specific kappa value (sample size), our results with only four observers are promising.

Regarding the classification of a scaphoid fracture, only limited data is available. Beeres et al (2008) and de Zwart et al (2012) assessed the interobserver variability of scaphoid fracture location (proximal, middle, distal) on MRI respectively CT for four observers and found a kappa value of 0.57 respectively 0.48 [52,54]. Interobserver agreement for scaphoid fracture classification by four observers in our study was substantial (κ 0.73, 95%CI 0.42-0.94). Although we have more than three categories, we have to keep in mind the limited number of patients in each of the five groups. This is an important limitation in our study. A higher number of scans should be assessed to evaluate the reliability of fracture classification between multiple observers.

Agreement rates in our study exceed those of previous studies, suggesting that HR-pQCT is reliable for fracture diagnosis and classification in patients with a clinically suspected scaphoid fracture. This might be explained by the considerable experience with other imaging techniques of all four observers in our study. Moreover, as resolution increases it is conceivable that distinction between vascular structures, motion artefacts and fractures is more apparent. Therefore, conventional CT with higher resolution than the investigated CT scanners in the previous paragraph might also increase interobserver agreement. However, the limited data available in the literature do not prove this hypothesis yet. Although interobserver agreement is just one aspect of diagnostic performance, it does reveal the reliability of a technique. In this study, intra-observer reliability was not determined.

Novel techniques such as HR-pQCT should be incorporated in further studies addressing accuracy and precision. Although no clear definition of a fracture on HR-pQCT is available, diagnosis based on expert opinion appears to be reliable in this study. Moreover, assessment in this study took place by both radiologists and treating orthopaedic trauma surgeons making extrapolation to clinical practice possible. The use of a uniform scan protocol and DICOM viewers in this study assures that implementation and assessment in a clinical setting is achievable sincp34873398comen 36classification to classify the fracture into type A, B or C. i.e. scaphoid fracture, distal radius fracture, e these viewers are available and used for multiple purposes in daily practice. The HR-pQCT scanner was designed to measure the bone density and to quantify the three-dimensional microarchitecture of the bone at the distal radius and distal tibia (both one stack of approximately 1 cm). To scan the scaphoid bone, a scan protocol was developed comprising three stacks (instead of one) to capture the entire scaphoid. The total scan procedure time of the scaphoid bone is 30 minutes (including patient position and scan time). Additionally, image processing and analysis requires 30 minutes and appurtenant computational hardware and software is required. This further increases the costs of HR-pQCT scanning of the scaphoid bone.

At present, the HR-pQCT is mainly used in research settings and its application is not yet ready to be implemented in clinical practice due to logistic (time consuming) and financial restrictions (HR-pQCT scans are not yet reimbursed). We estimate that the costs of a HR-pQCT scan are roughly three times higher than the costs of a regular CT scan.

Based on the current developments, standard scan protocols for scanning the scaphoid will be developed and image processing and analysis time will most likely be reduced in the near future. The availability of HR-pQCT scanners worldwide remains a limitation.

We conclude that diagnosis of scaphoid and other fractures is reliable with HR-pQCT in patients with a clinically suspected scaphoid fracture. Further research should address the comparison of scaphoid fracture detection with currently used imaging techniques and HR-pQCT to explore other diagnostic performance characteristics of this promising novel technique.

References

1. Groves, A.M., et al., *An international survey of hospital practice in the imaging of acute scaphoid trauma.* AJR Am J Roentgenol, 2006. 187(6): p. 1453-6.
2. Mallee, W.H., et al., *Computed tomography versus magnetic resonance imaging versus bone scintigraphy for clinically suspected scaphoid fractures in patients with negative plain radiographs.* Cochrane Database Syst Rev, 2015(6): p. Cd010023.
3. Karl, J.W., et al., *Diagnosis of Occult Scaphoid Fractures: A Cost-Effectiveness Analysis.* J Bone Joint Surg Am, 2015. 97(22): p. 1860-8.
4. Memarsadeghi, M., et al., *Occult scaphoid fractures: comparison of multidetector CT and MR imaging--initial experience.* Radiology, 2006. 240(1): p. 169-76.
5. de Zwart, A.D., et al., *Comparison of MRI, CT and bone scintigraphy for suspected scaphoid fractures.* Eur J Trauma Emerg Surg, 2016. 42(6): p. 725-731.
6. Adey, L., et al., *Computed tomography of suspected scaphoid fractures.* J Hand Surg Am, 2007. 32(1): p. 61-6.
7. Ring, D. and Lozano-Calderon S., *Imaging for suspected scaphoid fracture.* J Hand Surg Am, 2008. 33(6): p. 954-7.
8. Buijze, G.A., et al., *Diagnostic performance of radiographs and computed tomography for displacement and instability of acute scaphoid waist fractures.* J Bone Joint Surg Am, 2012. 94(21): p. 1967-74.
9. Rhemrev, S.J., et al., *Current methods of diagnosis and treatment of scaphoid fractures.* Int J Emerg Med, 2011. 4: p. 4.
10. De Zwart, A.D., et al., *MRI as a reference standard for suspected scaphoid fractures.* Br J Radiol, 2012. 85(1016): p. 1098-101.
11. Rhemrev, S.J., et al., *Early computed tomography compared with bone scintigraphy in suspected scaphoid fractures.* Clin Nucl Med, 2010. 35(12): p. 931-4.
12. Yin, Z.G., et al., *Diagnosing suspected scaphoid fractures: a systematic review and meta-analysis.* Clin Orthop Relat Res, 2010. 468(3): p. 723-34.
13. Gemme, S. and Tubbs, R.,, *What physical examination findings and diagnostic imaging modalities are most useful in the diagnosis of scaphoid fractures?* Ann Emerg Med, 2015. 65(3): p. 308-9.
14. Carpenter, C.R., et al., *Adult scaphoid fracture.* Acad Emerg Med, 2014. 21(2): p. 101-21.
15. Link, T.M., *Osteoporosis imaging: state of the art and advanced imaging.* Radiology, 2012. 263(1): p. 3-17.
16. Burghardt A.J., Krug, R. and Majumdar, S., *High-Resolution Imaging Techniques for Bone Quality Assessment*. Vitamin D (Fourth Edition), 2018.
17. Chapurlat, R.D., et al., *Effect of oral monthly ibandronate on bone microarchitecture in women with osteopenia-a randomized placebo-controlled trial.* Osteoporos Int, 2013. 24(1): p. 311-20.
18. Vilayphiou, N., et al., *Finite element analysis performed on radius and tibia HR-pQCT images and fragility fractures at all sites in postmenopausal women.* Bone, 2010. 46(4): p. 1030-1037.
19. Dalzell, N., et al., *Bone micro-architecture and determinants of strength in the radius and tibia: age-related changes in a population-based study of normal adults measured with high-resolution pQCT.* Osteoporos Int, 2009. 20(10): p. 1683-94.
20. Burghardt, A.J., et al., *Multicenter precision of cortical and trabecular bone quality measures assessed by high-resolution peripheral quantitative computed tomography.* J Bone Miner Res, 2013. 28(3): p. 524-36.
21. Khosla, S., et al., *Effects of sex and age on bone microstructure at the ultradistal radius: a population-based noninvasive in vivo assessment.* J Bone Miner Res, 2006. 21(1): p. 124-31.
22. Bacchetta, J., et al., *Early impairment of trabecular microarchitecture assessed with HR-pQCT in patients with stage II-IV chronic kidney disease.* J Bone Miner Res, 2010. 25(4): p. 849-57.
23. Romme, E.A., et al., *Bone stiffness and failure load are related with clinical parameters in men with chronic obstructive pulmonary disease.* J Bone Miner Res, 2013. 28(10): p. 2186-93.
24. Shimizu, T., et al., *Assessment of 3-month changes in bone microstructure under anti-TNFalpha therapy in patients with rheumatoid arthritis using high-resolution peripheral quantitative computed tomography (HR-pQCT).* Arthritis Res Ther, 2017. 19(1): p. 222.
25. Okazaki, N., et al., *Bone microstructure in men assessed by HR-pQCT: Associations with risk factors and differences between men with normal, low and osteoporosis-range areal BMD.* Bone Rep, 2016. 5: p. 312-319.
26. Burghardt, A.J., et al., *Quantitative in vivo HR-pQCT imaging of 3D wrist and metacarpophalangeal joint space width in rheumatoid arthritis.* Ann Biomed Eng, 2013. 41(12): p. 2553-64.
27. Rizzoli, R., et al., *Effects of strontium ranelate and alendronate on bone microstructure in women with osteoporosis. Results of a 2-year study.* Osteoporos Int, 2012. 23(1): p. 305-15.
28. Bala, Y., et al., *Risedronate slows or partly reverses cortical and trabecular microarchitectural deterioration in postmenopausal women.* J Bone Miner Res, 2014. 29(2): p. 380-8.

29. Sornay-Rendu, E., et al., *Bone Microarchitecture Assessed by HR-pQCT as Predictor of Fracture Risk in Postmenopausal Women: The OFELY Study.* J Bone Miner Res, 2017. 32(6): p. 1243-1251.
30. Stach, C.M., et al., *Periarticular bone structure in rheumatoid arthritis patients and healthy individuals assessed by high-resolution computed tomography.* Arthritis Rheum, 2010. 62(2): p. 330-9.
31. de Jong, J.J., et al., *Assessment of the healing process in distal radius fractures by high resolution peripheral quantitative computed tomography.* Bone, 2014. 64: p. 65-74.
32. Hosseini, H.S., et al., *Fast estimation of Colles' fracture load of the distal section of the radius by homogenized finite element analysis based on HR-pQCT.* Bone, 2017. 97: p. 65-75.
33. Donner, A. and Rotondi, M.A., *Sample size requirements for interval estimation of the kappa statistic for interobserver agreement studies with a binary outcome and multiple raters.* Int J Biostat, 2010. 6(1): p. Article 31.
34. Landis, J.R. and Koch G.G., *The measurement of observer agreement for categorical data.* Biometrics, 1977. 33(1): p. 159-74.
35. Kozin, S.H., *Incidence, mechanism and natural history of scaphoid fractures.* Hand Clin, 2001. 17(4): p. 515-24.
36. Jenkins, P.J., et al., *A comparative analysis of the accuracy, diagnostic uncertainty and cost of imaging modalities in suspected scaphoid fractures.* Injury, 2008. 39(7): p. 768-74.
37. Rhemrev, S.J., et al., *Clinical prediction rule for suspected scaphoid fractures: A prospective cohort study.* Injury, 2010. 41(10): p. 1026-30.
38. Pichler, W., et al., *Computer-assisted 3-dimensional anthropometry of the scaphoid.* Orthopedics, 2010. 33(2): p. 85-8.
39. Manske, S.L., et al., *Human trabecular bone microarchitecture can be assessed independently of density with second generation HR-pQCT.* Bone, 2015. 79: p. 213-21.
40. Pialat, J.B., et al., *Visual grading of motion induced image degradation in high resolution peripheral computed tomography: impact of image quality on measures of bone density and micro-architecture.* Bone, 2012. 50(1): p. 111-8.
41. Commission, U.S.N.R., *Background radiation, natural background sources.* 2018.
42. Rijksinstituut voor Volksgezondheid en Milieu, *Straling in kaart.* 2018.
43. Herbert, T.J. and Fisher, W.E., *Management of the fractured scaphoid using a new bone screw.* J Bone Joint Surg Br, 1984. 66(1): p. 114-23.
44. *Measuring nominal scale agreement among many raters*. 1971, American Psychological Association: US. p. 378-382.
45. Tiel-van Buul, M.M., et al., *The value of radiographs and bone scintigraphy in suspected scaphoid fracture. A statistical analysis.* J Hand Surg Br, 1993. 18(3): p. 403-6.
46. Mallee, W.H., et al., *6-week radiographs unsuitable for diagnosis of suspected scaphoid fractures.* Arch Orthop Trauma Surg, 2016. 136(6): p. 771-8.
47. Ghane, M.R., et al., *How Trustworthy Are Clinical Examinations and Plain Radiographs for Diagnosis of Scaphoid Fractures?* Trauma Mon, 2016. 21(5): p. e23345.
48. Low, G. and Raby, N., *Can follow-up radiography for acute scaphoid fracture still be considered a valid investigation?* Clin Radiol, 2005. 60(10): p. 1106-10.
49. Balci, A., et al., *Wrist fractures: sensitivity of radiography, prevalence and patterns in MDCT.* Emerg Radiol, 2015. 22(3): p. 251-6.
50. Wijetunga, A.R., et al., *The utility of cross-sectional imaging in the management of suspected scaphoid fractures.* J Med Radiat Sci, 2019. 66(1): p. 30-37.
51. Amrami, K.K., et al., *Imaging for Acute and Chronic Scaphoid Fractures.* Hand Clin, 2019. 35(3): p. 241-257.
52. Beeres, F.J., et al., *Observer variation in MRI for suspected scaphoid fractures.* Br J Radiol, 2008. 81(972): p. 950-4.
53. Beeres, F.J., et al., *Reliability of bone scintigraphy for suspected scaphoid fractures.* Clin Nucl Med, 2007. 32(11): p. 835-8.
54. de Zwart, A.D., et al., *Interobserver variability among radiologists for diagnosis of scaphoid fractures by computed tomography.* J Hand Surg Am, 2012. 37(11): p. 2252-6.

Improved detection of scaphoid fractures with High Resolution peripheral Quantitative Computed Tomography compared to conventional CT

A.M. Daniels, M.S.A.M. Bevers, S. Sassen, C.E. Wyers, B. van Rietbergen, P.P.M.M. Geusens, S. Kaarsemaker, P.F.W. Hannemann, M. Poeze, J.P. van den Bergh, H.M.J. Janzing

J Bone Joint Surg Am. 2020; 102(24):2138-2145

Abstract

Background
Computed tomography (CT), magnetic resonance imaging and bone scintigraphy are frequently used second-line imaging techniques in patients with a clinically suspected scaphoid fracture. However, no true reference standard exists for scaphoid fracture diagnosis as a result of varying diagnostic performance results. We hypothesized that the use of High Resolution peripheral Quantitative CT (HR-pQCT) in patients with a clinically suspected scaphoid fracture could improve scaphoid fracture detection in clinical setting compared to conventional CT.

Methods
Between December 2017 and October 2018, a total of 91 consecutive patients (≥18 years) presenting at the emergency department with a clinically suspected scaphoid fracture were included in this study. All patients were clinically reassessed within 14 days after first presentation followed by CT and HR-pQCT. If a scaphoid fracture was present, the fracture type was determined based on the Herbert classification system and correlation between CT and HR-pQCT was estimated using the Kendall's W statistic or coefficient of concordance (W); the closer to 1, the higher the correlation.

Results
The cohort consisted of 45 men and 46 women with a median age of 52 years (IQR 29-67). HR-pQCT revealed a scaphoid fracture in 24 patients (26%), whereas CT revealed a scaphoid fracture in 15 patients (16%). Patients with a scaphoid fracture were younger and more often men. The correlation between CT and HR-pQCT was high for scaphoid fracture type based on the Herbert classification system (W 0.793, 95% CI 0.57-0.91, p<0.001) and very high for scaphoid fracture location (W 0.955, 95% CI 0.90-0.98, p<0.001).

Conclusions
In this study, the number of patients diagnosed with a scaphoid fracture was 60% higher when using HR-pQCT compared to CT. These findings imply that a substantial proportion of fractures, in this study more than one-third, will be missed by the current application of CT scanning in patients with a clinically suspected scaphoid fracture.

Introduction

The scaphoid bone is the most commonly fractured carpal bone. Scaphoid fractures represent 2-6% of all fractures and occur mainly in young and active patients aged 15 to 40 years. In the Netherlands, scaphoid fractures account for 90% of all carpal fractures [1-4]. The scaphoid bone articulates with five surrounding bones and therefore serves a key role in the function of the wrist [5]. Inadequate treatment of a scaphoid fracture can lead to malunion, nonunion and early osteoarthritis [1,6,7]. These complications are associated with pain, decreased range of motion, reduced grip strength and worse functional outcome. Consequently, early and accurate diagnosis is important. Since up to 25% of scaphoid fractures remain radiographically occult with conventional imaging [1,8-10], patients with a suspected scaphoid fracture are generally treated with cast immobilization and reassessment takes place after approximately 10 days. This results in a diagnostic delay of up to two weeks. According to existing literature, only 10-20% of clinically suspected fractures are true fractures [4,8,11-14]. This implies that most patients are over-treated with unnecessary socio-economic effects as result of cast immobilization.

Radiological diagnosis of scaphoid fractures is difficult due to the unique shape, size and orientation of this carpal bone. Various imaging techniques have been suggested for the improvement of diagnosis and the reduction of overtreatment. Computed tomography (CT), magnetic resonance imaging (MRI) and bone scintigraphy (BS) are most frequently used nowadays but all have limitations [11-13,15-24]. None of the investigated diagnostic modalities is both sensitive and specific and therefore no true reference standard exists. Despite advanced knowledge and imaging methods, diagnosing scaphoid fractures remains challenging and the preferred imaging technique differs per hospital. The technique used in the hospital involved in this study is CT.

The development of High Resolution peripheral Quantitative CT (HR-pQCT), a novel high resolution and low-dose radiation technique, allows assessment of cortical and trabecular bone microarchitecture at the distal radius and tibia [25,26]. Recent research showed that studying the fracture healing process of stable distal radius fractures [27,28] and scanning the scaphoid bone in patients with a clinically suspected scaphoid fracture is feasible with HR-pQCT [29]. We hypothesized that the use of HR-pQCT in patients with a clinically suspected scaphoid fracture would improve scaphoid fracture detection in a clinical setting compared to conventional CT.

Methods

This study was approved by the Medical Ethics Committee (NL 62476.068.17) and conducted according to the principles of the Declaration of Helsinki and in accordance with the Medical Research Involving Human Subjects Act (WMO). The funder, being the hospital research foundation, had no input in the study design, data collection and analysis and preparation of the manuscript.

Study population

For this study (level of evidence II), all patients with a clinically suspected scaphoid fracture presenting at the emergency department (ED) within one week after trauma were screened for eligibility. Pregnant women and patients with a previous ipsilateral scaphoid fracture were excluded. Between December 2017 and October 2018, a total of 91 patients aged 18 years or older were included in our study [Figure 1]. At the ED, conventional radiographs were obtained in four views: posteroanterior (PA), true lateral, semi-pronated oblique and PA with the wrist in ulnar deviation. Independent of the diagnosis on these initial radiographs, cast immobilization was applied until definite diagnosis was obtained. All patients, regardless of the outcome of the initial radiographs, received written study information from their treating physician at the ED and were, after permission, contacted by telephone within the next four days by the investigator to answer any remaining questions regarding the study. After obtaining informed consent, CT and HR-pQCT were scheduled immediately following reassessment. This was, according to current clinical practice, within 7-14 days after trauma at the outpatient clinic. Informed consent was obtained during this visit and followed by physical examination, questionnaires, CT and HR-pQCT. Medical history, smoking status, alcohol use, medication use, hand domination and trauma mechanism were registered.

CT scan

Computed tomography of the affected forearm was conducted using the Siemens SOMATOM Definition AS. This scanner contains an 80-kW generator and Ultra-Fast Ceramic detector with a rotation time of one second (tube voltage 120 kV, tube current range 35 μA, pitch 0.6, 128 slices, slice thickness 1.0 mm, slice increment 0.5mm). The effective radiation dose of one CT scan of the hand/wrist is 46 μSv. All scans were conducted with the wrist in a fiber cast. According to the local protocol, all scans were reconstructed in transversal, coronal and sagittal direction of the wrist. In the cases where no fracture was detected on the conventional three reconstructed planes, reconstruction in the plane of the scaphoid was obtained. CT images were uploaded into IMPAX Client software.

Figure 1. Flowchart illustrating inclusion and exclusion of patients with a clinically suspected scaphoid fracture at the ED

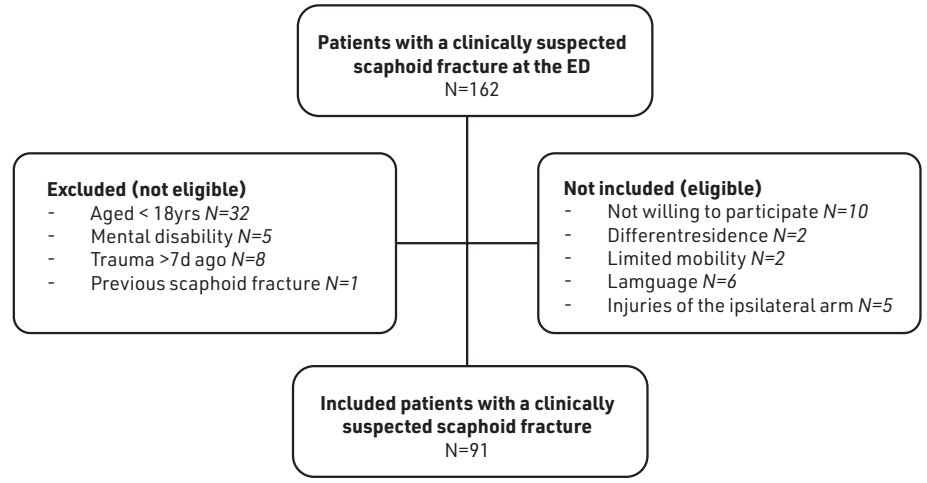

Fx Fracture
* Concurrent Fx of the ipsilateral lower/upper arm

HR-pQCT scan

The second-generation HR-pQCT (XtremeCT II; Scanco Medical AG, Brüttisellen, Switzerland) was used to scan the affected forearm. All scans were conducted with the wrist in a fiber cast with a detachable fiber cast around the thumb. this latter was applied during the HR-pQCT procedure for added stability. The patients' forearm was placed into an anatomically shaped holder to obtain a standardized position. Based on a scout view, the region of interest was determined and a reference line was placed on the rim at the joint surface of the distal radius. The standard scan protocol of the distal radius, with an isotropic voxel size of 0.061 mm, was adapted to three consecutive stacks of 10.2 mm resulting in a scanned region of 30.6 mm to cover the entire scaphoid bone. The effective radiation dose of HR-pQCT scanning of the scaphoid is 15 μSv. The maximum dose patients were exposed to was 30 μSv when repetition of the scan was necessary due to motion artefacts (grade 4-5) [30-33]. Motion-induced artefacts of the images were graded according to the manufacturer protocol and

the method of Pialat *et al.* [32]. In this study, all scans were of acceptable quality for fracture assessment, including three scans with a grade 4 quality in one out of three stacks. Scans were exported in Digital Imaging and Communications in Medicine (DICOM) format. Source images were reconstructed into transversal, coronal and sagittal planes. All HR-pQCT images and reconstructions were anonymized and uploaded into the local workstation.

Scan evaluation

All CT scans were evaluated by a radiologist (within 48 hours) and a dedicated hand and wrist orthopedic trauma surgeon (within one week); both were blinded for each other's assessment. They were asked to state the type of fracture (*i.e.* scaphoid, distal radius, carpal fracture) based on their expert opinion and to classify the scaphoid fracture, if present, according to the Herbert classification system [Figure 2][34]. Additional assessment by a third investigator was used for scans with a discrepant judgement by the two observers (N=4). Subsequent decision of diagnosis was based on majority assessment.

Figure 2. Herbert scaphoid fracture classification, 1984

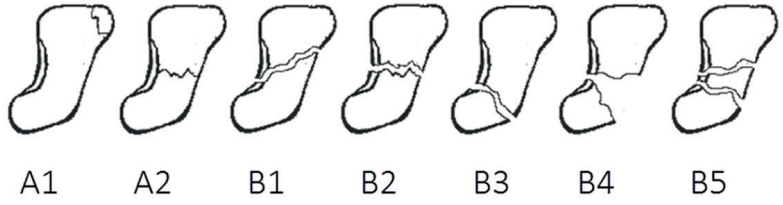

All HR-pQCT scans were evaluated by a musculoskeletal radiologist. In a previous study, the interobserver agreement for four observers (two musculoskeletal radiologists and two orthopedic trauma surgeons) was shown to be almost perfect regarding scaphoid fracture diagnosis with HR-pQCT in patients with a clinically suspected scaphoid fracture [35]. The observers evaluated each HR-pQCT scan independently and were asked to determine the presence of a scaphoid or other (*i.e.* distal radius, carpal, metacarpal) fracture based on their expert opinion and to classify the scaphoid fracture, if present, according to the Herbert classification system [Figure 2] [34]. The observers were aware of the fact that all patients were clinically suspected of having a scaphoid fracture based on physical examination at the ED. All observers were blinded for diagnosis on conventional radiographs and CT and were not aware of each other's assessment. The observers did not have access to any clinical data of the patients.

Statistical analysis

IBM SPSS Statistics, version 24 (IBM Corporation 1989, 2016) was used for statistical analysis. Distribution of data was tested with Q-Q plots and Kolmogorov-Smirnov analysis. Normally distributed data are presented as mean and standard deviation (SD). Age was non-normally distributed and therefore presented as median with interquartile range (IQR min-max). Chi-square and independent sample t-tests were used to analyze differences between patients with (scaphoid/other) and without a fracture. Crosstab calculation with McNemar testing was conducted to compare the proportion of scaphoid fractures diagnosed on CT and HR-pQCT. The correlation between scaphoid fracture classification and location by CT and HR-pQCT was estimated using the Kendall's W statistic or coefficient of concordance (W); the closer to 1, the higher the correlation. Diagnostic performance characteristics were calculated using MedCalc's diagnostic test evaluation calculator and presented as percentages with 95% confidence interval (CI). Significance level was set as α=0.05.

Results

Patient characteristics

All patients were reassessed at the outpatient clinic within 14 days after presentation at the ED (median 10days, IQR 6-14). The cohort consisted of 45 men and 46 women with a median age of 52 years (IQR 29-67). Men were significantly younger compared to women (37yrs vs 62yrs, p<0.001). On CT, 15 patients, with a median age of 41 years (IQR 22-53), were diagnosed with a scaphoid fracture. On HR-pQCT, 24 patients with a median age of 44 years (IQR 35-65) were diagnosed with a scaphoid fracture. Number and proportion of scaphoid fractures on CT and HR-pQCT according to sex and age is shown in Table 1.

Table 1. Distribution of scaphoid fracture incidence by sex and age group for CT and HR-pQCT diagnosis

		19-29 yrs	30-49 yrs	50-69 yrs	70+ yrs	Total
CT	Men	5 (33.3)	3 (20.0)	1 (6.7)	1 (6.7)	10 (66.7)
	Women	1 (6.7)	2 (13.3)	1 (6.7)	1 (6.7)	5 (33.3)
HR-pQCT	Men	7 (29.2)	5 (20.8)	2 (8.3)	1 (4.2)	15 (62.5)
	Women	3 (12.5)	3 (12.5)	2 (8.3)	1 (4.2)	9 (37.5)

Data are presented as number (%)

Fracture diagnosis

In the entire cohort, one patient was diagnosed with a nondisplaced triquetral fracture on HR-pQCT but not on CT and six distal radius fractures were not diagnosed on HR-pQCT due to the restricted scanned region; those fractures were not registered as missed diagnoses. Nine scaphoid fractures (37.5%) diagnosed with HR-pQCT were not diagnosed with CT [Figure 3A/B], resulting in a significant difference in proportion of patients with a scaphoid fracture on CT and HR-pQCT (p=0.004). Figure 4 and 5 demonstrate the CT and HR-pQCT images of two patients with a scaphoid fracture detected on HR-pQCT where CT was negative.

Figure 3. Presence of a scaphoid fracture on CT (A) and HR-pQCT (B), p=0.004

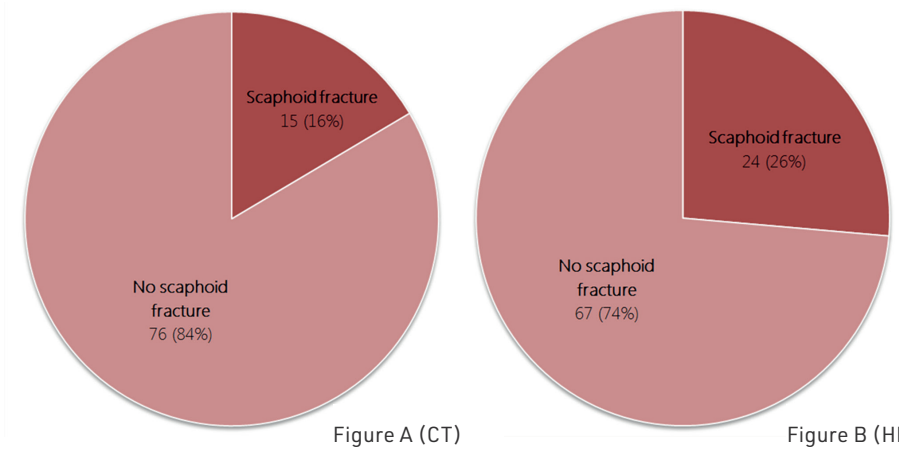

Figure A (CT) Figure B (HR-pQCT)

Figure 4. Transversal (A), coronal (B) and sagittal (C) negative CT section of a 25 year old female patient with a scaphoid fracture, type B3, diagnosed on HR-pQCT (transversal –D, coronal –E and sagittal –F)

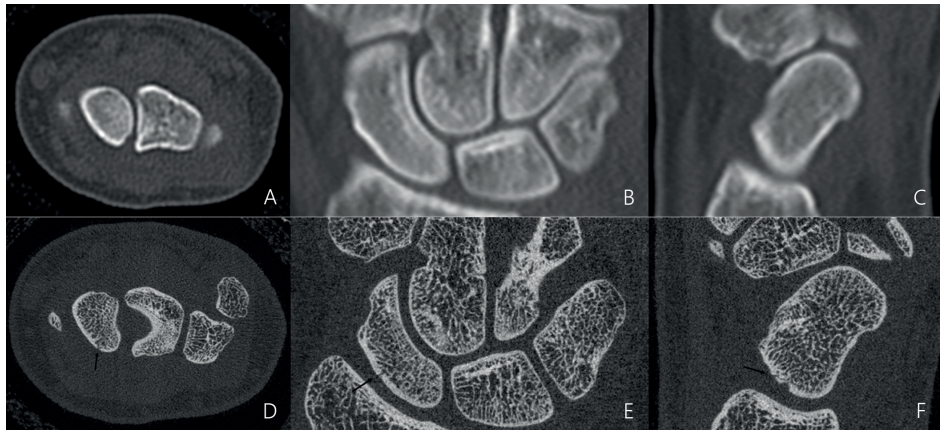

Figure 5. Transversal (A), coronal (B) and sagittal (C) negative CT section of a 38 year old female patient with a scaphoid fracture, type A2, diagnosed on HR-pQCT (transversal –D, coronal –E and sagittal –F)

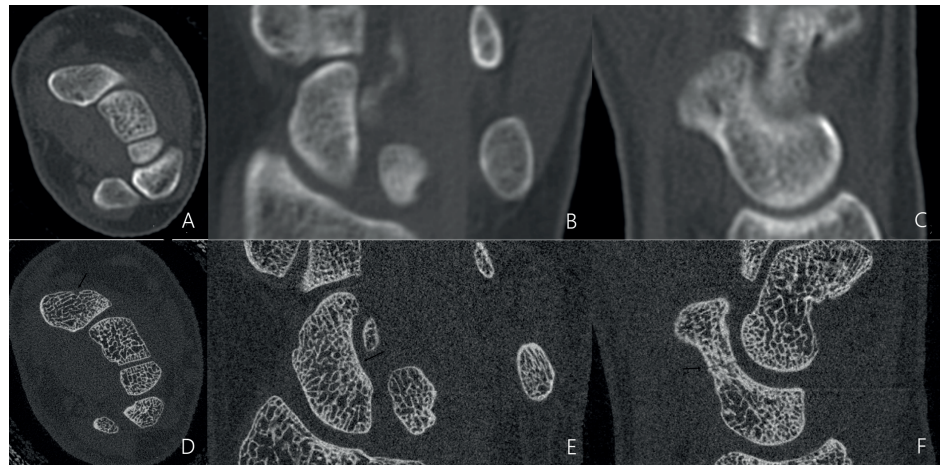

Two out of the nine patients diagnosed with a scaphoid fracture on HR-pQCT only did not want to be treated since they experienced no discomfort of the fracture and refused follow-up. The other seven patients were treated with cast immobilization for at least six weeks as were the patients with a scaphoid fracture on both CT and HR-pQCT. One of these seven patients had a concurrent hamate bone fracture, diagnosed on both CT and HR-pQCT.

There was no significant difference in median age between men and women or in trauma mechanism (low energy trauma vs high energy trauma vs sports/bicycle accidents) between patient with or without a scaphoid fracture (based on CT or HR-pQCT).

Scaphoid fracture classification

The highest proportion of fracture types according to the Herbert classification were type A1 on CT (40%) and type A2 on HR-pQCT (29%) [Figure 6A/B]. The most common location was the scaphoid waist [Figure 7A/B]. The correlation between CT and HR-pQCT was high for the scaphoid fracture type (Herbert classification) (W 0.793, 95% CI 0.57-0.91, p<0.001) and very high for scaphoid fracture location (W 0.955, 95% CI 0.90-0.98, p<0.001). There was no significant difference in sex, age and trauma mechanism (low/high energy and sports/bicycle accidents) between type A and B fractures as diagnosed on both CT and HR-pQCT.

Figure 6. Herbert scaphoid fracture classification on CT (A) and HR-pQCT (B), W=0.793

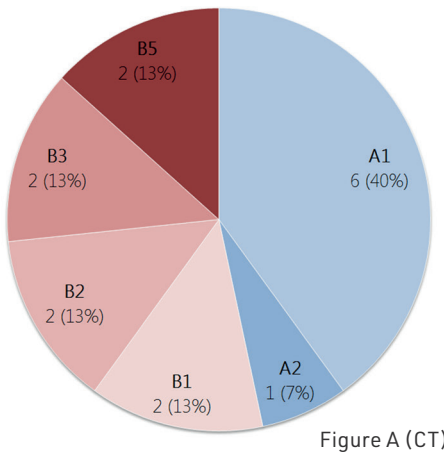

Figure A (CT)

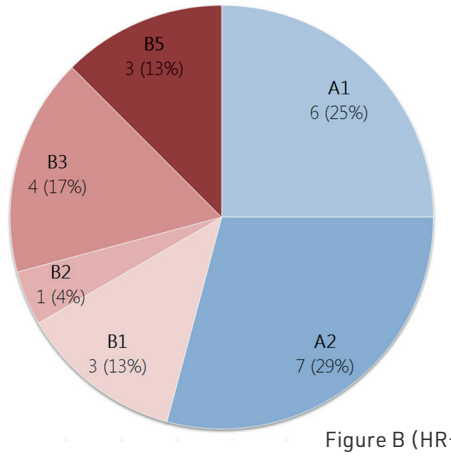

Figure B (HR-pQCT)

Figure 7. Scaphoid fracture location assessment on CT (A) and HR-pQCT (B), W=0.955

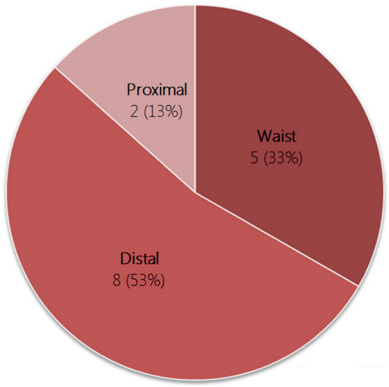

Figure A (CT)

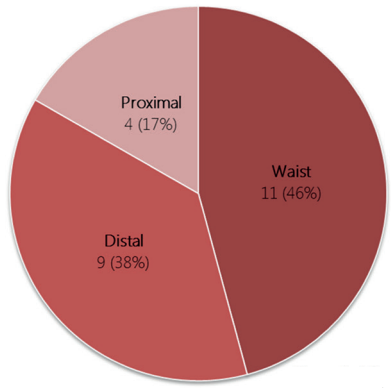

Figure B (HR-pQCT)

Discussion

This study is the first clinical study comparing CT and HR-pQCT for diagnosing scaphoid fractures. Many studies have examined the use of CT, MRI and BS for diagnosing scaphoid fractures [11,18,21,22,36], reporting a wide variation in diagnostic performance. This variation might be a result of the low incidence of scaphoid fractures and the use of different scan protocols. MRI is an appropriate imaging technique to exclude a scaphoid fracture (specificity 94-100%) [17,20,22,37,38]. However, MRI is time consuming, has restricted availability in many hospitals and is relatively expensive [16]. In contrary, CT is readily available and less expensive. A limitation of CT in diagnosing scaphoid fractures is the relative low sensitivity compared to MRI and BS and the radiation exposure to patients [11,18,21,36]. BS is highly sensitive but poorly specific [17,21,22,37,38], invasive, time consuming and it leads to a delay of 3-5 days. Most studies used an unreliable method, namely repeated radiographs after six weeks [22,39-42], as reference standard [11,16-18]. The lack of a universal reference standard makes it difficult to compare results of the previous mentioned studies and contributes to the described variation.

Current clinical imaging techniques as described above lack the ability to assess bone microarchitecture and thereby separately assess cortical and trabecular bone. A non-invasive method recently available for the assessment of bone microarchitecture at the distal radius and tibia is HR-pQCT [43]. Validation and reproducibility studies of HR-pQCT have been performed extensively for the distal radius [44-47] and in the last decade widespread experience has been gathered concerning the use of this technique in clinical research [48,49]. It is conceivable that distinction between a vascular structure, motion artefact and fracture is more apparent due to the higher resolution, which may help improving scaphoid fracture diagnosis. In our study, in only five patients the HR-pQCT scan had to be repeated due to poor quality, resulting in a mean radiation dose of 16 µSv per patient. This difference with the dose of a CT of the hand/wrist (46 µSv) can be explained by the length of the scanned region since HR-pQCT covers only 30.6 mm at the level of the scaphoid bone and CT covers the scaphoid bone as well the distal radius as all carpal bones. Accordingly, the effective radiation dose of HR-pQCT is very little compared to CT but can be interpreted as equal if the length of the scanned region is taken into account.

Since HR-pQCT was not previously used as imaging technique for scaphoid fractures, we investigated the feasibility of HR-pQCT in patients with a clinically suspected scaphoid fracture [29] and the interobserver variability for four independent investigators and have shown that it is a feasible and reliable

technique for scaphoid fracture diagnosis with a Fleiss' kappa of 0.91 representing 'almost perfect agreement' according to the guidelines by Landis and Koch [35]. The number of patients diagnosed with a scaphoid fracture was 60% higher when using HR-pQCT compared to CT.

In correspondence with previous studies [8,50,51], our data showed male predominance and relatively young age in patients with scaphoid fractures. We found no difference in mechanism of injury between patients with a scaphoid fracture, with another fracture and without a fracture in our study. Regarding scaphoid fracture location, previous papers on adults reported waist fractures as most common location, inconsistently followed by proximal [4,33,52] and distal [53-55] fractures. In our study, the most common fractures were type A1 (tubercle) fractures based on CT and A2 fractures based on HR-pQCT [Figure 6A/B]. This implies that HR-pQCT detects more clinically relevant fractures. As result of the relatively small numbers, no hard conclusions can be drawn on this topic yet.

This study is limited by the lack of a true reference standard; one of the important challenges in diagnosing scaphoid fractures is to develop such a true reference standard. In this study, we compared for the first time a novel technique (HR-pQCT) to an existing technique (CT) in scaphoid fracture detection and found that HR-pQCT detects scaphoid fractures in patients where CT does not. These findings are promising, but need to be replicated in other studies and further research should address the clinical consequences of missed scaphoid fractures by CT and investigate the cost-effectiveness of HR-pQCT. Although implementation of HR-pQCT is achievable in daily practice since scanning time of the scaphoid is only six minutes, HR-pQCT is currently used for research purposes and substantial processing time is required.

In our facility, the costs of a HR-pQCT scan are roughly three times higher than the costs of a regular CT scan. Based on the current developments, standard scan protocols for scanning the scaphoid will be developed and image processing and analysis time will most likely be reduced in the near future. The availability of HR-pQCT scanners worldwide remains a limitation. Another limitation of our study is the absence of intra-observer variability as the observers only assessed the scans once.

This study is strengthened by the relatively large cohort of patients with a clinically suspected scaphoid fracture. Moreover, all included patients underwent both CT and HR-pQCT at the same day.

In conclusion, scaphoid fracture detection with HR-pQCT is superior compared to CT. The number of patients diagnosed with a scaphoid fracture was 60% higher when using HR-pQCT compared to CT. HR-pQCT could be a promising new application for the detection of scaphoid fractures.

References

1. Tiel-van Buul, M.M., et al., *Radiography and scintigraphy of suspected scaphoid fracture. A long-term study in 160 patients.* J Bone Joint Surg Br, 1993. 75(1): p. 61-5.
2. Beeres, F.J., et al., *Scaphoid fractures: diagnosis and therapy.* Ned Tijdschr Geneeskd, 2007. 151(13): p. 742-7.
3. van der Molen, A.B., et al., *Time off work due to scaphoid fractures and other carpal injuries in The Netherlands in the period 1990 to 1993.* J Hand Surg Br, 1999. 24(2): p. 193-8.
4. Kozin, S.H., *Incidence, mechanism and natural history of scaphoid fractures.* Hand Clin, 2001. 17(4): p. 515-24.
5. Taljanovic, M.S., et al., *Imaging and treatment of scaphoid fractures and their complications.* Semin Musculoskelet Radiol, 2012. 16(2): p. 159-73.
6. Divelbiss, B.J. and Adams, B.D., *Electrical and ultrasound stimulation for scaphoid fractures.* Hand Clin, 2001. 17(4): p. 697-701, x-xi.
7. Dias, J.J. and Singh H.P., *Displaced fracture of the waist of the scaphoid.* J Bone Joint Surg Br, 2011. 93(11): p. 1433-9.
8. Jenkins, P.J., et al., *A comparative analysis of the accuracy, diagnostic uncertainty and cost of imaging modalities in suspected scaphoid fractures.* Injury, 2008. 39(7): p. 768-74.
9. Cheung, G.C., et al., *X-ray diagnosis of acute scaphoid fractures.* J Hand Surg Br, 2006. 31(1): p. 104-9.
10. Lozano-Calderon, S., et al., *Diagnosis of scaphoid fracture displacement with radiography and computed tomography.* J Bone Joint Surg Am, 2006. 88(12): p. 2695-703.
11. Mallee, W.H., et al., *Computed tomography versus magnetic resonance imaging versus bone scintigraphy for clinically suspected scaphoid fractures in patients with negative plain radiographs.* Cochrane Database Syst Rev, 2015(6): p. Cd010023.
12. Adey, L., et al., *Computed tomography of suspected scaphoid fractures.* J Hand Surg Am, 2007. 32(1): p. 61-6.
13. Ring, D. and Lozano-Calderon S.,, *Imaging for suspected scaphoid fracture.* J Hand Surg Am, 2008. 33(6): p. 954-7.
14. Rhemrev, S.J., et al., *Clinical prediction rule for suspected scaphoid fractures: A prospective cohort study.* Injury, 2010. 41(10): p. 1026-30.
15. Karl, J.W. et al., *Diagnosis of Occult Scaphoid Fractures: A Cost-Effectiveness Analysis.* J Bone Joint Surg Am, 2015. 97(22): p. 1860-8.
16. Memarsadeghi, M., et al., *Occult scaphoid fractures: comparison of multidetector CT and MR imaging--initial experience.* Radiology, 2006. 240(1): p. 169-76.
17. de Zwart, A.D., et al., *Comparison of MRI, CT and bone scintigraphy for suspected scaphoid fractures.* Eur J Trauma Emerg Surg, 2016. 42(6): p. 725-731.
18. Buijze, G.A., et al., *Diagnostic performance of radiographs and computed tomography for displacement and instability of acute scaphoid waist fractures.* J Bone Joint Surg Am, 2012. 94(21): p. 1967-74.
19. Rhemrev, S.J., et al., *Current methods of diagnosis and treatment of scaphoid fractures.* Int J Emerg Med, 2011. 4: p. 4.
20. De Zwart, A.D., et al., *MRI as a reference standard for suspected scaphoid fractures.* Br J Radiol, 2012. 85(1016): p. 1098-101.
21. Rhemrev, S.J., et al., *Early computed tomography compared with bone scintigraphy in suspected scaphoid fractures.* Clin Nucl Med, 2010. 35(12): p. 931-4.
22. Yin, Z.G., et al., *Diagnosing suspected scaphoid fractures: a systematic review and meta-analysis.* Clin Orthop Relat Res, 2010. 468(3): p. 723-34.
23. Gemme, S. and Tubbs R., *What physical examination findings and diagnostic imaging modalities are most useful in the diagnosis of scaphoid fractures?* Ann Emerg Med, 2015. 65(3): p. 308-9.
24. Carpenter, C.R., et al., *Adult scaphoid fracture.* Acad Emerg Med, 2014. 21(2): p. 101-21.
25. Link, T.M., *Osteoporosis imaging: state of the art and advanced imaging.* Radiology, 2012. 263(1): p. 3-17.
26. Burghardt A.J., Krug, R. and Majumdar S., *High-Resolution Imaging Techniques for Bone Quality Assessment*. Vitamin D, 2018.
27. de Jong, J.J.A., et al., *Contra-lateral bone loss at the distal radius in postmenopausal women after a distal radius fracture: A two-year follow-up HRpQCT study.* Bone, 2017. 101: p. 245-251.
28. de Jong, J.J.A., et al., *Fracture Repair in the Distal Radius in Postmenopausal Women: A Follow-Up 2 Years Postfracture Using HRpQCT.* J Bone Miner Res, 2016. 31(5): p. 1114-22.
29. Bevers, M., et al., *The Feasibility of High-Resolution Peripheral Quantitative Computed Tomography (HR-pQCT) in Patients with Suspected Scaphoid Fractures.* J Clin Densitom, 2019.
30. Pichler, W., et al., *Computer-assisted 3-dimensional anthropometry of the scaphoid.* Orthopedics, 2010. 33(2): p. 85-8.
31. Manske, S.L., et al., *Human trabecular bone microarchitecture can be assessed independently of density with second generation HR-pQCT.* Bone, 2015. 79: p. 213-21.
32. Pialat, J.B., et al., *Visual grading of motion induced image degradation in high resolution peripheral computed tomography: impact of image quality on measures of bone density and micro-architecture.* Bone, 2012. 50(1): p. 111-8.

33. Luria, S., et al., *3-dimensional analysis of scaphoid fracture angle morphology.* J Hand Surg Am, 2015. 40(3): p. 508-14.
34. Herbert, T.J. and Fisher W.E., *Management of the fractured scaphoid using a new bone screw.* J Bone Joint Surg Br, 1984. 66(1): p. 114-23.
35. Daniels A.M., et al., *Scaphoid fractures; interobserver reliability of diagnosis and classification using High Resolution peripheral Quantitative CT.* Bone Joint J, 2019.
36. Ilica, A.T., et al., *Diagnostic accuracy of multidetector computed tomography for patients with suspected scaphoid fractures and negative radiographic examinations.* Jpn J Radiol, 2011. 29(2): p. 98-103.
37. Beeres, F.J., et al., *Early magnetic resonance imaging compared with bone scintigraphy in suspected scaphoid fractures.* J Bone Joint Surg Br, 2008. 90(9): p. 1205-9.
38. Buijze, G.A., et al., *Diagnostic performance tests for suspected scaphoid fractures differ with conventional and latent class analysis.* Clin Orthop Relat Res, 2011. 469(12): p. 3400-7.
39. Low, G. and Raby N., *Can follow-up radiography for acute scaphoid fracture still be considered a valid investigation?* Clin Radiol, 2005. 60(10): p. 1106-10.
40. Munk, B., et al., *Diagnosis of scaphoid fractures. A prospective multicenter study of 1,052 patients with 160 fractures.* Acta Orthop Scand, 1995. 66(4): p. 359-60.
41. Tiel-van Buul, M.M., et al., *Diagnosing scaphoid fractures: radiographs cannot be used as a gold standard.* Injury, 1992. 23(2): p. 77-9.
42. Jacobsen, S., et al., *Suspected scaphoid fractures. Can we avoid overkill?* Acta Orthop Belg, 1995. 61(2): p. 74-8.
43. Muller, R., et al., *Morphometric analysis of noninvasively assessed bone biopsies: comparison of high-resolution computed tomography and histologic sections.* Bone, 1996. 18(3): p. 215-20.
44. Pistoia, W., et al., *Image-based micro-finite-element modeling for improved distal radius strength diagnosis: moving from bench to bedside.* J Clin Densitom, 2004. 7(2): p. 153-60.
45. Macneil, J.A. and Boyd, S.K., *Bone strength at the distal radius can be estimated from high-resolution peripheral quantitative computed tomography and the finite element method.* Bone, 2008. 42(6): p. 1203-13.
46. Varga, P., et al., *HR-pQCT based FE analysis of the most distal radius section provides an improved prediction of Colles' fracture load in vitro.* Bone, 2010. 47(5): p. 982-8.
47. Mueller, T.L., et al., *Computational finite element bone mechanics accurately predicts mechanical competence in the human radius of an elderly population.* Bone, 2011. 48(6): p. 1232-8.
48. van Rietbergen, B. and Ito K., *A survey of micro-finite element analysis for clinical assessment of bone strength: the first decade.* J Biomech, 2015. 48(5): p. 832-41.
49. de Jong, J.J., et al., *Assessment of the healing process in distal radius fractures by high resolution peripheral quantitative computed tomography.* Bone, 2014. 64: p. 65-74.
50. van Tassel, D.C., et al., *Incidence estimates and demographics of scaphoid fracture in the U.S. population.* J Hand Surg Am, 2010. 35(8): p. 1242-5.
51. Bohler, L., et al., *The results of treatment of 734 fresh, simple fractures of the scaphoid.* J Hand Surg Br, 2003. 28(4): p. 319-31.
52. Schaefer, M. and Siebert, H.R., *Fracture of the semilunar bone.* Unfallchirurg, 2002. 105(6): p. 540-52; quiz 52-3.
53. Brondum, V., et al., *Fracture of the carpal scaphoid: frequency and distribution in a well-defined population.* Eur J Radiol, 1992. 15(2): p. 118-22.
54. Dias, J. and Kantharuban, S., *Treatment of Scaphoid Fractures: European Approaches.* Hand Clin, 2017. 33(3): p. 501-509.
55. Dias, J.J., et al., *Should acute scaphoid fractures be fixed? A randomized controlled trial.* J Bone Joint Surg Am, 2005. 87(10): p. 2160-8.

Diagnostic performance of conventional radiographs and clinical reassessment compared with High Resolution peripheral Quantitative CT scaphoid fracture diagnosis

A.M. Daniels, J. Kranendonk, C.E. Wyers, H.M.J. Janzing, S. Sassen, B. van Rietbergen, P.P.M.M. Geusens, S. Kaarsemaker, P.F.W. Hannemann, M. Poeze, J.P. van den Bergh

Clin Orthop Relat Res. 2023; 481(1):97-104

Abstract

Background
Conventional radiographs and clinical reassessment are considered guiding in managing clinically suspected scaphoid fractures. As a result of the absence of a true reference standard, diagnostic performance results regarding these diagnostic tools vary.

Methods
Between December 2017 and October 2018, 162 patients with a clinically suspected scaphoid fracture presented at the emergency department (ED). A total of 46 patients was excluded and another 25 were not willing or able to participate, this resulted in 91 included patients. All patients underwent conventional radiography in the ED and clinical reassessment 7 to 14 days later, together with CT and HR-pQCT. The diagnostic performance characteristics and accuracy of conventional radiographs and clinical reassessment were compared with those of HR-pQCT for the diagnosis of fractures since this was proven to be superior to CT scaphoid fracture detection.

Results
The cohort included 45 men and 46 women with a median age of 52 years (interquartile range (IQR), 29 to 67 years). A total of 24 patients with a median age of 44 years (IQR, 35 to 65 years) were diagnosed with a scaphoid fracture on HR-pQCT. Conventional radiographs alone, compared with HR-pQCT had a sensitivity of 67%, specificity of 85%, positive predictive value (PPV) of 62%, negative predictive value (NPV) of 88% and a positive and negative LR of 4.5 respectively 0.4. Clinical reassessment alone, compared with HR-pQCT, resulted in a sensitivity of 58%, specificity of 42%, PPV of 26%, NPV of 74% and a positive and negative LR of 1.0. Combining clinical examination with conventional radiography produced a sensitivity of 50%, specificity of 91%, PPV of 67%, NPV of 84% and a positive and negative LR of 5.6 resp. 0.6.

Conclusion
The accuracy of conventional radiographs (80% compared with HR-pQCT) and clinical reassessment (46% compared with HR-pQCT) indicate that the value of clinical reassessment is limited in diagnosing scaphoid fractures and cannot be considered directive in managing scaphoid fractures.

Introduction

Background
Diagnosing scaphoid fractures is challenging because of the unique shape, size and orientation of this carpal bone. Various imaging techniques have been suggested for the improvement of diagnosis. Computed tomography (CT), magnetic resonance imaging (MRI) and bone scintigraphy (BS) are most frequently used today, but all have limitations [1-16]. Because of varying diagnostic performance results, no true reference standard exists regarding the preferred imaging technique.

Clinical suspicion is most often based on tenderness in the anatomic snuffbox after a fall on an outstretched hand [17,18]. Conventional radiography is performed at the emergency department (ED) but is insufficient to exclude a scaphoid fracture because 20% to 40% of patients with normal initial radiographic findings have a fracture on additional imaging, according to existing studies [7,18-22]. Therefore, regardless of the outcome of conventional radiography, patients with a clinically suspected scaphoid fracture are immobilized with a cast and reassessed within one to two weeks. If a scaphoid fracture is still suspected at the patient's clinical reassessment, additional imaging is performed to obtain a definite diagnosis [14,23-25].

Rationale
This is a unique study as it assessed the value of conventional radiographs and clinical reassessment in a cohort of patients subjected to additional imaging, regardless of the outcome of conventional radiographs and clinical reassessment. High-resolution peripheral quantitative CT (HR-pQCT), a novel imaging technique that allows an assessment of the microstructure of cortical and trabecular bone at the distal radius and tibia, has recently been introduced [26-32].Because there is no consensus regarding the reference imaging technique for diagnosing scaphoid fractures, we have studied HR-pQCT as a diagnostic tool and have shown that it is feasible [33,34] and superior [35] to CT for detecting fractures in patients with a clinically suspected scaphoid fracture. We therefore compared the results of conventional radiographs and clinical reassessment with HR-pQCT in this study.

Methods

Study population and design

In this prospective study, all patients aged ≥ 18 years with a clinically suspected scaphoid fracture who presented to the ED between December 2017 and October 2018 within 1 week after trauma were eligible for study participation. This yielded a total number of 162 patients of which 46 were excluded based on age < 18 years, mental disability, trauma > 7days ago and a previous scaphoid fracture. Another 25 patients were eligible but not willing or able to participate, resulting in 91 included patients [Figure 1].

At the ED, conventional radiographs were obtained in four views: posteroanterior, true lateral, semi-pronated oblique and posteroanterior with the wrist in ulnar deviation. Conventional radiographs were assessed by an experienced team of radiologists. Independent of the outcome of these radiography findings, cast immobilization was applied and patients received written study information from their treating physician in the ED. Standard outpatient visits were planned within 7-14 days after trauma (for patients for whom non-operative treatment was appropriate) according to current clinical practice. If patients were eligible and willing to participate, informed consent was obtained during this visit, followed by a clinical examination and questionnaires, including pain and functioning scores, medical history, smoking status, alcohol use, medication use, dominant hand and trauma mechanism.

Clinical reassessment was conducted by a surgical resident and was classified as positive if at least one of the following was present: anatomic snuffbox tenderness, scaphoid tubercle tenderness or axial compression pain on the thumb (with the thumb in extension and abduction). This clinical workup was in accordance with regional treatment protocols and published studies [14,23-25]. Conventional CT and HR-pQCT scanning of the scaphoid bone region was conducted on the same day, regardless of the outcome of clinical reassessment. Since there is currently no true reference standard available we have decided to compare the results of conventional radiographs and clinical reassessment to HR-pQCT as this technique was superior to conventional CT in our previous conducted study [35]. The radiologist and trauma surgeon assessing the CT and HR-pQCT were blinded to the other's assessment of the patients as well as to their clinical data.

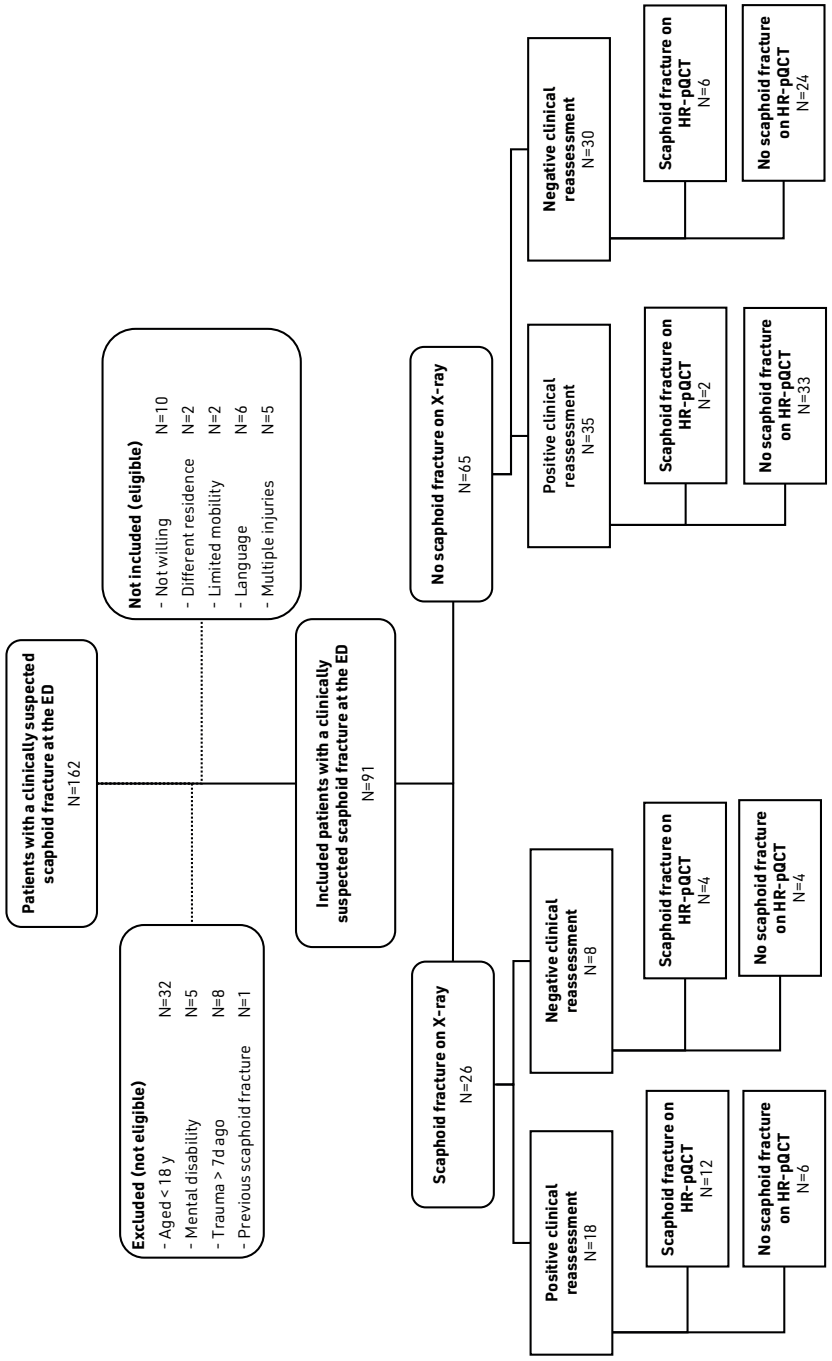

Figure 1. Flowchart with the patient selection for, inclusion in and results of this study

ED=emergency department | X-ray=conventional radiographs

Study outcome

Our primary study goal was assessing the diagnostic performance of conventional radiographs and clinical reassessment compared to HR-pQCT. To achieve this we have obtained conventional radiographs at first presentation of all patients and have conducted clinical reassessment at the outpatient clinic and compared this to the results of the HR-pQCT as our chosen gold standard. Our secondary study goal was to assess the diagnostic performance of conventional radiographs and clinical reassessment combined compared with HR-pQCT. To achieve this we have combined the data and classified it as positive if a scaphoid fracture was seen on conventional radiographs and clinical reassessment was positive and classified it as negative if there was no scaphoid fracture on conventional radiographs or clinical reassessment was negative.

Patient characteristics

The median age in our cohort, which consisted of 45 men and 46 women, was 52 years (IQR 29-67 years). The presence of a scaphoid fracture was suggested on the conventional radiographs of 29% (26/91) of the patients and 58% (53/91) of the patients had clinical suspicion of a scaphoid fracture at reassessment. Overall, a scaphoid fracture was diagnosed in 26% (24/91) on HR-pQCT.

The median age was lower in patients with a scaphoid fracture on HR-pQCT (44 years; IQR 35-65 years) than in those without a scaphoid fracture (65 years; IQR 52-74 years) (p = 0.001). Fifteen of the 24 patients with a scaphoid fracture on HR-pQCT were men.

HR-pQCT

HR-pQCT (XtremeCT II; Scanco Medical AG, Brüttisellen, Switzerland) scanning of the scaphoid bone was performed on a 30.6-mm region of the wrist (three consecutive 10.2-mm stacks with an isotropic voxel size of 0.061 mm), with a reference line at the longitudinal sagittal ridge between the scaphoid bone and lunate fossa at the articular surface of the distal radius. The standard protocol of the distal radius, with an isotropic voxel size of 0.061 mm, was adapted to three consecutive stacks (30.6 mm) to cover the entire scaphoid [36-38].

All scanning was conducted with the wrist in a synthetic cast with a removable cast around the thumb, this latter was applied during the HR-pQCT procedure for added stability. The patient's forearm was placed in an anatomically shaped motion-restraining holder to obtain a standardized position. Detailed information regarding the scanning procedures, image reconstruction and fracture assessment was described previously [33,35].

Statistical analysis

Data were analyzed using IBM SPSS Statistics, version 25.0 (IBM Corp., Armonk, NY, USA). Categorical data are presented as frequencies with a percentage. Distributions of data were tested with Q-Q plots and a Kolmogorov-Smirnov analysis. Normally distributed data are presented as the mean and SD; non-normally distributed data are presented as the median and IQR. Chi-square tests were used to analyze differences in patient characteristics between patients with a scaphoid fracture and those without a scaphoid fracture on HR-pQCT. The level of significance was set at $\alpha = 0.05$. The diagnostic performance characteristics of conventional radiographs and clinical reassessment, including sensitivity, specificity, positive predictive value (PPV) and negative predictive value (NPV), positive and negative likelihood ratio (LR) and accuracy were calculated using MedCalc: Clinical Online Calculator, diagnostic test evaluation calculator (MedCalc Software Ltd, Ostend, Belgium)compared with HR-pQCT.

Results

Conventional radiographs

We have found a sensitivity of 67% (95% CI, 45% to 84%), specificity of 85% (95% CI, 74% to 93%), PPV of 62% (95% CI, 46% to 75%), NPV of 88% (95% CI, 80% to 93%) and a positive and negative LR of 4.5 (95% CI, 2.4 to 8.5) and 0.4 (95% CI, 0.2 to 0.8) respectively for conventional radiographs compared with HR-pQCT scaphoid fracture diagnosis [Table 1]. Eight of the 24 patients with scaphoid fractures diagnosed with HR-pQCT did not have a scaphoid fracture on conventional radiographs and 10 patients were diagnosed with a scaphoid fracture on conventional radiographs, although they appeared to have no fracture on HR-pQCT.

Clinical Reassessment

We have found a sensitivity of 58% (95% CI, 37% to 78%), specificity of 42% (95% CI, 30% to 54%), PPV of 26% (95% CI, 19% to 35%), NPV of 74% (95% CI, 62% to 83%) and positive and negative LR of 1.0 (95% CI, 0.7 to 1.5) respectively 1.0 (95% CI, 0.57 to 1.73) [Table 1]. Clinical reassessment results were negative in 10 of the 24 patients with a scaphoid fracture on HR-pQCT and positive in 39 patients without a scaphoid fracture on HR-pQCT. Of the 39 patients with a positive clinical reassessment result without a scaphoid fracture on HR-pQCT, nine had a diagnosis of a non-displaced fracture of one of the other carpal bones and two had a fracture of the distal radius.

Table 1. Diagnostic performance characteristics of conventional radiographs at the ED and out-patient clinical reassessment 7-14 later using HR-pQCT diagnosis as reference (scaphoid Fx vs no scaphoid Fx)

Diagnostic performance characteristic	X-ray vs HR-pQCT	CR vs HR-pQCT	X-ray & CR vs HR-pQCT
Sensitivity	67%	58%	50%
Specificity	85%	42%	91%
PPV	62%	26%	67%
NPV	88%	74%	84%
Positive LR	4.47	1.00	5.58
Negative LR	0.39	1.00	0.55
AUC	0.76	0.50	0.71
95% CI	[0.64-0.88]	[0.37-0.64]	[0.57-0.84]
p-value	< 0.001	0.993	0.003

X-ray=conventional radiographs | CR=clinical reassessment | PPV=positive predictive value | NPV=negative predictive value | LR=likelihood ratio | AUC=area under the curve | CI=confidence interval | Fx=fracture

Conventional radiographs and clinical reassessment

The combination of conventional radiographs and clinical reassessment resulted in the following diagnostic performance characteristics compared with HR-pQCT; sensitivity of 50% (95% CI, 29% to 71%), specificity of 91% (95% CI, 82% to 97%), PPV of 67% (95% CI, 46% to 83%), NPV of 84% (95% CI, 77% to 88%) and positive and negative LR of 5.6 (95% CI, 2.4 to 13.2) respectively 0.6 (95% CI, 0.4 to 0.8) [Table 1].

Discussion

In this study, the diagnostic performance of conventional radiographs and clinical reassessment was investigated in a cohort of patients with clinically suspected scaphoid fractures. We have addressed the diagnostic performance of conventional radiographs and clinical reassessment alone as well as combined compared with HR-pQCT diagnosis.

Conventional radiographs

Conventional radiographs can be helpful to diagnose other fractures but are insufficient to diagnose scaphoid fractures without any additional imaging. Although the value of conventional radiographs has been studied frequently in the past [2,3,39,40], comparing the results is difficult because of variation in the reference standard that was used. Overall, 20% to 40% of scaphoid fractures are initially occult on conventional radiographs [12,21,41,42]. This is similar to the 33% proportion we found compared with HR-pQCT in our study. Because initially occult fractures are the focus of most studies, patients with positive conventional radiographic findings are not considered.

This results in the absence of adequate diagnostic performance characteristics regarding false-positive radiographic diagnoses. If these patients were considered to have a scaphoid fracture without additional imaging, they would unnecessarily be immobilized, resulting in concurrent physical and socioeconomic consequences. In our opinion, the suggestion of a scaphoid fracture on conventional radiographs in the ED justifies early second-line imaging to confirm the diagnosis and assess the anatomic position of the fracture to rule out displacement or proximal pole localization, or reject the diagnosis of a scaphoid fracture. However, studies have used repeated conventional radiographs, an unreliable method, as the reference standard [10,16].

Clinical reassessment

The diagnostic accuracy of a clinical assessment for detecting suspected scaphoid fractures is limited. A large number of physical examination tests have been described to support diagnosing scaphoid fractures. The most common tests evaluate for tenderness in the anatomic snuffbox, scaphoid tubercle tenderness and axial compression pain of the thumb [4,43-45]. In a systematic review and meta-analysis [45], sensitivity ranges appeared to be relatively high, whereas specificity results were poor for tenderness in the anatomic snuffbox and axial compression on the thumb. We think that in contrast to Unay et al. [46], the focus of a clinical assessment should be to minimize missed scaphoid fractures instead

of preventing unnecessary additional imaging. In our study, we combined the diagnostic findings and classified patients as having positive findings if at least one of these findings was positive at clinical reassessment. Despite this low threshold, we identified a substantial number (N=10) of missed diagnoses compared with HR-pQCT if patients with negative clinical examination findings did not receive additional imaging.

Conventional radiographs and clinical reassessment

The combination of conventional radiographs and clinical reassessment does not increase the accuracy of these diagnostic tests compared with the accuracy of conventional radiographs alone. Some studies combined clinical tests or developed a clinical decision rule to increase the post-test fracture probability [18,43,47-49]. However, the proportion for predicting a true fracture remains relatively low (40%) [18] and implementation in daily practice is not always feasible because of the extensiveness and difficulty of the tests that are used [49]. Tenderness in the anatomic snuffbox is the most-sensitive clinical diagnostic test but is insufficient to safely rule out a scaphoid fracture.

Limitations

This study is limited because HR-pQCT is not yet readily available in a hospital setting, as it is exclusively used as research tool. Since the patients in our study were a selection out of consecutive patients from the ED who all underwent HR-pQCT, we are convinced that this does not affect our results. Although this limited availability may complicate research involving the HR-pQCT in the near future, implementation in a hospital setting will follow in the upcoming years and thereby this limitation will be overcome. Furthermore, other fractures were detected on additional imaging. The presence of fractures (other than scaphoid fractures) may influence the clinical assessment findings since patients might experience pain as a result of this 'other' fracture interfering with the assessment for scaphoid fractures as known from previously conducted studies [4,22,50]. In our study, other non-displaced carpal fractures or distal radius fractures were present in 11 of the 39 patients with positive clinical reassessment results (without a scaphoid fracture on HR-pQCT). Third, since there were 'only' 24 patients with a scaphoid fracture the 95% confidence intervals of mainly the sensitivity and PPV rates are wider and therefore the uncertainty is greater for those values. However, we believe there is still enough prevision to make decisions about the utility of these diagnostics.

Conclusion

Based on our study results and the results of previously mentioned studies [45] reporting varying and disappointing diagnostic performance values, we conclude that clinical assessment is an inadequate indicator of the presence or absence of scaphoid fractures. We acknowledge that clinical investigation remains important in daily practice and that part of this assessment is useful; however, deciding to dismiss a patient from further follow-up with a 33% (HR-pQCT) chance of having a scaphoid fracture is not desirable. Therefore, clinical assessment alone cannot be considered directive in managing scaphoid fractures. The combination of conventional radiographs and clinical reassessment does not increase the accuracy of these diagnostic tests compared with the accuracy of conventional radiographs alone and is therefore also limited in diagnosing scaphoid fractures. Based on the accuracy for clinical reassessment of only 50%, we suggest that additional imaging should not be conducted in addition to or based upon clinical reassessment but should rather immediately replace the current clinical reassessment. By introducing early additional imaging (high resolution CT) in all patients instead of decision making (including the decision to perform imaging) based on clinical reassessment, the time to definite diagnosis will be accelerated and decisions on treatment can be made more reliable.

References

1. Adey, L., et al., *Computed tomography of suspected scaphoid fractures*. J Hand Surg Am, 2007. 32:61-66.
2. Breitenseher, M.J., et al., *Radiographically occult scaphoid fractures: value of MR imaging in detection.* Radiology, 1997. 203:245-250.
3. Buijze, G.A., et al., *Diagnostic performance of radiographs and computed tomography for displacement and instability of acute scaphoid waist fractures.* J Bone Joint Surg Am, 2012. 94:1967-1974.
4. Carpenter, C.R., et al., *Adult scaphoid fracture.* Acad Emerg Med, 2014. 21:101-121.
5. de Zwart A.D., et al., *Comparison of MRI, CT and bone scintigraphy for suspected scaphoid fractures.* Eur J Trauma Emerg Surg, 2016. 42:725-731.
6. de Zwart, A.D., et al., *MRI as a reference standard for suspected scaphoid fractures*. Br J Radiol, 2012. 85:1098-1101.
7. Duckworth, A.D., Ring D. and McQueen M.M., Assessment of the suspected fracture of the scaphoid. J Bone Joint Surg Br, 2011. 93:713-719.
8. Gemme, S. and Tubbs, R., *What physical examination findings and diagnostic imaging modalities are most useful in the diagnosis of scaphoid fractures?* Ann Emerg Med, 2015. 65:308-309.
9. Karl ,J.W., Swart, E. and Strauch, R.J., *Diagnosis of Occult Scaphoid Fractures: A Cost-Effectiveness Analysis.* J Bone Joint Surg Am, 2015. 97:1860-1868.
10. Low, G. and Raby, N., *Can follow-up radiography for acute scaphoid fracture still be considered a valid investigation?* Clin Radiol, 2005. 60:1106-1110.
11. Mallee, W.H., et al., *Computed tomography versus magnetic resonance imaging versus bone scintigraphy for clinically suspected scaphoid fractures in patients with negative plain radiographs.* Cochrane Database Syst Rev, 2015
12. Memarsadeghi, M., et al., *Occult scaphoid fractures: comparison of multidetector CT and MR imaging - initial experience.* Radiology, 2006. 240:169-176.
13. Rhemrev, S.J., et al., *Early computed tomography compared with bone scintigraphy in suspected scaphoid fractures.* Clin Nucl Med, 2010. 35:931-934.
14. Rhemrev, S.J., et al., *Current methods of diagnosis and treatment of scaphoid fractures.* Int J Emerg Med, 2011. 4:4.
15. Ring, D. and Lozano-Calderon, S., *Imaging for suspected scaphoid fracture.* J Hand Surg Am, 2008. 33:954-957.
16. Yin, Z.G., et al., *Diagnosing suspected scaphoid fractures: a systematic review and meta-analysis.* Clin Orthop Relat Res, 2010. 468:723-34.
17. Dias, J. and Kantharuban, S., *Treatment of Scaphoid Fractures: European Approaches.* Hand Clin, 2017. 33:501-509.
18. Duckworth, A.D., et al., *Predictors of fracture following suspected injury to the scaphoid.* J Bone Joint Surg Br, 2012. 94:961-968.
19. Beeres, F.J., et al., *Outcome of routine bone scintigraphy in suspected scaphoid fractures.* Injury, 2005. 36:1233-1236.
20. Cheung, G.C., Lever, C.J. and Morris, A.D., *X-ray diagnosis of acute scaphoid fractures.* J Hand Surg Br, 2006. 31:104-109.
21. Gabler, C., et al., *Diagnosis of occult scaphoid fractures and other wrist injuries. Are repeated clinical examinations and plain radiographs still state of the art?* Langenbecks Arch Surg, 2001. 386:150-154.
22. Jenkins, P.J., et al., *A comparative analysis of the accuracy, diagnostic uncertainty and cost of imaging modalities in suspected scaphoid fractures.* Injury, 2008. 39:768-774.
23. Beeres, F.J., et al., *Scaphoid fractures: diagnosis and therapy*. Ned Tijdschr Geneeskd, 2007. 151:742-747.
24. Buijze, G.A., *Scaphoid fractures: anatomy, diagnosis and treatment.* Faculty of Medicine (AMC-UvA), 2012. Amsterdam, The Netherlands.
25. Machin, E., Blackham, J. and Benger, J., *Management of suspected scaphoid fractures in the emergency department*. Guidelines in Emergency Medicine Department,2018.
26. Burghardt, A.J., Krug, R., Majumdar, S., *High-Resolution Imaging Techniques for Bone Quality Assessment.* Vitamin D (Fourth Edition), 2018.
27. Cheung, A.M., et al., *High-resolution peripheral quantitative computed tomography for the assessment of bone strength and structure: a review by the Canadian Bone Strength Working Group.* Curr Osteoporos Rep, 2013. 11:136-146.
28. de Jong, J.J., et al.,.*Assessment of the healing process in distal radius fractures by high resolution peripheral quantitative computed tomography*. Bone, 2014. 64:65-74.
29. de Jong, J.J.A., et al., *Contra-lateral bone loss at the distal radius in postmenopausal women after a distal radius fracture: A two-year follow-up HRpQCT study.* Bone, 2017. 101:245-251.
30. de Jong, J.J.A., et al., *Fracture Repair in the Distal Radius in Postmenopausal Women: A Follow-Up 2 Years Postfracture Using HRpQCT*. J Bone Miner Res, 2016. 31:1114-1122.
31. Link, T.M., *Osteoporosis imaging: state of the art and advanced imaging.* Radiology, 2012. 263:3-17.

32. Mueller, T.L., et al., *Non-invasive bone competence analysis by high-resolution pQCT: an in vitro reproducibility study on structural and mechanical properties at the human radius.* Bone, 2009. 44:364-371.
33. Bevers, M., et al., *The Feasibility of High-Resolution Peripheral Quantitative Computed Tomography (HR-pQCT) in Patients with Suspected Scaphoid Fractures.* J Clin Densitom, 2020. 23:432-444.
34. Daniels, A.M., et al., *The interobserver reliability of the diagnosis and classification of scaphoid fractures using high-resolution peripheral quantitative CT.* Bone Joint J, 2020. 102:478-484.
35. Daniels, A.M., et al., *Improved Detection of Scaphoid Fractures with High-Resolution Peripheral Quantitative CT Compared with Conventional CT.* J Bone Joint Surg Am, 2020. 16:2138-2145.
36. Manske, S.L., et al., *Human trabecular bone microarchitecture can be assessed independently of density with second generation HR-pQCT.* Bone, 2015. 79:213-221.
37. Pialat, J.B., et al., *Visual grading of motion induced image degradation in high resolution peripheral computed tomography: impact of image quality on measures of bone density and micro-architecture.* Bone, 2012. 50:111-118.
38. Pichler, W., et al., Computer-assisted 3-dimensional anthropometry of the scaphoid. Orthopedics, 2010. 33:85-88.
39. Balci, A., et al., *Wrist fractures: sensitivity of radiography, prevalence and patterns in MDCT.* Emerg Radiol, 2015. 22:251-256.
40. Beeres, F.J., et al., *Early magnetic resonance imaging compared with bone scintigraphy in suspected scaphoid fractures.* J Bone Joint Surg Br, 2008. 90:1205-1209.
41. Nguyen, Q., et al., *The clinical scaphoid fracture: early computed tomography as a practical approach.* Ann R Coll Surg Engl, 2008. 90:488-491.
42. Tiel-van Buul, M.M., et al., *Radiography and scintigraphy of suspected scaphoid fracture. A long-term study in 160 patients.* J Bone Joint Surg Br, 1993. 75:61-65.
43. Bergh, T.H., et al., *Clinical scaphoid score (CSS) to identify scaphoid fracture with MRI in patients with normal x-ray after a wrist trauma.* Emerg Med J, 2014. 31:659-664.
44. Ghane, M.R., et al., *How Trustworthy Are Clinical Examinations and Plain Radiographs for Diagnosis of Scaphoid Fractures?* Trauma Mon, 2016. 21:23345.
45. Mallee, W.H., et al., *Clinical diagnostic evaluation for scaphoid fractures: a systematic review and meta-analysis.* J Hand Surg Am, 2014. 39:1683-1691
46. Unay, K., et al., *Examination tests predictive of bone injury in patients with clinically suspected occult scaphoid fracture.* Injury, 2009. 40:1265-1268.
47. Mallee, W.H., et al., *Detecting scaphoid fractures in wrist injury: a clinical decision rule.* Arch Orthop Trauma Surg, 2020. 140:575-581.
48. Parvizi, J., et al., *Combining the clinical signs improves diagnosis of scaphoid fractures. A prospective study with follow-up.* J Hand Surg Br, 1998. 23:324-327.
49. Rhemrev, S.J., et al., *Clinical prediction rule for suspected scaphoid fractures: A prospective cohort study.* Injury, 2010. 41:1026-1030.
50. Gibney, B., et al., *Trapezium fracture: a common clinical mimic of scaphoid fracture.* Emerg Radiol, 2019. 26:531-540.

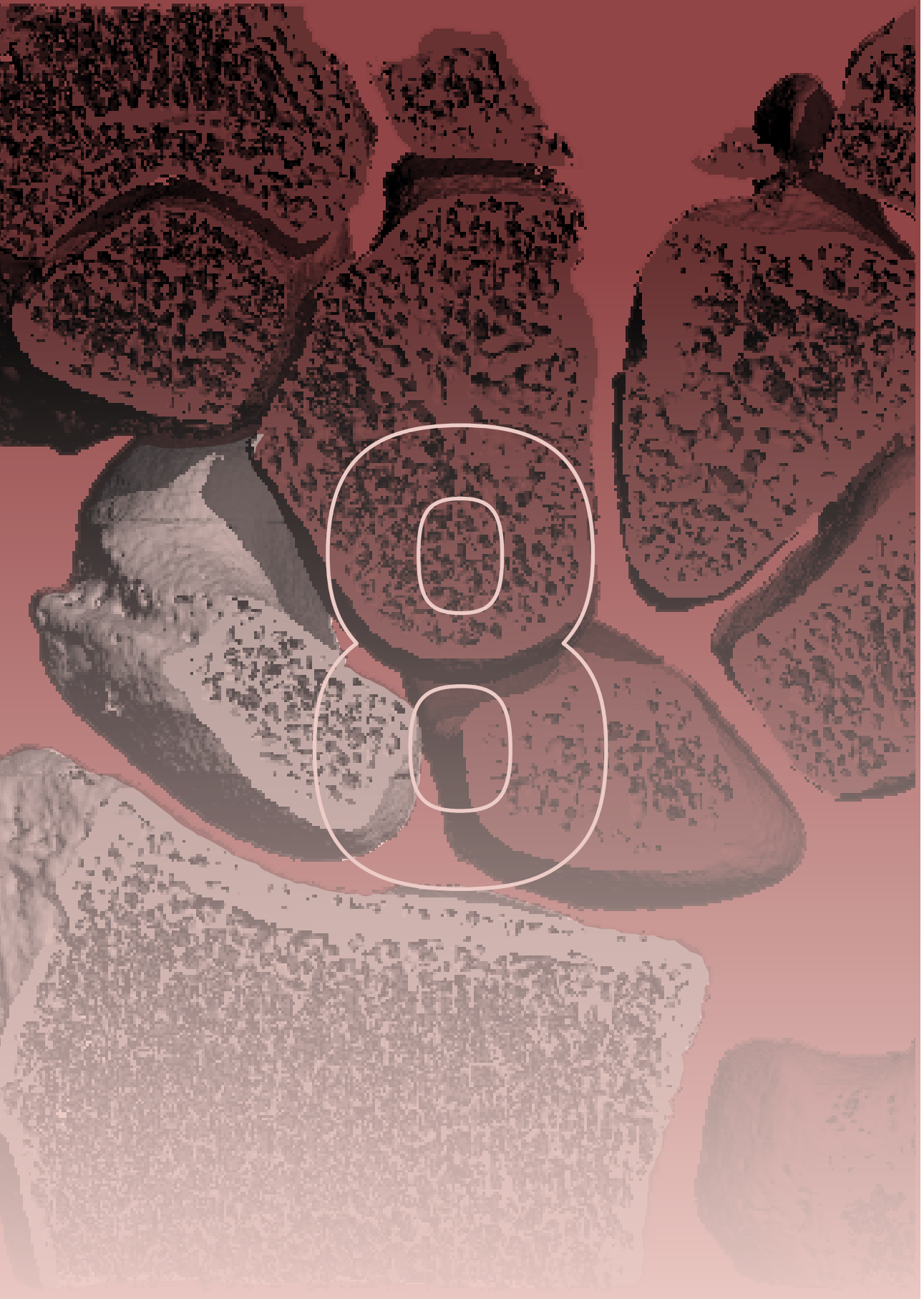

Chapter 8

Discussion

Discussion

This thesis describes the value of High Resolution peripheral Quantitative CT (HR-pQCT) to investigate factors associated with fracture pattern complexity (chapter 2) and secondary displacement (chapter 3) of distal radius fractures (DRFs) and the novel application of HR-pQCT for detection of scaphoid fractures (chapter 4-7).

Distal radius fractures

Several clinical risk factors are known to be associated with fracture risk, such as age, low body mass index (BMI), smoking, alcohol use, osteoporosis, previous fractures and the number and severity of prevalent vertebral fractures [1]. Although bone mineral density (BMD) is an important risk factor for fractures, inconsistent outcomes on the association of decreased BMD (measured by dual-energy X-ray absorptiometry (DXA)) with DRF pattern complexity [2-6] and secondary displacement [3,7] have been reported. It is hypothesized that poorer bone microarchitecture (assessed with DXA and HR-pQCT) and lower strength (assessed with HR-pQCT) might be associated with more complex fracture pattern [2-5,8-11]. In chapter 2 however, we have shown that bone microarchitecture and strength, assessed with HR-pQCT, were not associated with fracture pattern complexity. We have demonstrated that higher age and male gender were independently associated with a more complex fracture pattern of DRFs, whereas other factors which are known to be associated with fracture risk (such as BMI, BMD, number and severity of prevalent vertebral fractures, smoking and alcohol use) were not associated with DRF pattern complexity. The finding that age and gender were associated with the complexity of DRFs might be explained by the mechanism of trauma. It is known that men are more frequently involved in high velocity/transportation/work related accidents [12]. The higher velocity might result in a higher direct impact on the affected limb and thereby cause a more complex fracture pattern. Elderly patients might have less capability to react adequate and safe to a fall whereby the impact on the affected limb increases. Moreover, the position of the wrist at the time of trauma determines the direction of the force and thereby the effect on bones as well as ligamentous structures. The position of the wrist at the moment of trauma is not always known and might therefore be an unpredictable factor involved in pattern complexity of DRFs[2].

In chapter 3 we have demonstrated that patients who underwent successful reduction at primary presentation were at high risk for secondary displacement. Thereby, successful primary reduction was the most important determinant for secondary displacement of a DRF as is known in literature [13]. In addition, we found that lower total and cortical volumetric BMD and lower cortical thickness at the distal radius (assessed with HR-pQCT) were independently associated with secondary displacement of a DRF. This implies that even though cortical bone quality does not influence the fracture pattern complexity (as described in chapter 2), it may be an important risk factor for secondary displacement of a DRF. Although cortical integrity was already suggested to play a role in fracture stability [14,15], this is the first study using quantitative measures of cortical bone microarchitecture at the distal radius to assess this hypothesis.

We have learned from our data that in patients with a dislocated fracture at the time of presentation at the ED and with suitable patient characteristics for surgery (such as age and comorbidities) early operative treatment should be considered rather than primary reduction and follow-up. Based on the Dutch guidelines [16], additional imaging (CT) should be obtained when surgical repair is considered in patients with a distal radius fracture. HR-pQCT might, besides providing this (pre-operative) additional fracture information, help to identify those patients with the highest risk for secondary displacement of the fracture based on a low cortical volumetric BMD and thickness.

The work presented in chapter 2 and 3 of this thesis has several limitations. First, HR-pQCT analyses were only conducted in a subset of 71 patients of the entire cohort of 251 patients with a DRF. Since there was no difference in patient characteristics, including gender, age, length, weight, AO Orthopedic Trauma Association (OTA) DRF classification, BMD measured by DXA and vertebral fracture assessment (VFA), between patients with and without HR-pQCT measurement, we consider the results as representative for the entire cohort of patients with a DRF. Secondly, we studied a selection of patients that presented at the emergency department (ED) with a DRF because we only obtained additional information in patients that attended the Fracture Liaison Service for systematic evaluation of their subsequent fracture risk and osteoporosis (including assessment of BMD, VFA and HR-pQCT). Healthy complier bias might be introduced due to the finding that the healthiest patients attended the FLS and participated in a clinical trial [17]. Finally, the fracture classification systems used in literature [18-22] vary and thereby comparison of our results with the results of previous studies is difficult. In contrast to other classification systems, the AO/OTA classification, which we used in our study, has a strong intra- and interobserver reliability when focusing on the main type only [18,19,23]. In concordance with this, consensus rate in our study for two independent investigators was 79.7% and classification of main type was in line with previous published papers [4,24].

Scaphoid fractures

According to existing literature, 10-20% of the patients with a clinically suspected scaphoid fracture are diagnosed with a fracture based on the current imaging modalities [25-30]. Although conventional radiographs, computed tomography (CT), magnetic resonance imaging (MRI) and bone scintigraphy (BS) are frequently used, there is no consensus regarding the best modality for detecting scaphoid fractures. This results in the use of varying imaging techniques for diagnostic procedures in patients with acute scaphoid injury [27,30-34]. In chapter 4 to 7 we studied the novel application of HR-pQCT for detection of scaphoid fractures, based on the concept that high resolution imaging might reveal fractures that may have been missed with current imaging modalities with a substantially lower resolution. In chapter 4, we have studied the feasibility of HR-pQCT imaging of the scaphoid bone and have shown that, after the adjustment of the cast with an additional (removable) thumb part, the proportion of poor-quality stacks in scaphoid scans (three stacks) was similar to radius and tibia scans (one stack). The additional thumb part was needed to reduce the substantial motion artifacts. Because of the high resolution and relatively long scan times (approximately six minutes), movement during scanning can result in movement artefacts and thereby have impact on the accuracy and reproducibility of the images [35-37]. Subsequently, we have investigated the reliability of scaphoid fracture diagnosis with HR-pQCT and have shown a 90% agreement rate between four independent observers regarding scaphoid fracture diagnosis (chapter 5). This result exceeds the agreement rates (κ-values) for follow-up radiographs [38], CT [28,39], MRI [39,40] and BS [41] ranging from 14 to 80% and therefore the HR-pQCT seems to be promising. The difference in favor of HR-pQCT is most likely explained by the fact that high resolution enables a more reliable distinction between a fracture, motion artefact or a vascular structure compared to radiographs, CT and BS. The results of our studies raise the question whether higher resolution CT results would be comparable to HR-pQCT. The difference between HR-pQCT and MRI agreement rates, also in favor of HR-pQCT, might be explained by the additional findings such as edema, which is frequently seen on MRI, but not necessarily accompanied by a fracture [42]. In chapter 6, we have shown that the number of patients that was diagnosed with a scaphoid fracture was 60% higher using HR-pQCT compared to CT. Based on these results we conclude that HR-pQCT appears to be superior to conventional CT for diagnosing scaphoid fractures in a clinical research setting. Implementation in a routine clinical setting would therefore be of additional value in patients with a clinical suspicion of a scaphoid fracture at first presentation (without another diagnosis).

Besides more advanced imaging techniques, in current clinical practice conventional radiographs and clinical (re)assessment play an important role in scaphoid fracture diagnosis. The lack of a true reference standard toughens the interpretation of the diagnostic performance of both conventional radiographs and clinical (re)assessment. Overall, it is suggested that 20-40% of the scaphoid fractures are initially occult on conventional radiographs [43-46]. This is comparable with the 33%(8 out of 24) of occult scaphoid fractures on conventional radiographs we found compared to HR-pQCT in our study. In chapter 7 we have demonstrated that the accuracy of conventional radiographs at first presentation was fair (accuracy of 0.76) compared to HR-pQCT. Mainly the false positive diagnosis on conventional radiographs (38% compared to HR-pQCT) indicates that its diagnostic value is limited in diagnosing scaphoid fractures. However, conventional radiographs at initial presentation might reveal other fractures such as another carpal bone, metacarpal or distal radius fracture and thereby result in a clear diagnosis at the ED. As a result of the limited scan region of a HR-pQCT scan, other fractures outside the scanned region can be missed on HR-pQCT. Overall, we consider conventional radiographs at first presentation (at the ED) as insufficient for definite diagnosis of a scaphoid fracture, but still of value to reveal other fractures in patients with a clinically suspected scaphoid fracture.

Moreover, the presence of other fractures may influence clinical assessment findings [26,47,48]. In chapter 7, the accuracy of clinical reassessment was failed (accuracy of 0.50) compared to HR-pQCT diagnosis. Eleven other fractures were detected on HR-pQCT in patients with a clinically suspected scaphoid fracture at the time of reassessment, nine were other carpal bone fractures and two patients had a DRF. The finding that patients with other fractures have a positive clinical reassessment for scaphoid fracture detection has been described in previous studies for CT, MRI and BS imaging as well [32,49].

This suggests that clinical assessment for the presence of a scaphoid fracture is obscured by the presence of other fractures and therefore has a poor specificity.

The work presented in chapter 4 to 7 of this thesis has several limitations. First, we compared a novel technique (HR-pQCT) to an existing technique (CT) as reference, although no true reference standard is available since CT, but also MRI and BS have limitations regarding scaphoid fracture diagnosis in current clinical practice. Secondly, the assessment of interobserver agreement for the classification of scaphoid fractures was limited due to the relatively small number of patients in each group. Preferably, a higher number of patients (and HR-pQCT scans) should have been assessed to evaluate the reliability of

fracture classification between multiple observers. The (clinical) consequence of diagnosis missed with conventional CT and detected with HR-pQCT is presently unknown, so the importance of diagnosing occult scaphoid fractures has to be further studied. Besides the limited availability of HR-pQCT devices in hospitals worldwide, scanning time is longer compared to CT and multiple-stack scanning is needed since the length of one HR-pQCT stack is limited to 1 cm [50]. Therefore, motion artefacts and stack shifts are frequently seen and remain challenging in HR-pQCT image assessment. In addition, due to motion artefacts, repeated measurements are needed in approximately one-third of HR-pQCT scans. On the other hand, the effective radiation dose of HR-pQCT is low compared to CT and can be interpreted as equal if the length of the total scanned region is taken into account.

Conclusions and future perspectives

Overall, we conclude that the application of HR-pQCT imaging has resulted in novel insights into factors associated with the pattern complexity and secondary displacement of distal radius fractures. Age and gender were independently associated with the pattern complexity of DRFs, whereas other factors including bone microarchitecture and bone strength were not. Regarding secondary displacement of a DRF, primary reduction was the most important determinant, as is known in literature. A novel finding of our study was, that lower total and cortical vBMD and lower cortical thickness of the distal radius were independently associated with secondary displacement of a DRF. Although this finding is of interest, it is desirable to further study this association in a prospective study. We also suggest to extend the age range by including a younger group of patients (for example > 18 years) which might result in a higher variation of bone microarchitectural parameters.

The application of HR-pQCT was assessed for the first time for scaphoid fracture diagnosis. We have demonstrated that in vivo HR-pQCT scanning of the scaphoid bone is feasible in patients with a clinically suspected scaphoid fracture when using a cast with thumb part during scan acquisition. Moreover, diagnosis of scaphoid and other fractures is reliable based on HR-pQCT scans in patients with a clinically suspected scaphoid fracture and resulted in a substantially (60%) higher number of patients diagnosed with a scaphoid fracture compared to CT. Therefore, it can be concluded that HR-pQCT was proven to be superior to conventional CT. It is however desirable to replicate this in larger prospective cohorts. In our opinion it is of added value to compare HR-pQCT with conventional CT (with higher resolution), MRI and BS in a combined approach in future studies to define a true reference standard for scaphoid fracture detection.

Further, based on our study revealing the accuracy for clinical reassessment of only 50%, we suggest that additional imaging should not be conducted in addition to or based upon clinical reassessment but should rather immediately replace the current clinical reassessment. By introducing early additional imaging (high resolution CT) in all patients instead of decision making (including the decision to perform imaging) based on clinical reassessment, the time to definite diagnosis will be accelerated and decisions on treatment can be made more reliably.

Most expediently would be future research addressing the (clinical) consequences of diagnosis missed with conventional CT and detected with HR-pQCT. Since it is unethical to withhold adequate treatment for patients with a scaphoid fracture this is only possible in a randomized controlled trial with informed consent and narrow follow-up so that early intervention is still possible in the group of patients with a scaphoid fracture on HR-pQCT but not subjected to cast immobilization. This would make these data more relevant to clinicians and contribute to the implementation of HR-pQCT in diagnosing scaphoid fractures in clinical practice. In line with this, microarchitectural bone evaluations in patients with a suspected scaphoid fracture and research into the healing process of scaphoid fractures should be addressed.

The implementation of HR-pQCT in clinical practice should go along with the development of standard imaging protocols for the scaphoid with longer stack regions, faster image processing and a reduced analysis time. This will reduce the costs of a HR-pQCT scan, which is now roughly three times higher than the costs of a regular CT in our facility.

References

1. van den Bergh, J.P., et al., *Osteoporosis, frailty and fracture: implications for case finding and therapy.* Nat Rev Rheumatol, 2012. 8(3): p. 163-72.
2. Itoh, S., et al., *Relationship between bone mineral density of the distal radius and ulna and fracture characteristics.* J Hand Surg Am, 2004. 29(1): p. 123-30.
3. Clayton, R.A., et al., *Association between decreased bone mineral density and severity of distal radial fractures.* J Bone Joint Surg Am, 2009. 91(3): p. 613-9.
4. Dhainaut, A., et al., *Exploring the relationship between bone density and severity of distal radius fragility fracture in women.* J Orthop Surg Res, 2014. 9: p. 57.
5. de Klerk, G., et al., *The relation between AO-classification of distal radial fractures and bone mineral density.* Injury, 2013. 44(11): p. 1657-8.
6. Bleibler, F., et al., *The health burden and costs of incident fractures attributable to osteoporosis from 2010 to 2050 in Germany--a demographic simulation model.* Osteoporos Int, 2013. 24(3): p. 835-47.
7. Robin, B.N., et al., *Relationship of bone mineral density of spine and femoral neck to distal radius fracture stability in patients over 65.* J Hand Surg Am, 2014. 39(5): p. 861-6.e3.
8. Burghardt, A.J., et al., *Age- and gender-related differences in the geometric properties and biomechanical significance of intracortical porosity in the distal radius and tibia.* J Bone Miner Res, 2010. 25(5): p. 983-93.
9. Rozental, T.D., et al., *Premenopausal women with a distal radial fracture have deteriorated trabecular bone density and morphology compared with controls without a fracture.* J Bone Joint Surg Am, 2013. 95(7): p. 633-42.
10. Oyen, J., et al., *Osteoporosis as a risk factor for distal radial fractures: a case-control study.* J Bone Joint Surg Am, 2011. 93(4): p. 348-56.
11. Oyen, J., et al., *Low bone mineral density is a significant risk factor for low-energy distal radius fractures in middle-aged and elderly men: a case-control study.* BMC Musculoskelet Disord, 2011. 12: p. 67.
12. Pape, M., et al., *Is there an association between female gender and outcome in severe trauma? A multi-center analysis in the Netherlands.* Scand J Trauma Resusc Emerg Med, 2019. 27(1): p. 16.
13. Nesbitt, K.S., et al., *Assessment of instability factors in adult distal radius fractures.* J Hand Surg Am, 2004. 29(6): p. 1128-38.
14. Lafontaine, M., et al., *Stability assessment of distal radius fractures.* Injury, 1989. 20(4): p. 208-10.
15. Mackenney, P.J., et al., *Prediction of instability in distal radial fractures.* J Bone Joint Surg Am, 2006. 88(9): p. 1944-51.
16. Nederlandse Vereniging voor Heelkunde, *Richtlijn distale radius fracturen.* Federatie Medisch Specialisten, 2021.
17. Vranken, L., et al., *The association between prevalent vertebral fractures and bone quality of the distal radius and distal tibia as measured with HR-pQCT in postmenopausal women with a recent non-vertebral fracture at the Fracture Liaison Service.* Osteoporos Int, 2019. 30(9): p. 1789-1797.
18. Lill, C.A., et al., *Impact of bone density on distal radius fracture patterns and comparison between five different fracture classifications.* J Orthop Trauma, 2003. 17(4): p. 271-8.
19. Plant, C.E., et al., *Is it time to revisit the AO classification of fractures of the distal radius? Inter- and intra-observer reliability of the AO classification.* Bone Joint J, 2015. 97-b(6): p. 818-23.
20. Arealis, G., et al., *Does the CT improve inter- and intra-observer agreement for the AO, Fernandez and Universal classification systems for distal radius fractures?* Injury, 2014. 45(10): p. 1579-84.
21. Andersen, D.J., et al., *Classification of distal radius fractures: an analysis of interobserver reliability and intraobserver reproducibility.* J Hand Surg Am, 1996. 21(4): p. 574-82.
22. Ferrero, A., et al., *Analysis of the inter- and intra-observer agreement in radiographic evaluation of wrist fractures using the multimedia messaging service.* Hand (N Y), 2011. 6(4): p. 384-9.
23. Belloti, J.C., et al., *Are distal radius fracture classifications reproducible? Intra and interobserver agreement.* Sao Paulo Med J, 2008. 126(3): p. 180-5.
24. Jayakumar, P., et al., *AO Distal Radius Fracture Classification: Global Perspective on Observer Agreement.* J Wrist Surg, 2017. 6(1): p. 46-53.
25. Kozin, S.H., *Incidence, mechanism and natural history of scaphoid fractures.* Hand Clin, 2001. 17(4): p. 515-24.
26. Jenkins, P.J., et al., *A comparative analysis of the accuracy, diagnostic uncertainty and cost of imaging modalities in suspected scaphoid fractures.* Injury, 2008. 39(7): p. 768-74.
27. Mallee, W.H., et al., *Computed tomography versus magnetic resonance imaging versus bone scintigraphy for clinically suspected scaphoid fractures in patients with negative plain radiographs.* Cochrane Database Syst Rev, 2015(6): p. Cd010023.
28. Adey, L., et al., *Computed tomography of suspected scaphoid fractures.* J Hand Surg Am, 2007. 32(1): p. 61-6.
29. Ring, D. and Lozano-Calderon, S., *Imaging for suspected scaphoid fracture.* J Hand Surg Am, 2008. 33(6): p. 954-7.

30. Rhemrev, S.J., et al., *Early computed tomography compared with bone scintigraphy in suspected scaphoid fractures.* Clin Nucl Med, 2010. 35(12): p. 931-4.
31. Buijze, G.A., et al., *Diagnostic performance tests for suspected scaphoid fractures differ with conventional and latent class analysis.* Clin Orthop Relat Res, 2011. 469(12): p. 3400-7.
32. de Zwart, A.D., et al., *Comparison of MRI, CT and bone scintigraphy for suspected scaphoid fractures.* Eur J Trauma Emerg Surg, 2016. 42(6): p. 725-731.
33. Yin, Z.G., et al., *Diagnosing suspected scaphoid fractures: a systematic review and meta-analysis.* Clin Orthop Relat Res, 2010. 468(3): p. 723-34.
34. Groves, A.M., et al., *An international survey of hospital practice in the imaging of acute scaphoid trauma.* AJR Am J Roentgenol, 2006. 187(6): p. 1453-6.
35. Pauchard, Y., et al., *Quality control for bone quality parameters affected by subject motion in high-resolution peripheral quantitative computed tomography.* Bone, 2012. 50(6): p. 1304-10.
36. Engelke, K., et al., *Short-term in vivo precision of BMD and parameters of trabecular architecture at the distal forearm and tibia.* Osteoporos Int, 2012. 23(8): p. 2151-8.
37. Sode, M., et al., *Quantitative characterization of subject motion in HR-pQCT images of the distal radius and tibia.* Bone, 2011. 48(6): p. 1291-7.
38. Mallee, W.H., et al., *6-week radiographs unsuitable for diagnosis of suspected scaphoid fractures.* Arch Orthop Trauma Surg, 2016. 136(6): p. 771-8.
39. de Zwart, A.D., et al., *Interobserver variability among radiologists for diagnosis of scaphoid fractures by computed tomography.* J Hand Surg Am, 2012. 37(11): p. 2252-6.
40. Beeres, F.J., et al., *Observer variation in MRI for suspected scaphoid fractures.* Br J Radiol, 2008. 81(972): p. 950-4.
41. Beeres, F.J., et al., *Reliability of bone scintigraphy for suspected scaphoid fractures.* Clin Nucl Med, 2007. 32(11): p. 835-8.
42. Tibrewal, S., et al., *Role of MRI in the diagnosis and management of patients with clinical scaphoid fracture.* Int Orthop, 2012. 36(1): p. 107-10.
43. Tiel-van Buul, M.M., et al., *Radiography and scintigraphy of suspected scaphoid fracture. A long-term study in 160 patients.* J Bone Joint Surg Br, 1993. 75(1): p. 61-5.
44. Gabler, C., et al., *Diagnosis of occult scaphoid fractures and other wrist injuries. Are repeated clinical examinations and plain radiographs still state of the art?* Langenbecks Arch Surg, 2001. 386(2): p. 150-4.
45. Nguyen, Q., et al., *The clinical scaphoid fracture: early computed tomography as a practical approach.* Ann R Coll Surg Engl, 2008. 90(6): p. 488-91.
46. Memarsadeghi, M., et al., *Occult scaphoid fractures: comparison of multidetector CT and MR imaging--initial experience.* Radiology, 2006. 240(1): p. 169-76.
47. Carpenter, C.R., et al., *Adult scaphoid fracture.* Acad Emerg Med, 2014. 21(2): p. 101-21.
48. Gibney, B., et al., *Trapezium fracture: a common clinical mimic of scaphoid fracture.* Emerg Radiol, 2019. 26(5): p. 531-540.
49. Beeres, F.J., et al., *Early magnetic resonance imaging compared with bone scintigraphy in suspected scaphoid fractures.* J Bone Joint Surg Br, 2008. 90(9): p. 1205-9.
50. van den Bergh, J.P., et al., *The clinical application of high-resolution peripheral computed tomography (HR-pQCT) in adults: state of the art and future directions.* Osteoporos Int, 2021. 32(8): p. 1465-1485.

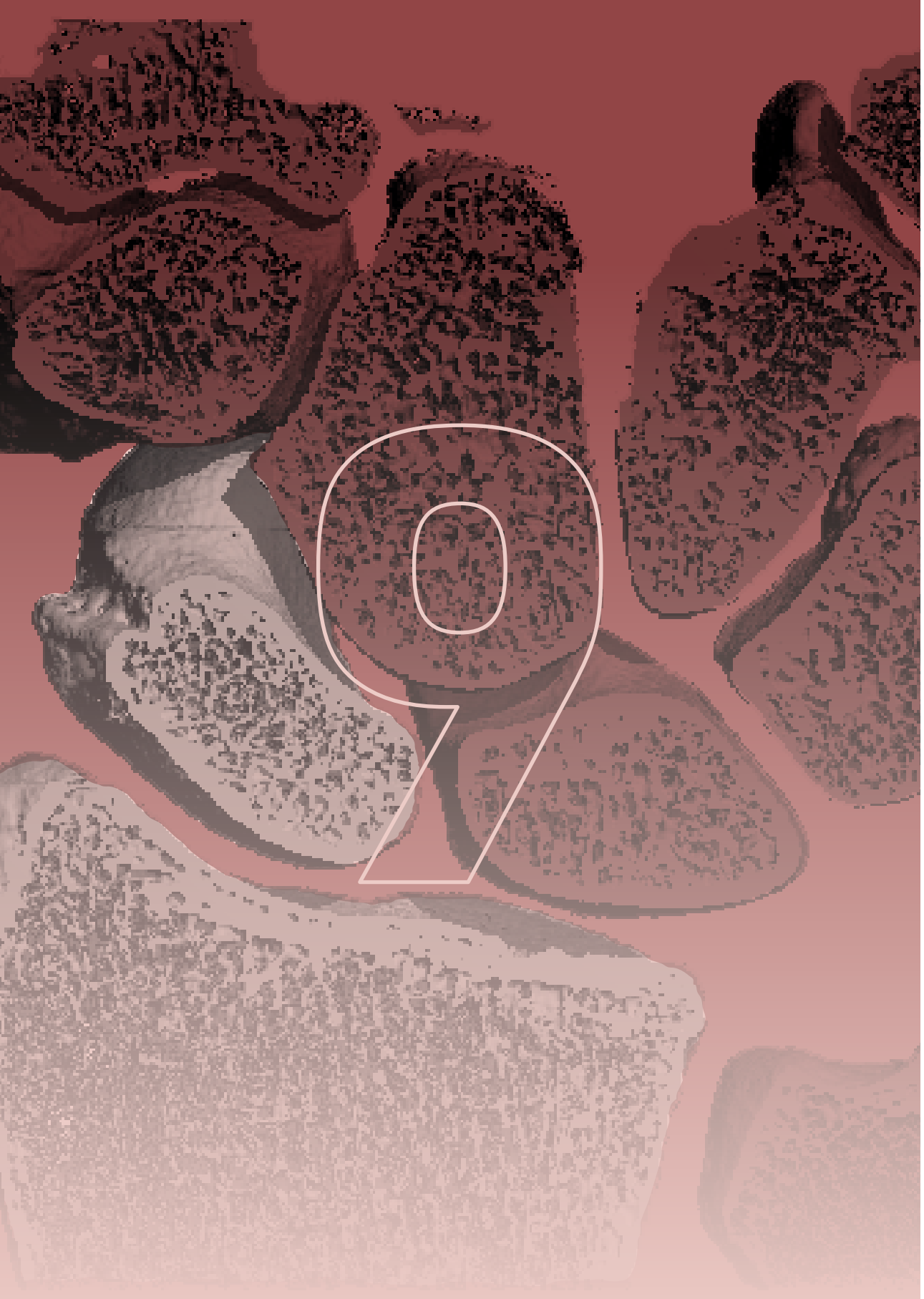

Chapter 9

Summary
Samenvatting (Dutch)

Summary

In this thesis, we studied the association of patient characteristics, bone mineral density (BMD, measured by Dual Energy X-ray Absorptiometry (DXA)), bone microarchitecture and calculated bone strength (by High Resolution peripheral Quantitative Computer Tomography (HR-pQCT)) with the pattern complexity and secondary displacement of distal radius fractures. Subsequently, we studied the novel application of HR-pQCT for detection of scaphoid fractures, compared to current diagnostic modalities such as Computed Tomography (CT), Magnetic Resonance Imaging (MRI) and Bone Scintigraphy (BS).

Chapter 1 sets out the background and outline of this thesis and presents an overview of the epidemiology, classification and treatment of distal radius and scaphoid fractures.

In ***chapter 2*** we have investigated the association of patient characteristics, BMD, bone microarchitecture and bone strength (assessed with HR-QCT) with the pattern complexity of distal radius fractures. In a cohort of 251 patients aged 50-90 years, we have demonstrated that age (Odds ratio (OR) 1.11, 95% CI 1.03-1.19) and male gender (OR 8.48, 95% CI 1.75-41.18) were independently associated with the pattern complexity of distal radius fractures. Other factors known to be associated with fracture risk, including body mass index, BMD, number and severity of prevalent vertebral fractures, smoking and alcohol use were not associated with distal radius fracture pattern complexity. In addition, bone microarchitecture and bone strength were not associated with fracture pattern complexity. This indicates that, besides age and gender, trauma mechanism may also be an important determinant for distal radius fracture pattern complexity.

Chapter 3 described the association of patient characteristics, BMD, bone microarchitecture and strength with secondary displacement of distal radius fractures based on radiographic alignment parameters. In our cohort of 251 patients, the most important determinant for secondary displacement of a distal radius fracture was primary reduction (OR 22.00, 95% CI 2.27-212.86). While age, gender, bone mineral density measured by dual-energy X-ray absorptiometry and prevalent vertebral fracture status were not associated with secondary fracture displacement, lower total (OR 0.16, 95% CI 0.04-0.68) and cortical volumetric bone mineral density (OR 0.19, 95% CI 0.05-0.80) and lower cortical thickness (OR 0.13, 95% CI 0.02-0.74) at the distal radius were independently associated with secondary displacement of a distal radius fracture. This implies that besides primary reduction, poor cortical bone quality may be important for the risk of secondary displacement of distal radius fractures.

In **chapter 4 to 7**, we studied the application of HR-pQCT for detection of scaphoid fractures. As there were no data available in literature regarding the feasibility of HR-pQCT imaging of the scaphoid bone, we performed a prospective cohort study in 91 consecutive patients, ≥ 18 years with a clinically suspected scaphoid fracture. In the emergency department (ED), conventional radiographs of the scaphoid bone were made. Independent of the diagnosis on these initial radiographs, cast immobilization was applied and reassessment at the outpatient clinic was performed within 7 to 14 days after trauma. Conventional CT and HR-pQCT of the scaphoid bone were scheduled immediately following reassessment.

In ***chapter 4*** we compared a fully automated and a semi-automated contouring procedure of the scaphoid bone and evaluated the microarchitectural indices in good- and poor- quality scans. We found that it was necessary to extend the standard cast with an additional (removable) thumb part in order to reduce motion artifacts. After this modification, the proportion of poor-quality stacks was similar to distal radius and tibia scans and automatic contouring starting from course hand-drawn pre-contours appeared to be appropriate in good and bad quality scans. We concluded that in vivo HR-pQCT scanning of the scaphoid bone is feasible in patients with a clinically suspected scaphoid fracture when using a cast with thumb part.

Based on the findings in chapter 4, we investigated the interobserver agreement of the diagnosis and classification of scaphoid fractures, in a randomly selected subgroup of 31 out of the 91 patients, in ***chapter 5***. We found an interobserver agreement of 91% for the identification of a scaphoid fracture of (κ = 0.91, 95% CI 0.76-1.00) and 80% for the identification of other fractures of (κ = 0.80, 95% CI 0.72-0.87). Additionally, the mean intra-class correlation coefficient for the classification of a scaphoid fracture in the seven patients diagnosed with scaphoid fracture by all four observers was 73% (95% CI 0.42-0.94). We concluded that the diagnosis of scaphoid and other fractures using HR-pQCT is reliable in patients with a clinically suspected scaphoid fracture.

To investigate whether the use of HR-pQCT increased scaphoid fracture detection, we compared this technique to conventional CT in our cohort of 91 patients with a clinically suspected scaphoid fracture in ***chapter 6***. The number of patients diagnosed with a scaphoid fracture was 60% higher when using HR-pQCT (N=24) compared to CT (N=15). The correlation between CT and HR-

pQCT was high for the Herbert classification of scaphoid fractures (Kendall rank correlation coefficient (W) 0.793, p<0.001) and very high (W 0.955, p<0.001) for scaphoid fracture location (proximal, waist, distal). We therefore concluded that scaphoid fracture detection with HR-pQCT is superior compared to conventional CT and that HR-pQCT could be a promising novel application for the detection of scaphoid fractures.

In ***chapter 7*** the performance of conventional radiographs (at first presentation at the ED) and clinical reassessment (after 7-14 days) for the diagnosis of scaphoid fractures was compared to HR-pQCT. The accuracy of conventional radiographs at the ED was fair (AUC 0.76) and clinical reassessment failed (AUC 0.50) compared to HR-pQCT, indicating that the value of initial radiographs and especially clinical reassessment is limited in diagnosing scaphoid fractures.

Chapter 8 provides a general discussion with conclusion following from this thesis.

Nederlandse samenvatting

In dit proefschrift hebben we onderzocht of er een associatie is tussen patiëntkenmerken, botdichtheid gemeten met Dual-energy X-ray absorptiometry (DXA), bot microarchitectuur en berekende botsterkte met hoog-resolutie kwantitatieve CT scanning (Engels: 'High Resolution peripheral Quantitative Computed Tomography', afgekort HR-pQCT) en de complexiteit en secundaire verplaatsing van pols (distale radius) breuken (fracturen). Daarnaast hebben we een nieuwe toepassing van HR-pQCT voor de detectie van fracturen van het scheepvormig handwortelbeentje (scaphoïd) bestudeerd en vergeleken met de huidige diagnostische modaliteiten zoals de CT (computed tomography) scan, de MRI (magnetic resonance imaging) scan en de bot scintigrafie (botscan).

Hoofdstuk 1 schetst de achtergrond en opzet van dit proefschrift en geeft een overzicht van de epidemiologie, classificatie en behandeling van distale radius- en scaphoïd fracturen.

In ***hoofdstuk 2*** hebben we de relatie tussen patiëntkenmerken, botdichtheid, bot microarchitectuur en botsterkte gemeten met HR-pQCT met de complexiteit van distale radiusfracturen onderzocht. In een cohort van 251 patiënten met een leeftijd tussen 50-90 jaar hebben we aangetoond dat leeftijd (Odds ratio (OR) 1.11, 95% BI 1.03-1.19) en mannelijk geslacht (OR 8.48, 95% BI 1.75-41.18) onafhankelijk geassocieerd waren met de complexiteit van distale radiusfracturen. Andere factoren waarvan bekend is dat ze geassocieerd zijn met het risico op fracturen, waaronder body mass index, botdichtheid, het aantal en de ernst van wervelfracturen, roken en alcoholgebruik, waren niet geassocieerd met de complexiteit van distale radius fracturen. Daarnaast waren ook bot microarchitectuur en botsterkte niet geassocieerd met de complexiteit van de fractuur. Dit geeft aan dat, naast leeftijd en geslacht, het traumamechanisme een belangrijke determinant kan zijn voor de complexiteit van distale radius fracturen maar dat HR-pQCT parameters geen voorspellende waarden zijn voor de complexiteit van een distale radius fractuur.

In ***hoofdstuk 3*** werd de relatie tussen patiëntkenmerken, botdichtheid, bot microarchitectuur en botsterkte gemeten met HR-pQCT met secundaire verplaatsing van distale radiusfracturen op basis van de stand van de fractuur op de röntgenfoto's beschreven. In ons cohort van 251 patiënten was primaire repositie de belangrijkste determinant voor secundaire verplaatsing van een distale radiusfractuur (OR 22.00, 95% BI 2.27-212.86). Leeftijd, geslacht, botdichtheid en prevalente wervelfracturen waren niet geassocieerd met secundaire fractuurverplaatsing, terwijl lagere totale (OR 0.16, 95% BI 0.04-0.68) en corticale volumetrische BMD (OR 0.19, 95% CI 0.05-0.80) en lagere corticale dikte (OR 0.13, 95% CI 0.02-0.74) van de distale radius wel onafhankelijk gerelateerd waren aan secundaire verplaatsing van een distale radiusfractuur. Dit impliceert dat naast primaire repositie, een verminderde corticale botkwaliteit kan bijdragen aan het risico op secundaire verplaatsing van een distale radius fractuur.

In ***hoofdstuk 4 tot en met 7*** hebben we de toepassing van HR-pQCT voor de detectie van scaphoïd fracturen bestudeerd. Omdat er in de literatuur geen gegevens beschikbaar waren over de haalbaarheid van HR-pQCT-beeldvorming van het scaphoïd, hebben we een prospectieve cohortstudie uitgevoerd bij 91 opeenvolgende patiënten, ≥18 jaar met een klinische verdenking op een scaphoïd fractuur. Op de spoedeisende hulp (SEH) werden conventionele röntgenfoto's van het scaphoïd gemaakt. Onafhankelijk van de diagnose op deze röntgenfoto's werd de patiënt geïmmobiliseerd in een onderarms gips en 7-14 dagen later opnieuw beoordeeld op de polikliniek. Bij alle patiënten werd ook een CT en HR-pQCT van het scaphoïd uitgevoerd op de dag van de herbeoordeling op de polikliniek.

In ***hoofdstuk 4*** vergeleken we een volledig geautomatiseerde en een semiautomatische procedure om de HR-pQCT beelden van het scaphoïd te contouren en evalueerden we de microarchitectuur parameters in scans van zowel goede als slechte kwaliteit. We stelden vast dat het noodzakelijk was om het standaard onderarms gips uit te breiden met een afneembare duimspalk om bewegingsartefacten op de scanbeelden te verminderen. Na deze wijziging was het percentage scans van slechte kwaliteit vergelijkbaar met de standaard distale radius- en tibia HR-pQCT scans, en bleek een automatische contourvorming beginnend met handgetekende pre-contouren geschikt te zijn bij scans van zowel goede als slechte kwaliteit. We concludeerden dat in vivo HR-pQCT-scanning van het scaphoïd goed uitvoerbaar is bij patiënten met een klinische verdenking op een scaphoïd fractuur bij gebruik van een additionele afneembare duimspalk.

Gebaseerd op de bevindingen in hoofdstuk 4, hebben we in ***hoofdstuk 5*** de inter-beoordelaar overeenkomst van de diagnose en classificatie van scaphoïd fracturen onderzocht in een willekeurig geselecteerde subgroep van 31 van de 91 patiënten. We vonden een inter-beoordelaar overeenkomst van 91% voor het diagnosticeren van een scaphoïd fractuur (κ = 0,91, 95% BI 0,76-1,00) en 80% voor het diagnosticeren van andere fracturen (κ = 0.80, 95% BI 0.72-0.87) wanneer we de HR-pQCT gebruikten. De gemiddelde intra-class correlatiecoëfficiënt (ICC) voor de classificatie van een scaphoïd fractuur in de zeven patiënten gediagnosticeerd met een scaphoïd fractuur door alle vier de beoordelaars was

73% (95% BI 0.42-0.94). We concludeerden dat de diagnose van scaphoïd- en andere fracturen met HR-pQCT betrouwbaar is bij patiënten met een klinische verdenking op een scaphoïd fractuur.

Om te onderzoeken of de toepassing van HR-pQCT zou kunnen leiden tot het frequenter vaststellen van een scaphoïd fractuur hebben we deze techniek in ***hoofdstuk 6*** vergeleken met de conventionele CT in ons cohort van 91 patiënten met een klinische verdenking op een scaphoïd fractuur. Het aantal patiënten gediagnosticeerd met een scaphoïd fractuur was 60% hoger bij gebruik van HR-pQCT (N=24) in vergelijking met CT (N=15). De correlatie tussen CT en HR-pQCT was hoog voor de Herbert-classificatie van scaphoïd fracturen (Kendall-rank correlatiecoëfficiënt (W) 0.793, p<0,001) en zeer hoog (W 0.955, p<0,001) voor de locatie van de scaphoïd fractuur (proximaal, taille, distaal). We concludeerden dat de detectie van scaphoïd fracturen met HR-pQCT superieur is in vergelijking met conventionele CT en dat HR-pQCT een veelbelovende nieuwe toepassing zou kunnen zijn voor de detectie van scaphoïd fracturen.

In ***hoofdstuk 7*** werd de diagnose van scaphoïd fracturen op basis van conventionele röntgenfoto's (bij eerste presentatie op de SEH) en klinische herbeoordeling (na 7-14 dagen) vergeleken met HR-pQCT. De nauwkeurigheid van conventionele röntgenfoto's op de SEH was redelijk (AUC 0,76) en klinische herbeoordeling onvoldoende (AUC 0,50) in vergelijking met HR-pQCT. Dit geeft aan dat de waarde van initiële röntgenfoto's en vooral klinische herbeoordeling beperkt is bij het diagnosticeren van scaphoïd fracturen.

Hoofdstuk 8 geeft een algemene discussie weer met de conclusie die volgt uit dit proefschrift.

Chapter 10

Impact Paragraph
Acknowledgements
Curriculum vitae
List of publications
List of abbreviations

Impact paragraph

Distal radius fractures (DRFs) are the most common fractures in adults and scaphoid fractures the most common carpal fractures. These injuries have a significant contribution to emergency department (ED) visits and a substantial impact on both patients' physical and mental health. As result of prolonged time off work and high healthcare costs, these injuries are responsible for a considerable socioeconomic burden. The consequences for the patient and thereby society reach further than only the economic impact. For example, functional limitations, pain, psychological stress and decreased social interactions are important factors that need to be taken into account.

It is well known that osteoporosis is related to fracture risk. The most common method to evaluate bone mineral density (BMD) is dual-energy X-ray absorptiometry (DXA). More recent, High Resolution peripheral Quantitative CT (HR-pQCT), a three-dimensional quantitative imaging technique of the distal radius and distal tibia has been developed. In addition to the BMD measured by DXA, this low radiation technique allows in vivo measurement of bone microarchitecture at the extremities by performing a 'virtual bone biopsy'. Moreover HR-pQCT provides higher resolution images of an bigger area than only the virtual biopsy whereby fracture detection might be improved. This thesis was set up to assess the value of HR-pQCT to investigate both the prognostic and diagnostic value in distal radius respectively scaphoid fractures. Although BMD is proven to be an important component of fracture risk, the contribution of decreased BMD (measured by DXA) to DRF pattern complexity and secondary displacement of a DRF is reported with controversial results. We have demonstrated that besides age and male gender there was no association between BMD, bone microarchitecture or other risk factors and DRF pattern complexity in our study. However, lower total and cortical volumetric BMD and lower cortical thickness at the distal radius (assessed with HR-pQCT) were independently associated with secondary displacement of a DRF. Besides these bone microarchitectural values, patients with a primary displaced fracture who underwent successful reduction at primary presentation were at high risk for secondary displacement.

We have learned from these data that in patients aged > 50 years with a dislocated fracture at presentation with suitable patient characteristics for surgery (such as age and comorbidities) early operative treatment should be considered rather than primary reduction and follow-up. HR-pQCT might help to identify the patient(s) at highest risk for secondary displacement in the future. On patient level this results in more customized treatment options leading to a deliberate decision. On economic/society level this might cause earlier return to work and participation in society with positive effects on both physical and mental health.

Reducing time to diagnosis and thereby a similar effect on economic/society level can be accomplished by our study assessing the diagnostic value of HR-pQCT in scaphoid fractures. Since HR-pQCT is a novel application, we have first demonstrated that HR-pQCT is feasible and reliable in patients with a clinically suspected scaphoid fracture. Secondly, we have proven that it is superior compared to conventional CT. This is relevant as there is no current true reference standard for diagnosing scaphoid fractures since all additional imaging techniques have their shortcomings. In current clinical practice, patients with a suspected scaphoid fracture are clinically reassessed in approximately 1-2 weeks. During this time the wrist of the patient is immobilized with a cast resulting in the inability to participate in the society (for example work). After reassessment the healthcare professional will make the decision to conduct additional imaging. However, our study indicates that the value of clinical reassessment is limited in diagnosing scaphoid fractures.

We therefore recommend to conduct early additional imaging with high resolution CT instead of clinical reassessment to obtain early definite diagnosis and reduce unnecessary immobilization in all patients with a clinically suspected scaphoid fracture aged ≥ 18 years presenting at the ED.

This is the first study assessing HR-pQCT as a prognostic tool for distal radius fracture complexity and displacement and as a diagnostic tool for scaphoid fractures. The results from the different studies in this PhD thesis will initiate and/or support future research and thereby be beneficial for researchers and healthcare professionals. More specifically, the gained knowledge regarding DRFs and scaphoid fractures will be beneficial for patients with a DRF aged over 50 years respectively patients with a clinically suspected scaphoid fracture aged 18 years and older. The novel information obtained in this thesis will assist both healthcare professionals as patients in choosing the appropriate treatment or diagnostic tool.

Transferring these research findings to healthcare professionals in order to instigate a change in the use of additional imaging, more specifically HR-pQCT, is one of the most important factors for success. This is and will be achieved by

the published articles and for example an already implemented updated protocol in the hospital involved in the studies. Widespread sharing of the results has occurred and will be pursued on both national and international congresses. The knowledge should than be transparently shared with the patient at for example the ED or outpatient clinic whereby the healthcare professional and the patient can make a deliberate decision together.

Acknowledgements

Save the best for last! Met het schrijven van mijn dankwoord komt ook het besef dat het écht klaar is. Na mijn afstuderen wilde ik ontzettend graag aan de slag als arts in de kliniek in plaats van non-stop achter een computer zitten (lees: promoveren). Ik heb de unieke kans gekregen om werken in de kliniek te kunnen combineren met mijn promotietraject en dat had ik niet kunnen doen zonder alle steun die ik van jullie heb gekregen.

Om te beginnen wil ik heel graag de *patiënten* bedanken die zo enthousiast hebben deelgenomen aan onze prospectieve studie. Zonder jullie was dit nooit gelukt!

Uiteraard wil ik heel graag mijn promotieteam bedanken; Prof. dr. Joop van den Bergh, Prof. dr. Martijn Poeze, dr. Heinrich Janzing en dr. Caroline Wyers. Jullie hebben mij de kans en het vertrouwen gegeven om te promoveren. Ook hebben jullie mij gesteund toen ik met het plan kwam om mijn promotietraject simultaan aan mijn ANIOS tijd te doorlopen. En ook al was niet iedereen even enthousiast toen ik wilde mee solliciteren voor de opleiding tot chirurg nog voordat mijn proefschrift af was (omdat jullie uit ervaring wisten dat het dan nog een paar jaar zou blijven liggen... en zo geschiedde), toch hadden jullie enorm veel begrip dat het tempo van mijn promotie iets omlaag ging en dat waardeer ik heel erg! De zowel chirurgische als internistische input heeft uiteraard vele voordelen maar kan ook af en toe haaks op elkaar staan, tsja... waarom zou het ook anders zijn dan in de kliniek?! Dank jullie wel voor jullie begeleiding in dit wetenschappelijke avontuur.

Joop, je oog voor detail heeft er voor gezorgd dat ieder stuk in optimale conditie is ingestuurd. De ontelbare aanvullende analyses waar we uiteindelijk niks mee gingen doen heb ik je absoluut niet altijd in dank afgenomen maar zijn zonder twijfel van aanvullende waarde geweest voor het begrijpen en interpreteren van de resultaten. Dankjewel voor alles!

Martijn, je wist op ieder moment precies hoe het er met mijn stukken voor stond dankzij alle notities op je Ipad. Je prikkelde me vanaf ons eerste gesprek om na te denken over een titel, iets waarvan ik toen dacht; 'dit is nog zó ver weg'.

Heinrich, dr. Janzing, bedankt voor de steun, het vertrouwen en alle goede zorgen. Ondanks de weinige woorden wist ik heel goed wanneer u enthousiast werd van mijn geratel door de glimlach op uw gezicht. Een van de grootste obstakels in mijn promotie periode was de aanhef van mijn mails; iedereen bij voornaam en dan 'dr Janzing', dat is toch vreemd. Dus vanaf heden zal u (lees: je) er toch aan moeten geloven, Heinrich ;).

Caroline, mijn back up, externe geheugen, epidemiologische ondersteuning en luisterend oor. Bij jou kon ik terecht als ik niet meer snapte waarom bovenstaande drie mannen allemaal een ander idee hadden, als ze het artikel hadden gereviseerd en het eigenlijk weer op mijn eerste versie leek en gewoon om het over van alles en nog wat te hebben. Jij was degene die me bij het laatste stuk toch nog even het zetje gaf dat ik nodig had om het af te maken. Ik had me geen betere copromotor kunnen wensen, dank je wel!

Frans Heyer, *Loes* Janssen en *Lisanne* Vranken: dank jullie wel voor de grondlegging van verschillende onderdelen waar ik verder mee aan de slag kon tijdens mijn promotietraject. Speciale dank aan *Frans* voor je voor je hulp bij het includeren van de patiënten en voor je technische hulplijn voor de HR-pQCT!

Josephine Kranendonk: ik vond het ontzettend leuk om jou te mogen begeleiden in de laatste fase van je opleiding. Je enthousiasme en betrokkenheid hebben ervoor gezorgd dat je een mooi artikel hebt geschreven. Mede dankzij de koffie pauzes en koptelefoons een groot succes!

Maud Strous, Maudje (of zoals Tess zegt 'grote Maud')... Dat kamertje in het leerhuis, waar het ooit allemaal begon. Eerst vele uren samen achter de computer in het leerhuis, toen ook nog heel veel uren samen in de kliniek en daaropvolgend mijn telefonische hotline voor onbegrijpelijke internistische problematiek. Dat alles resulteerde in een goeie vriendschap met veel koffie en pannenkoeken dates! En om het dan compleet te maken zullen we het toch maar doen he, promoveren. Wie wil ik dan liever als paranimf dan iemand die vanaf moment één aan mijn zij heeft gestaan?! Dank je wel!

Alle *chirurgen* van het VieCuri: zonder jullie steun was dit niet gelukt. Als semi arts mocht ik blijven en als ANIOS kon ik in enkele dagdelen per week mijn patiënten includeren. Dankzij jullie steun kon ik als AIOS verder leren in dit vertrouwde nest en hebben jullie op alle vlakken, zowel werk (klinisch wat enthousiaster dan onderzoeks-gerelateerd, begrijpelijk...) als privé altijd heel veel interesse getoond en mij ondersteund waar nodig. Jullie flexibiliteit, betrokkenheid en eerlijkheid hebben me ontzettend veel geboden. Dank jullie wel!

Alle *assistenten* van het VieCuri: een heel komen en gaan in de afgelopen jaren. Aan iedereen die heeft geholpen met inclusies van de patiënten; dank jullie wel. Aan iedereen die me heeft ondersteund bij het afmaken bij mijn proefschrift; dank jullie wel. En aan iedereen die gewoon af en toe even luisterde als ik blij was dat er iets was gepubliceerd of baalde dat het niet ging zoals ik had gehoopt; bedankt!

Alle *orthopeden*, *SEH-artsen* en *SEH-assistenten*: bedankt voor jullie hulp bij het includeren van de patiënten, de mailtjes als er eentje tussendoor was geglipt en het aanleveren van leesvoer. Speciale dank aan *Okke Lambers Heerspink* om als opponent op te treden tijdens mijn verdediging.

Bert van Rietbergen en *Melissa* Bevers: dank jullie wel voor alle input op technisch gebied. *Melissa*, ik vond het heel leuk om tijdens mijn promotie de kans te krijgen om jou mee te mogen begeleiden en ben heel blij en trots dat jij aan de slag bent gegaan met de plannen die voort zijn gevloeid uit ons onderzoek. Daarnaast wil ik je ongelofelijk bedanken voor je hulp bij het maken van de 3D afbeeldingen voor mijn boekje, zonder jou was ik nog altijd bezig geweest...

Angelique, *Eric*, *Evelien*, *Yvonne*, *Hans*, *Loes* en *Peter*: ontzettend bedankt voor alles wat jullie voor me hebben gedaan. Iedere patiënt mocht ik tussendoor plannen, dank voor het meedenken/meehelpen en de peptalks op de momenten dat mijn eigen planning me een beetje voorbij liep. Ik had me geen betere gipsverbandmeesters kunnen wensen!

Annemarie, *Marian*, *Rudie*, *Tia* en *Tiny*; de HR-pQCT operators die de patiënt van me overnamen als ik weer eens aangesneld kwam omdat ik stiekem toch niet echt veel tijd had en het dan met alle liefde en rust van me overnamen. Ontzettend bedankt hiervoor en ik weet zeker ook namens de patiënten voor de goede zorgen voor hen.

Prof. dr. P. Willems, bedankt om op te treden als voorzitter van de beoordelingscommissie van dit proefschrift. Ook aan de andere leden van mijn beoordelingscommissie en oppositie; *Prof. dr. A.E. Boonen*, *dr. A.J.M. Janus*, d*r. ir. J.J.A. de Jong* en *Prof. dr. M.H.J. Verhofstad* bedankt voor uw tijd en interesse!

Natuurlijk wil ik ook alle *co-auteurs* bedanken voor hun feedback. Dankzij jullie kritische blik zijn de artikelen verbeterd en hebben we samen mooie ideeën voor nu en de toekomst gevonden.

In het bijzonder *Pascal* Hannemann: dé scaphoid kenner. Dank voor al je input en je betrokkenheid!

Stacey Willems (oh jee, nu mevrouw van Hoof), lieve Stace; vanuit Utrecht kwam je 'terug' naar het zuiden voor de master geneeskunde. Vanaf dat moment een onafscheidelijk duo en ondanks onze uiteenlopende interesse op medisch gebied zaten en zitten we altijd op een lijn. Daarnaast kan wellicht elke chirurg wel een psychiater aan z'n zij gebruiken dus die heb ik dan alvast in de pocket! Aangezien je zo'n groot fan bent van onderzoek en promoties kon ik je de kans niet ontnemen om naast me te staan als paranimf. Dank je wel dat je dit wil doen en dank je wel voor alles, aapie!

Munt en *Kiek*; zonder de inhoud van mijn proefschrift te kennen hadden jullie bedacht dat jullie toch wel de meeste geschikte kandidaten zouden zijn als paranimf. Wat het eigenlijk was dat deed er niet zo veel toe, klonk in ieder geval leuk. Sorry dat jullie deze rol nu niet kunnen vervullen, jullie hadden het ongetwijfeld geweldig gedaan! Maar veel belangrijker ben ik heel blij met jullie als vriendinnen; jullie vertellen me de waarheid als ik het liever niet wil horen, zijn altijd jullie heerlijke (en drukke) zelf en al zien we elkaar lang niet zo vaak als we zouden willen, des te meer genieten we als we wel samen zijn. Dank jullie wel om er altijd voor mij te zijn en zoveel interesse te hebben getoond in mijn onderzoek!

Aan al mijn *vrienden en familie*, mijn boekje is klaar dus nu kunnen jullie eindelijk lezen wat ik in de afgelopen jaren in mijn 'vrije tijd' heb gedaan (tip: ga voor de Nederlandse samenvatting, scheelt je een paar uur). Ik wil jullie bedanken voor de steun en misschien nog meer wel voor de niet werk- en onderzoeks-gerelateerde afleiding.

In het bijzonder natuurlijk *papa* en *mama*, bedankt dat jullie er altijd voor me zijn. Ook al vinden jullie het waarschijnlijk vanzelfsprekend, toch wil ik jullie heel graag hier bedanken want mede dankzij jullie sta ik hier. Mama, als een van de weinigen zal je dit hele boek woord voor woord hebben gelezen. Ik kreeg het boekwerk met heel veel waardevolle opmerkingen en soms een rijtje vraagtekens van onbegrip van je terug. Mocht het een troost zijn, ik snap het ook niet allemaal hoor. Dank jullie wel voor de ongelofelijke hulp in ons soms iets te drukke leven, jullie maken het allemaal haalbaar en Maarten, ik en de meisjes zijn jullie daar héél dankbaar voor!

Lieve *Maarten*, mijn steun en toeverlaat. Behalve op het gebied van een proefschrift afronden dan... Maar we hebben het toch maar mooi gedaan hè schatje! Allebei onze opleiding, ons gezin met twee heerlijke dochters en een derde op komst, ons droomhuis dat dankzij jou inmiddels af is en ons hele leven daaromheen. In het afgelopen jaar hoopten of dachten we vaak dat er bij ons meer dan 24 uur in een dag zouden zitten. Dat bleek niet het geval, dus dan maar wat minder slaap. Maar dankzij jou positieve instelling heb ik geleerd om bepaalde dingen naast me neer te leggen als ze even niet zo soepel gaan, en dat komt toch stiekem wel heel vaak van pas. Nu we dit hoofdstuk hebben afgerond hebben we weer wat meer tijd voor elkaar (en wat meer tijd om te slapen), ik hou heel veel van je! Lieve *Tess* en *Maud*, jullie brengen zoveel liefde en vreugde in ons leven en daar kan ik jullie niet genoeg voor bedanken! Dikke kus van mama.

Curriculum vitae

Anne Daniels was born on the 11th of November 1991 in Sittard, the Netherlands. She obtained her Atheneum degree at Trevianum in Sittard in 2010.

After being eliminated for studying medicine, she studied European Public Health at Maastricht University. In 2011 she started her medical study at the Maastricht University where she received her medical doctor degree in 2017. After graduation, she started working as a surgical resident not in training at VieCuri Medical Centre in Venlo. Simultaneously she conducted research in this center resulting in her PhD under supervision of Prof. dr. Joop van den Bergh and Prof. dr. Martijn Poeze. In July 2019 she started her surigcal training at VieCuri Medical Centre in Venlo under the supervision of dr. Heinrich Janzing and dr. Frits Aarts. In April 2023, she continued her training at Maastricht Univeristy Medical Centre under supervision of dr. Jarno Melenhorst.

She lives happily together with Maarten van Heinsbergen and their two (soon to be three) daughters, Tess and Maud.

List of publications

Daniels A.M., Vogelaar F.J. *Late onset pulmonary metastasis more than 10 years after primary sigmoid carcinoma.* World Journal of Gastrointestinal Pathophysiology, May 2017; 15-8(2):96-99

Bloemen A., **Daniels A.M.,** Samyn M.G., Janssen R.J., Elshof J.W. *ECG guided tip positioning technique for Peripherally Inserted Central Catheters in a Dutch teaching hospital: feasibility and cost-effectiveness analysis in a prospective cohort study.* Journal of Vascular Access. Nov 2018; 19(6):578-584

Daniels A.M., Theelen L.M.A., Wyers C.E., Janzing H.M.J., van Rietbergen B., Vranken L., van der Velde R.Y., Geusens P.P.M.M., Kaarsemaker S., Poeze M., van den Bergh J.P. *Bone microarchitecture and distal radius fracture pattern complexity.* Journal of Orthopaedic Research. Aug 2019; 37(8):1690-1697

Daniels A.M., Wyers C.E., Janzing H.M.J., Sassen S., Loeffen D., Kaarsemaker S., van Rietbergen B., Hannemann P.F.W., Poeze M., van den Bergh J.P. *The interobserver reliability of the diagnosis and classification of scaphoid fractures using High Resolution peripheral Quantitative CT.* Bone and Joint Journal. Apr 2020; 102-B(4):478-484

Bevers M.S.A.M., **Daniels A.M.**, Wyers C.E., van Rietbergen B., Geusens P.P.M.M., Kaarsemaker S., Janzing H.M.J., Hannemann P.F.W., Poeze M., van den Bergh J.P. *The feasibility of High-Resolution Peripheral Quantitative Computed Tomography in patients with suspected scaphoid fractures.* Journal of Clinical Densitometry. Jul 2020; 23(3):432-442

Strous M.T.A., **Daniels A.M.**, Zimmermann F.M., van Erning F.N., Gidron Y., Vogelaar F.J. *Is pre-operative heart rate variability a prognostic indicator for overall survival and cancer recurrence in patients with primary colorectal cancer.* Plos One. Aug 2020; 15(8): 237-244

Daniels A.M., Bevers M.S.A.M., Sassen S., Wyers C.E., van Rietbergen B., Geusens P.P.M.M., Kaarsemaker S., Hannemann P.F.W., Poeze M., van den Bergh J.P., Janzing H.M.J. *Improved detection of scaphoid fractures with High Resolution peripheral Quantitative Computed Tomography compared with conventional CT.* Journal of Bone and Joint Surgery. Dec 2020; 102(24):2138-2145

Daniels A.M., Janzing H.M.J., Wyers C.E., van Rietbergen B., Vranken L., van der Velde R.Y., Geusens P.P.M.M., Kaarsemaker S., Poeze M., van den Bergh J.P. *Association of secondary displacement of distal radius fractures with cortical bone quality at the distal radius.* Archives of Orthopaedic and Trauma Surgery. Nov 2021; 141(11):1909-1918

Bevers M.S.A.M., Wyers C.E., **Daniels A.M.**, Audenaert E.A., van Kuijk S.M.J., van Rietbergen B., Geusens P.P.M.M., Kaarsemaker S., Janzing H.M.J., Hannemann P.F.W., Poeze M., van den Bergh J.P. *Association between bone shape and the presence of a fracture in patients with a clinically suspected scaphoid fracture.* Journal of Biomechanics. Nov 2021; 128

Bevers M.S.A.M., **Daniels A.M.**, van Rietbergen B., Geusens P.P.M.M., van Kuijk S.M.J., Sassen S., Kaarsemaker S., Hannemann P.F.W., Poeze M., Janzing H.M.J., van den Bergh J.P., Wyers C.E. *Assessment of the healing of conservatively-treated scaphoid fractures using HR-pQCT.* Bone. Dec 2021; 153:116-161

Daniels A.M., Kranendonk J., Wyers C.E., Janzing H.M.J., Sassen S., van Rietbergen B., Geusens P.P.M.M., Kaarsemaker S., Hannemann P.F.W., Poeze M., van den Bergh J.P. *What Is the diagnostic performance of conventional radiographs and clinical reassessment compared with HR-pQCT scaphoid fracture diagnosis?* Clinical Orthopaedics and Related Research. Jan 2023; 481(1):97-104

List of abbreviations

AO	Arbeitsgemeinschaft für Osteosynthesefragen
AUC	Area Under the Curve
BMD	Bone Mineral Density
BMI	Body Mass Index
BS	Bone Scintigraphy
CI	Confidence Interval
CT	Computed Tomography
DA	Dorsal Angulation
DRF	Distal Radius Fracture
DXA	Dual-energy X-ray Absorptiometry
ED	Emergency Department
FLS	Fracture Liaison Service
FN	Femoral Neck
Fx	Fracture
HR-pQCT	High Resolution peripheral Quantitative CT
IQR	Inter Quartile Range
LS	Lumbar Spine
MRI	Magnetic Resonance Imaging
NS	Not Significant
OR	Odds Ratio
OTA	Orthopaedic Trauma Association
RI	Radial Inclination
SD	Standard Deviation
TH	Total Hip
UV	Ulnar Variance
vBMD	volumetric Bone Mineral Density
VA	Volar Angulation
VF	Vertebral Fracture
VFA	Vertebral Fracture Assessment
µFEA	micro Finite Element Analysis